DEPARTMENT REPORT
UWME-DR-501-103-1

IOSIPESCU SHEAR PROPERTIES OF GRAPHITE FABRIC/EPOXY COMPOSITE LAMINATES

DAVID E. WALRATH
DONALD F. ADAMS

JUNE 1985

FINAL TECHNICAL REPORT

NASA-LANGLEY RESEARCH CENTER
HAMPTON, VA 23665
GRANT NO. NAG-1-272

COMPOSITE MATERIALS RESEARCH GROUP
MECHANICAL ENGINEERING DEPARTMENT
UNIVERSITY OF WYOMING
LARAMIE, WYOMING 82071

1. Report No.	2. Government Accession No.	3. Recipient's Catalog No.

4. Title and Subtitle	5. Report Date
Iosipescu Shear Properties of Graphite Fabric/ Epoxy Composite Laminates	June 1985
	6. Performing Organization Code

7. Author(s)	8. Performing Organization Report No.
David E. Walrath Donald F. Adams	UWME-DR-501-103-1
	10. Work Unit No.
9. Performing Organization Name and Address Composite Materials Research Group University of Wyoming Laramie, WY 82071	11. Contract or Grant No. NAG-1-272
	13. Type of Report and Period Covered Final Technical Report May 1984-May 1985
12. Sponsoring Agency Name and Address National Aeronautics and Space Administration Washington, D.C. 20546	14. Sponsoring Agency Code

15. Supplementary Notes

Langley Technical Monitor:
Mr. Jerry Deaton
Materials Division

16. Abstract

The Iosipescu shear test method was used to measure the in-plane and interlaminar shear properties of four T300 graphite fabric/934 epoxy composite materials. Different weave geometries tested included an Oxford weave, a 5-harness satin weave, an 8-harness satin weave, and a plain weave with auxiliary warp yarns. Both orthogonal and quasi-isotropic layup laminates were tested.

In-plane and interlaminar shear properties were obtained for laminates of all four fabric types. Overall, little difference in shear properties attributable to the fabric weave pattern was observed. The auxiliary warp material was significantly weaker and less stiff in interlaminar shear parallel to its fill direction.

A conventional strain gage extensometer was modified to measure shear strains for use with the Iosipescu shear test. While preliminary results were encouraging, several design iterations failed to produce a reliable shear transducer prototype. Strain gages are still the most reliable shear strain transducers for use with this test method.

Analytical and experimental studies of the Iosipescu shear test method conducted during previous years of the investigation are also summarized. Recent experimental verifications of the Iosipescu shear method conducted by other investigators are compared to the results obtained in the present effort.

17. Key Words (Suggested by Author(s))	18. Distribution Statement
composite materials fabric composites shear properties shear test methods	**Unclassified, Unlimited**

19. Security Classif. (of this report)	20. Security Classif. (of this page)	21. No. of Pages	22. Price*
Unclassified	Unclassified	125	

* For sale by the National Technical Information Service, Springfield, Virginia 22161

TABLE OF CONTENTS

PREFACE

This final technical report summarizes results of a combined analytical and experimental study performed for the National Aeronautics and Space Administration-Langley Research Center under Grant Number NAG-1-272, University of Wyoming Project Number 5-32452. During the first year of this three-year grant, Mr. Marvin B. Dow served as the NASA-LRC Technical Monitor. For the subsequent two years, Mr. Jerry W. Deaton served in this capacity.

All work conducted as part of this grant was performed by members of the Composite Materials Research Group within the Mechanical Engineering Department at the University of Wyoming. The CMRG is led by Dr. Donald F. Adams, Professor of Mechanical Engineering. Mr. David E. Walrath, Supply Assistant Professor of Mechanical Engineering, served as Principal Investigator for this research program. Also participating in this program were Mr. Russ Porter and Mr. John Miller, Mechanical Engineering Machine Shop, and Mr. Robert Wakelee and Mr. Douglas McLarty, undergraduate students in Mechanical Engineering.

SECTION 1

INTRODUCTION AND SUMMARY

1.1 Background

The measurement of anisotropic composite material shear stress-shear strain behavior, including shear strength and shear modulus, has been a problem of special interest to the composites community for a number of years. Many different test methods have been proposed; the interested investigator will find lists of references to many different shear test methods in References [1-4], for example.

One particular class of shear tests has gained increased interest in recent years. The tests in this class all employ some form of beam loaded laterally, and make use of edge notches in the test region to induce a uniform shear stress distribution. Variations of this shear test method have been reported by Arcan et al. [5-7], Iosipescu [8], and Slepetz [9].

At the University of Wyoming, the Iosipescu version of this shear test method has been used to measure shear properties of various materials for approximately seven years. Our experiences with this test method prior to initiation of the present NASA grant are summarized in References [1,10].

1.2 Synopsis of Previous Work

The work presented here was performed during the final year of a three-year NASA-Langley Research Center grant to study and use the Iosipescu shear test method. The purposes of this grant were two-fold. First, the Iosipescu shear test method was to be examined, both analytically and experimentally, for its applicability in making in-plane and interlaminar shear property measurements of laminated composite materials. Second, the method was to be used to measure the in-plane and interlaminar shear properties of selected composite material systems, specifically graphite fabric/epoxy composite laminates.

During the first year of this NASA grant, the effort was entirely analytical [11]. An extensive finite element analysis of the test specimen was conducted to determine the influence of geometric and

material variations on simulated test results. Nine different notch configurations were modeled, including three different notch depths, three notch angles, and three notch root radii. These different configurations were analyzed using three different material systems, representing differing degrees of orthotropy. The first material was isotropic (aluminum), representing a stiffness orthotropy ratio (E_{11}/E_{22}) of 1. The second material had an orthotropy ratio of 13 (e.g., T300/934 or AS/3501-6 graphite/epoxy). A third highly orthotropic material, with an orthotropy ratio of 49 (e.g., GY70/934 graphite/epoxy) was also modeled. These materials were all assumed to remain linearly elastic.

A major conclusion of the first-year study was that the positions of the inner loading points in the then current Wyoming version of the Iosipescu shear fixture were too near the center test region of the specimen. Compressive stresses induced by the applied load were intruding into the region of supposedly pure shear stress. Thus, the first recommendation made was to redesign the test fixture such that the inner loading points were positioned farther from the center of the test specimen.

Notch geometry and the degree of material orthotropy in the test specimen were also found to affect modeled test results. A shear stress concentration was predicted to exist at the roots of the notches. The most significant geometric parameter affecting this stress concentration was found to be the notch root radius. Sharp notches produced higher stress concentrations than did notches with rounded root radii. The included angle of the notch was found to have a secondary effect on modeled test results; this notch angle dependency was also a function of the degree of material orthotropy. Notch depth was shown to be less important as long as the variation maintained the depth between 20 and 25 percent of overall specimen height. Results from this first-year analysis are summarized and compared to recent experimental data in Section 2 of the present report.

During the second year of the program, a new test fixture was designed and built [12]. This improved test fixture incorporated three major changes from the previous fixture design. The specimen size was increased from 50 mm x 12 mm (2.0 in x 0.5 in) to 76 mm x 19 mm (3.0 in

x 0.75 in), to provide increased area for shear strain measurement and easier access to the center test region of the specimen for instrumentation purposes. The inner loading points were moved away from the center of the test specimen, to a distance of 6.3 mm (0.25 in). This distance was 2.5 mm (0.1 in) in the first Wyoming version of the Iosipescu shear test fixture [11]. Finally, a sliding block clamping mechanism was incorporated into each fixture half in order to provide a close fit between the specimen and the fixture, thus eliminating the need for close dimensional tolerances on specimen height. Further details of the test fixture design, including machine drawings and instructions for its use, are included in Appendix A of the present report.

Additional finite element analyses of the Iosipescu shear test specimen were also conducted during the second year of this grant [12]. The new test configuration, with inner loading points positioned farther from the test region, was analyzed for two different notch geometries. Specifically, notch angles of 90° and 110° were modeled. Notch depth was modeled as being 20 percent of the specimen height, with notch root radii of 1.27 mm (0.050 in). Nonlinear material behavior was included in these analyses, an important consideration in shear testing of many materials, particularly polymer matrix composites. Two materials were modeled, viz., an (isotropic) 6061 aluminum alloy ($E_{11}/E_{22} = 1$) and an (orthotropic) unidirectional AS4/3501-6 graphite/epoxy ($E_{11}/E_{22} = 16$).

Analytically, notch angle was shown to have an influence on predicted shear modulus. However, this influence of notch angle was less when rounded notch root radii rather than sharp notches were modeled.

Experimentally, variations in shear modulus with notch geometry were shown to exhibit trends similar to those predicted by the finite element analysis. Cracks tended to initiate at one or both of the notch roots in 0° orientation tests of unidirectional composite materials (i.e., in specimens with the fibers oriented along the specimen length). These cracks propagated away from the notch root in a direction parallel to the fiber direction. This cracking was most prevalent in materials which tended to be brittle, and was a result of the shear stress concentration in the notch root region. In an effort to understand the effect of these cracks on test results, finite element models containing

cracks at the notch roots were also analyzed during the second year of this research program. These cracks were modeled as gaps formed by deleted elements. Thus, the crack width was larger as modeled than that which occurred in actual test specimens. Then preliminary results were considered to be more qualitative than quantitative, but still reasonably representative of the general stress state within the specimen. It was found that these cracks at the notch root tended to relieve the shear stress concentration, as would be expected. However, these cracks did not significantly alter the stress state in the test region of the Iosipescu shear specimen. Thus, it was concluded that the cracks which may occur at the notch roots do not significantly affect the results of the test, and may in fact be favorable. These analytical results, originally reported in Reference [12], are summarized in Section 2 of the present report.

1.3 Summary of the Present Third Year Effort

During the present third year of this grant, in-plane and interlaminar shear tests were performed on ten graphite fabric/epoxy composite laminates provided by NASA-Langley. These test panels had been fabricated using four different types of woven fabric, viz., an Oxford weave, a 5-harness satin weave, an 8-harness satin weave, and a special plain weave with auxiliary warp yarns. The Oxford, 5-harness, and 8-harness weave fabrics had been fabricated into both orthogonal and quasi-isotropic laminates. The plain weave auxiliary warp fabric was provided as an orthogonal laminate only. The term orthogonal laminate is used here to define a multi-ply fabric laminate in which the warp direction of every ply is oriented in the same direction, i.e., the 0° direction. The term quasi-isotropic laminate is used here to define a multi-ply fabric laminate in which the warp directions of the successive plies are laid up in the pattern $[45/0/[45/90]_{3S}$, the angle representing the orientation of the warp direction of the individual ply.

In-plane and interlaminar shear tests were conducted on all four types of fabric. For the Oxford, 5-harness satin and 8-harness satin weave laminates, little influence of weave was observed in the in-plane shear properties. The quasi-isotropic laminates did exhibit higher in-plane shear strengths and shear moduli than the orthogonal laminates,

as would be expected due to the presence of fibers oriented at ±45°. Some panel to panel variations in interlaminar shear properties were observed. However, little or no difference in interlaminar shear properties attributable to weave geometry was observed. Possible explanations for the panel to panel variations are discussed in Section 3. Laminated fabric shear properties measured during the second year of the grant [12] have also been included in the discussion contained in Section 3. All individual shear test results obtained during the present third year of this grant are listed in Appendix B.

A second task to be performed during the present third year was to further study the feasibility of modifying a standard extensometer for use as a shear strain transducer. One technique often used to measure the shear strain in an Iosipescu specimen utilizes strain gages oriented at ±45° to the specimen length. This strain measure method works very well, producing accurate, repeatable results for most materials. However, strain gages are relatively expensive, not reusable, and are limited in the magnitude of shear strain that can be measured. The optimum shear strain transducer could be mounted quickly, would be reusable, would have a large strain range, and would be compatible with instrumentation available in most mechanical testing laboratories.

A modified extensometer for shear strain measurement had been previously developed and used at the University of Wyoming [1,10]. While the device did demonstrate the possibility of performing shear strain measurements in this manner, it was not easily mounted. Results obtained were highly dependent on how the device was attached to the test specimen. During the second-year analytical effort [12], the feasibility of determining shear strains via this method of measuring relative displacements was again established. Therefore, during the present third-year program, an effort was made to design a better attachment mechanism for this shear transducer.

An attachment mechanism was designed and a prototype was built. Initial tests showed reasonable agreement between shear strains measured with the modified extensometer and shear strains measured with strain gages. Unfortunately considerable hysteresis was apparent in the results obtained with the modified extensometer. No hysteresis was present in the strain gage results as long as the test specimen was not loaded

beyond its yield point. Furthermore, repetitive tests on the same specimen resulted in a 10 to 20 percent variation in shear strain from test to test as measured by the modified extensometer. Negligible variation was present in the strain gage shear strain results. Several different design modifications were performed, and some improvement in the shear response of the modified extensometer was achieved. However, the test-to-test variation in results measured by the modified extensometer was still unacceptable. Strain gages are still the optimum shear strain measurement technique for use with the Iosipescu shear test method. Further discussion of the modified extensometer shear strain transducer is included in Section 2.

SECTION 2
CURRENT STATUS OF THE IOSIPESCU SHEAR TEST METHOD

2.1 Test Configuration

The basic loading diagram for an Iosipescu shear test specimen is illustrated in Figure 1. Forces are applied to the test specimen as shown in Figure 1a. These lateral forces produce a net shear loading P through the center region of the test specimen while the moments induced by these forces exactly cancel at midspan. Thus a state of pure shear loading exists at the midlength of the test specimen, as illustrated in Figures 1b and 1c.

In a beam of constant cross section, the shear stress distribution due to lateral shear loading will be parabolic, as described in most elementary mechanics of materials textbooks. In order to alter this shear stress distribution from parabolic to uniform, Iosipescu machined 90° included angle notches at the specimen midspan [8]. The depth and shape of these notches and the shear stress distribution produced have been the subjects of extensive investigation by the present investigators and others during the past few years.

The Iosipescu shear test fixture used at the University of Wyoming has evolved through two basic designs. The original test fixture, shown in Figure 2, was copied from a fixture used by T. R. Place at the Aeronutronic Division of Ford Aerospace and Communications Corporation. There, the Iosipescu shear test was used to test three-dimensionally reinforced ceramic matrix composite materials [13]. This first Wyoming version of the Iosipescu fixture was used to measure shear properties for a wide variety of materials including three-dimensionally reinforced carbon-carbon composites [14-16], unidirectionally reinforced glass/epoxy and graphite/epoxy, chopped glass fiber-reinforced polyester sheet molding compound (SMC) [10,17,18], neat (unreinforced) epoxy resins [19], and even such materials as wood and foam [20]. The test method worked well, resulting in apparent shear failures and reproducible shear strengths and shear moduli. Eventually, drawings of the fixture were sent to other interested investigators, at their request, that they might build their own test fixtures. Some

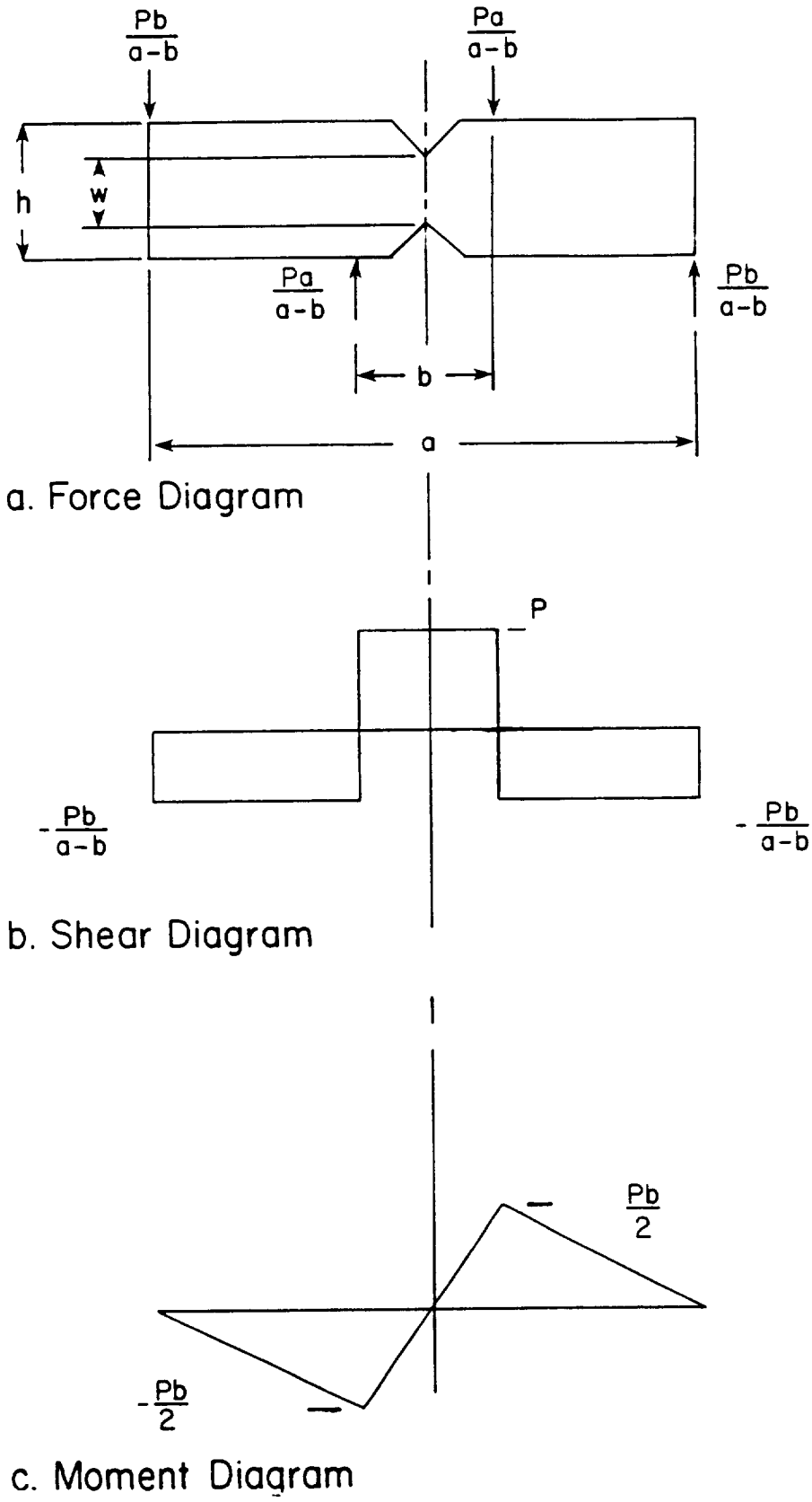

Figure 1. Force, Shear, and Moment Plots for the Iosipescu Shear Test Specimen.

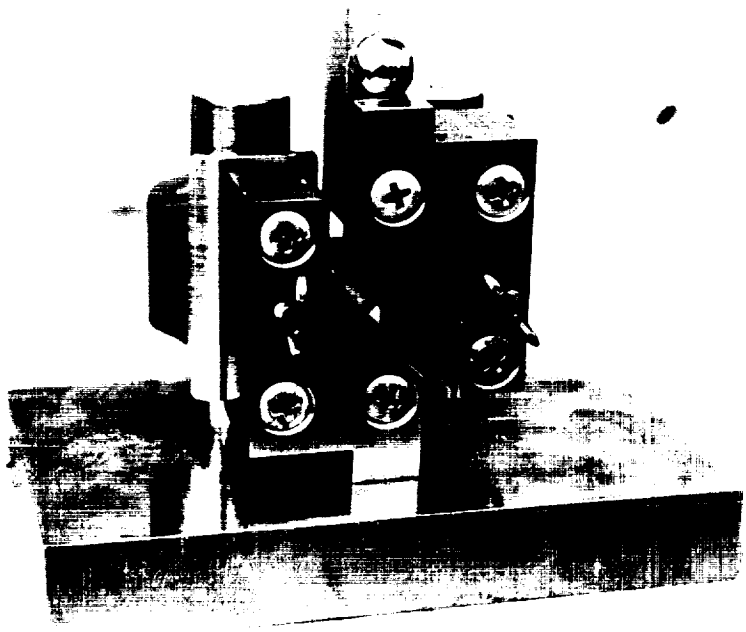

Figure 2. Original Wyoming Version of the Iosipescu Shear Test Fixture.

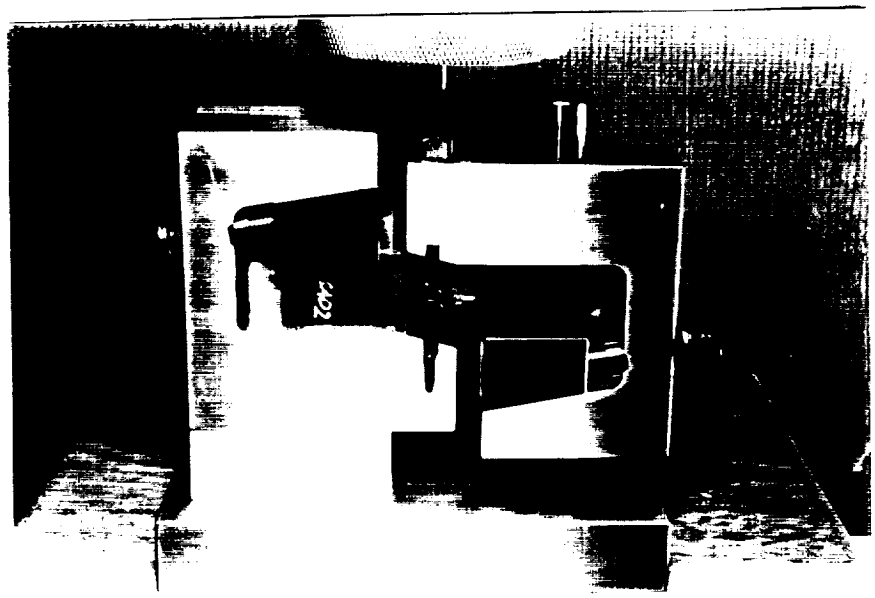

Figure 3. Redesigned Wyoming Version of the Iosipescu Shear Test Fixture.

organizations preferred to have a fixture built for them at the University of Wyoming, which was done.

During the first year of the present NASA grant, it was found that compression stresses from the inner loading points intruded into the test region of the specimen [11]. Therefore, during the second year of this grant, the text fixture was redesigned, repositioning the inner loading points and incorporating changes to make the test fixture more convenient to use [12]. The redesigned Wyoming version of the Iosipescu shear test fixture, shown in Figure 3, was used for all subsequent testing performed as part of the second and third years of this NASA funded study. Detail drawings and parts descriptions for this newer Wyoming version of the Iosipescu shear test fixture are included in Appendix A.

During this same time period, additional investigators were also beginning to use the Iosipescu shear test. Work was performed by Spigel [4] using a test fixture similar to that shown in Figure 2. Sullivan, et al., [3] used a Wyoming built fixture, like that shown in Figure 2, to measure the shear properties of a vinyl ester resin. Sullivan, et al., also concluded that the inner loading points of the test fixture were too near the test region of the specimen. When the inner loading points were moved away from the center of the specimen, to 10 mm (0.39 in), the compression stresses induced by the loading forces no longer intruded into the test region. They did report problems with load post binding in their modified fixture, however, which would obviously make measured numerical results questionable until the binding was eliminated. A linear ball bushing had already been incorporated into the design of the newer version of the Iosipescu shear fixture shown in Figure 3.

2.2 Notch Geometry and Shear Stress Distribution

Most of the detailed analyses of the stress states within double edge notched beam shear test specimens have been conducted using finite element techniques. A major concern of these various investigations has been the configuration, i.e., the notch angle, root radius and depth, of these edge notches in the test specimen.

Slepetz, et al., [9] modeled three notch configurations, viz., a sharp notch, a notch with a fillet or root radius, and a specimen with

no notch at all, i.e., a beam of constant cross section. In this linear elastic analysis, properties for aluminum, glass/epoxy, and graphite/epoxy were used. The analysis of Slepetz, et al., was actually performed on a test configuration then called the Asymmetric Four-Point Bend (AFPB) test. This differs somewhat from the Iosipescu loading technique in that the test fixture is divided into top and bottom sections rather than left and right fixture halves. However in the notch region, the net effect is the same, i.e., pure shear loading. Slepetz, et al., showed that for orthotropic as well as isotropic materials, the shear stress distribution in a specimen of constant cross section, i.e., a beam without notches, was indeed nearly parabolic as predicted by beam theory. Edge notches at the test specimen midlength did transform the shear stress distribution from parabolic towards a uniform distribution. However, for sharp notches in orthotropic unidirectional composites, there was a shear stress concentration at the notch root. They only modeled 90° notches with depths equal to 25 percent of the overall specimen height.

Bergner and Herakovich also modeled a slightly different test geometry [21,22]. In their modeled fixture, end pieces were attached to the beam specimen ends in order to apply the lateral shear loading. A linear elastic, plane stress finite element analysis was used to model one notch geometry, a sharp 90° notch with a depth equal to 22.5 percent of the specimen height. Material properties for unidirectional and quasi-isotropic $[0/90/\pm45]_S$ graphite/polyimide as well as (isotropic) steel were used. These investigators also noted the presence of a shear stress concentration at the notch root for the unidirectional composites. No experimental work was performed.

Marloff [23] analyzed the Arcan, et al. [5-7] version of a double edge notch beam shear test specimen. Marloff demonstrated that failures tended to initiate slightly away from the test specimen centerline. Therefore, the stress state causing initiation of this failure was not pure shear, but some combination of normal bending stress and shear stress. Marloff did conclude that uniform pure shear existed in the test specimen and that measurements of in-plane shear modulus should be quite accurate.

During the first year of the present NASA-funded grant, finite element investigations of the Iosipescu loading method were conducted [11]. Nine different notch geometries were modeled using three different sets of linear elastic material properties. Notch depths equal to 10, 20, and 30 percent of the specimen height were modeled. Notch root radii of 0 mm, 0.64 mm, and 1.27 mm (0 in, 0.025 in, and 0.050 in) were studied. Notch angles of 90°, 110°, and 120° were also examined. Linear elastic material properties for aluminum (E_{11}/E_{22} = 1), unidirectional AS/3501-6 graphite/epoxy (E_{11}/E_{22} = 13) and GY70/934 graphite/epoxy (E_{11}/E_{22} = 49) were used in analyzing nine geometric models, resulting in 27 different finite element solutions.

Iosipescu had originally determined the optimum notch depth to be equal to 22.5 percent of the overall specimen height, although he used notch depths of 25 percent in his experimental work [8]. However, Iosipescu studied only isotropic materials. Slepetz, et al., [9] modeled and tested orthotropic materials, but examined only two notch depths, 0 percent (a beam of constant cross section) and 25 percent of overall specimen height. Finite element models analyzed by the present authors during this study indicated that notch depth had little effect on test results as long as it was in the range of 20-25 percent of overall specimen height.

Notch root radius was shown to influence test results much more significantly than notch depth. A sharp notch root radius produces a shear stress concentration at the notch root in orthotropic materials, also observed by Slepetz, et al. [9] and Bergner et al., [21,22]. This shear stress concentration was shown to be alleviated by rounding the bottom of the notch root. It was recommended that notch root radii of at least 1.27 mm (0.050 in) be used to minimize shear stress concentrations [12]. It was also noted, however, that the point of maximum shear stress in the test specimen tended to shift away from the centerline of the specimen with increasing notch root radius. Similar results were obtained by Marloff in his finite element investigations [23].

Iosipescu [8] had concluded that for isotropic materials a 90° notch was optimum, as the sides of the notch would coincide with the principal stress directions. For orthotropic materials, a relationship between notch angle and stress distribution was observed during the

first year of the present research [11]. It appeared from the finite element analyses that the optimum notch angle might be greater than 90°.

During the second year of this research program [12], finite element analysis of the Iosipescu shear test specimen were extended to include nonlinear material behavior. An incremental analysis employing a tangent modulus technique was used to model inelastic material behavior [24,25]. The influence of notch angle was modeled using notch angles of 90° and 110°. Material properties for an isotropic aluminum and an inelastic (in shear) orthotropic AS4/3501-6 graphite/epoxy were used.

Analytically, the effect of inelastic material behavior was to blunt the shear stress concentration at the notch root within the test specimen. Centerline shear stress distributions calculated during this second year for the orthotropic AS4/3501-6 material are replotted here as Figures 4 and 5. Shear stresses have been normalized by the average applied shear stress. The notch geometry for the model of Figure 4 was a 90° notch with a root radius of 1.27 mm (0.050 in). The stress distribution plotted in Figure 4a is for the initial (linearly elastic) first increment of the analysis. Note the approximate 1.3 magnitude of the shear stress concentration. At Increment 4, depicted in Figure 4b, the first elements are beginning to behave inelastically. At Increment 8, most elements in the test region of the specimen are inelastic. It will be noted that the shear stress distribution has become more uniform. Finally, in Increment 12, where stresses are approaching ultimate, the stress distribution is nearly uniform.

In Figure 5, for the same orthotropic material, the shear stress distributions for a 110°, 1.27 mm (0.050 in) root radius notch are plotted. An approximately 1.2 magnitude of shear stress concentration for the linearly elastic first increment, plotted in Figure 5a, will be noted. Comparing the shear stress distribution of Figure 5a with that of 4a, it can be seen that the shear stress concentration for the 110° notch is slightly less than that for the 90° notch. The same slight difference was still present just after the onset of inelastic behavior, as can be seen by comparing Figure 5b (for Increment 4) with Figure 4b. However, at larger applied shear stresses, e.g., Increments 8 and 12 plotted in Figures 5c and 5d, the stress distributions have again become nearly uniform.

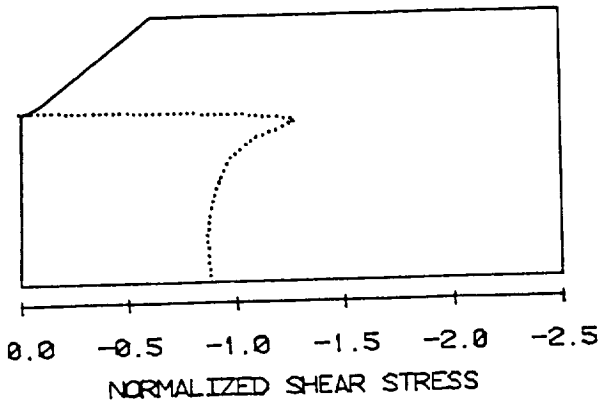

a) Increment 1, $\bar{\tau}$ = 11.7 MPa (1.70 ksi)

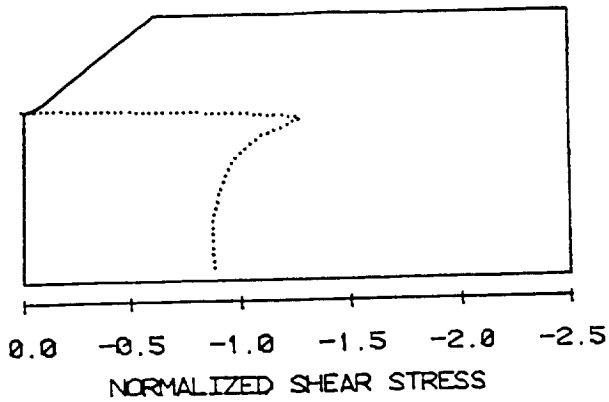

b) Increment 4, $\bar{\tau}$ = 44.9 MPa (6.51 ksi)

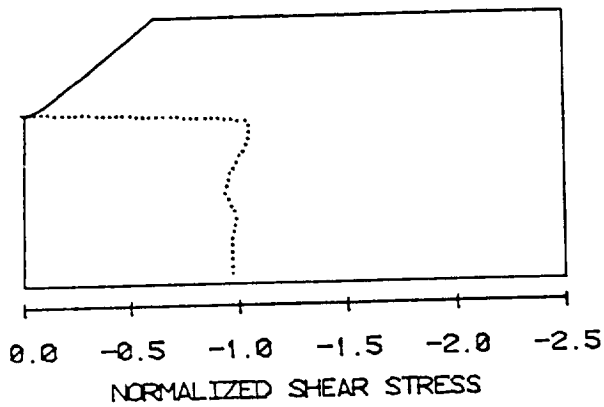

c) Increment 8, $\bar{\tau}$ = 85.1 MPa (12.34 ksi)

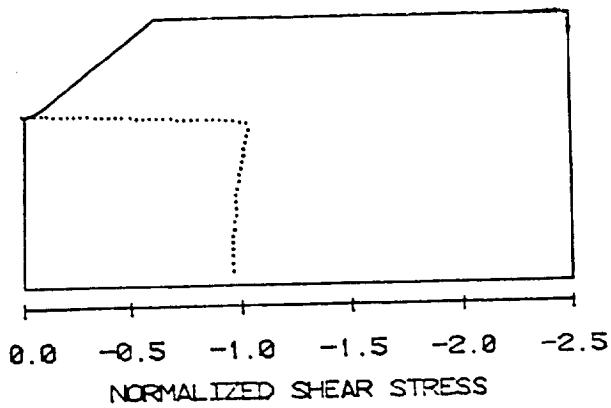

d) Increment 12, $\bar{\tau}$ = 109.2 MPa (15.84 ksi)

Figure 4. Normalized Centerline Shear Stress Profiles $\tau_{xy}/\bar{\tau}$ for a 90° Notch Iosipescu Shear Test Specimen of AS4/3501-6 Graphite/ Epoxy Unidirectional Composite.

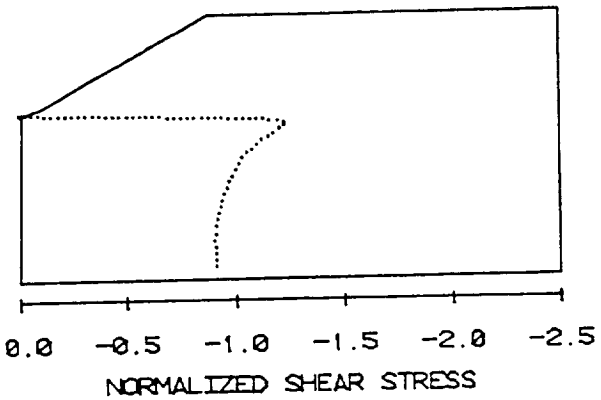

a) Increment 1, 14.5 MPa (2.11 ksi)

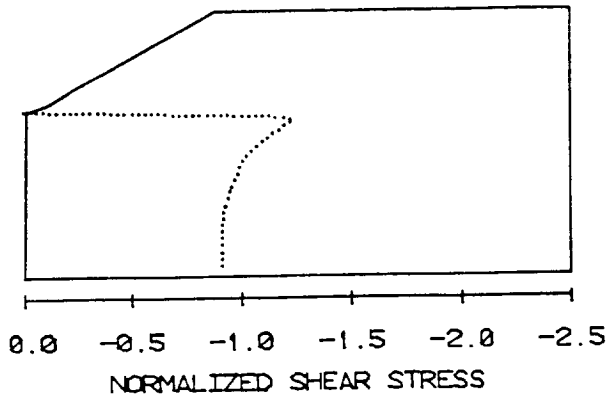

b) Increment 4, 57.1 MPa (8.28 ksi)

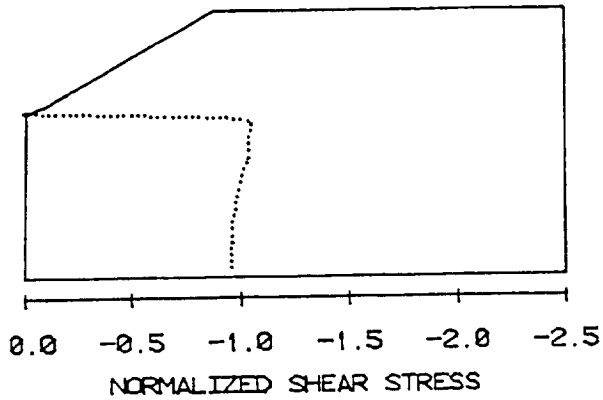

c) Increment 8, 95.0 MPa (13.78 ksi)

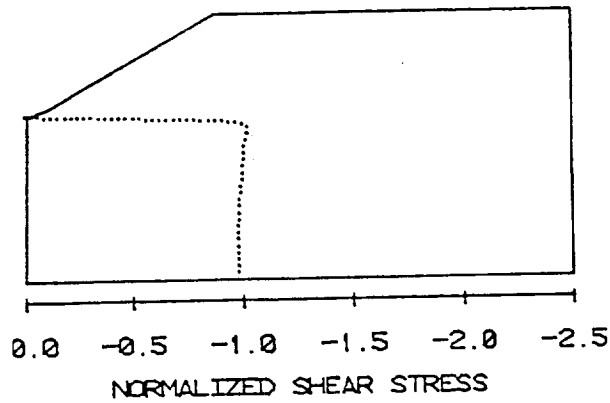

d) Increment 12, 114.0 MPa (16.53 ksi)

Figure 5. Normalized Centerline Shear Stress Profiles $\tau_{xy}/\bar{\tau}$ for a 110° Notch Iosipescu Shear Test Specimen of AS4/3501-6 Graphite/ Epoxy Unidirectional Composite.

2.3 Apparent Shear Properties

Much of the analytical work performed during the first two years of this grant was geared towards predicting the shear stress-shear strain response obtained when using the different specimen geometries. Shear stress, to the testing machine operator, is the applied load divided by the cross-sectional area of the test specimen between the notch roots. Applied stress in the analysis was calculated from the total nodal forces at the loading points divided by the cross-sectional area between the notch roots. Shear strains as would be measured by a strain rosette, were calculated from analytical results as the average shear strain in the central region of the test specimen covered by an area equivalent to that of the shear strain rosette. Thus, error estimates were made by comparing the calculated apparent shear modulus as predicted by the finite element analysis with the actual shear modulus used as input to the analysis.

The effect of notch root radius on apparent shear modulus is plotted in Figure 6, from the results of the first-year linear finite element analysis [11]. It will be noted that for all three types of materials, isotropic (E_{11}/E_{22} = 1), orthotropic (E_{11}/E_{22} = 13), and highly orthotropic (E_{11}/E_{22} = 49), the apparent shear modulus decreased with increasing notch root radius. An isotropic material tested with a 90° sharp notched test specimen (root radius equal to 0.0) was predicted to exhibit an apparent shear modulus approximately 10 percent greater than the actual value. As the modeled notch root radius was increased the difference between the predicted and the measured shear modulus decreased. For the highly orthotropic material, characteristic of a high modulus graphite/epoxy, the error in the predicted shear modulus was quite high, viz., 27 percent when a sharp notch root radius was modeled. This difference decreased to 17 percent when the 1.27 mm (0.050 in) root radius was modeled.

Two conclusions were drawn from the results plotted in Figure 6. First, both the notch root radius and the degree of material orthotropy affected the predicted shear modulus in these finite element models of the Iosipescu shear test. Second, the predicted shear modulus decreased with increasing notch root radius. It should be remembered that these finite element results were obtained during the first year of this

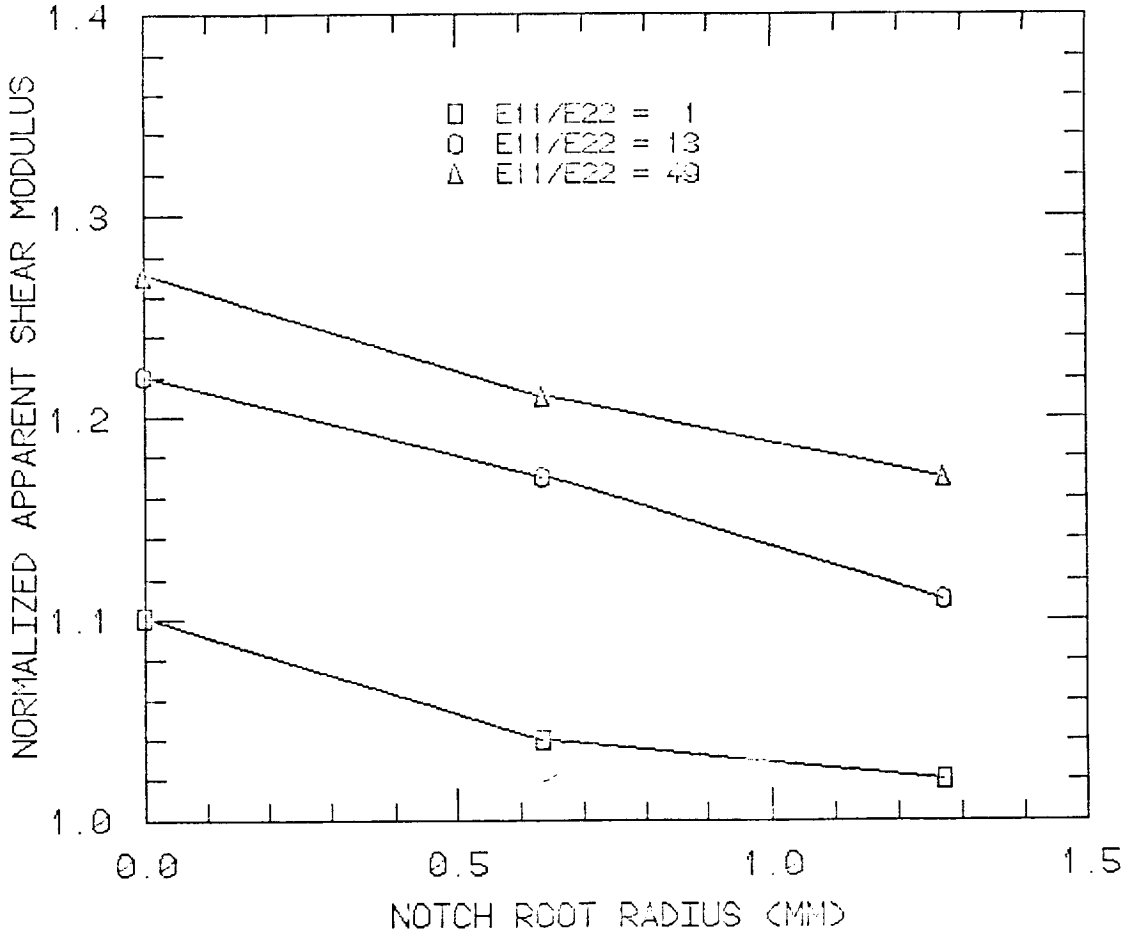

Figure 6. Normalized Apparent Shear Modulus versus Notch Root Radius, 90° Notch Angle.

grant, in which the first Wyoming version of the test fixture was modeled. Some compressive stresses from the inner loading faces infringed on the test region.

The influence of notch angle was modeled during both the first and second years of this grant. During the first year, notch angles of 90°, 110°, and 120° were modeled, for sharp notches [11]. The effect of these three notch angles on predicted (apparent) shear modulus is plotted in Figure 7. The predicted shear modulus decreases, for all three types of material, with increasing notch angle. For the isotropic (E_{11}/E_{22} = 1) cases, the larger notch angle specimens were predicted to have shear moduli lower than actual input values. For the unidirectional orthotropic graphite/epoxy materials, the effect of increasing notch angle was to decrease the predicted shear modulus, but results were still greater than the input shear modulus.

During the second year of this research effort, nonlinear material behavior was included. Also, notches were modeled with root radii equal to 1.27 mm (0.050 in), as opposed to the sharp notches modeled during the first year. The apparent shear moduli for 90° and 110° notched specimens, using material properties with orthotropy ratios of 1 and 16, are plotted in Figure 8. Predicted shear modulus again decreases with increasing notch angle. It will be noted that for the isotropic materials (E_{11}/E_{22} = 1), the predicted (apparent) shear modulus is less than the input shear modulus for both the 90° and the 110° notch angles. The apparent shear moduli plotted in Figure 8 are lower than those predicted for the sharp notch models plotted in Figure 7 due to the increased notch root radii of 1.27 mm (0.050 in). It will also be noted in Figures 7 and 8 that the decrease in apparent shear modulus with increasing notch angle is much less pronounced for notches with rounded root radii. The finite element meshes used during the second year [12] were more detailed, incorporating 778 elements as opposed to the 256 elements used during the first year [11]. It can also be seen from Figures 7 and 8 that both analyses predict decreasing apparent shear modulus with increasing notch angle.

The effect of notch root radius and notch angle has been experimentally investigated by Spigel [4]. Unfortunately for the present purposes, the major portion of this test work was conducted on

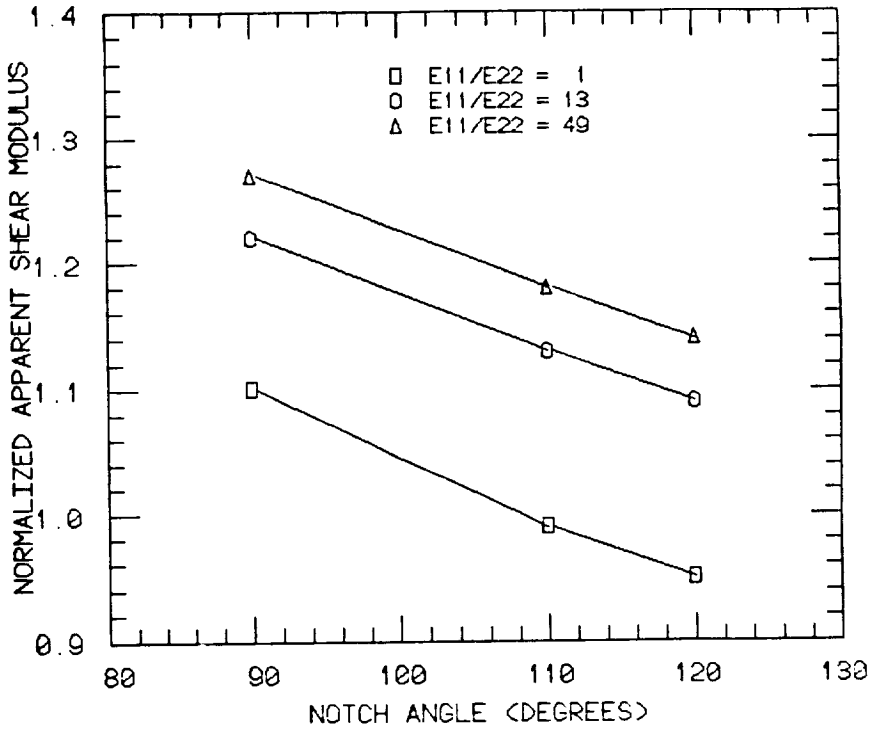

Figure 7. Normalized Apparent Shear Modulus versus Notch Angle, Sharp Notch.

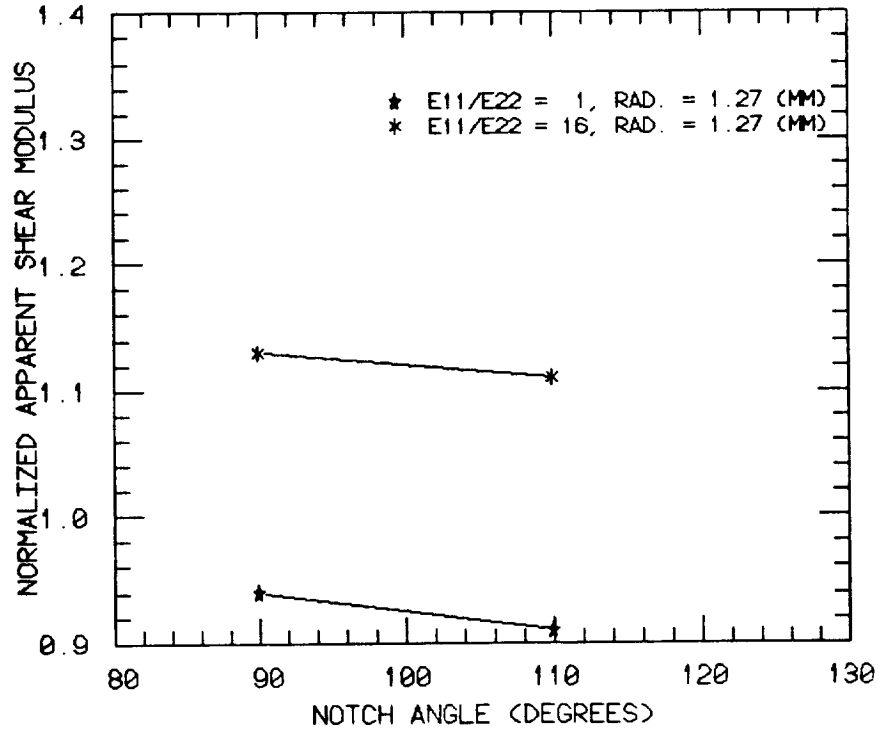

Figure 8. Normalized Apparent Shear Modulus versus Notch Angle, Root Radius = 1.27 mm.

quasi-isotropic $[0/\pm45/90]_S$ laminates. Thus, the experimental data were not directly comparable to the analysis conducted as part of this grant. Spigel did make some comparisons between his data and the analytical results of this present program. However, all finite element analyses performed as part of this grant were for isotropic or unidirectional orthotropic materials. Comparisons of isotropic plane stress analytical results with experimental Iosipescu shear results for quasi-isotropic laminates must be made with caution. The stress state within a quasi-isotropic laminate is three-dimensional near free edges. Thus, the stress distribution in an Iosipescu shear specimen at the notch root for a quasi-isotropic laminate could be dominated by interlaminar stresses. This fact was also noted by Spigel in his work [4]. Complex failure modes were also observed for the quasi-isotropic graphite fabric/epoxy laminates tested during the present third-year work, as discussed in Section 3.

Spigel did observe a relationship between measured shear properties and notch geometry for his quasi-isotropic laminates [4]. His results indicated that both the measured shear strength and measured shear modulus decreased with increasing notch angle and increasing notch root radius. Spigel suggested that these experimental trends contradicted the results of the analyses reported in Reference [11]. However, the only analytical results from Reference [11] which could be compared with Spigel's experimental work were the shear modulus results for an isotropic material. As was shown in Figures 6 through 8, finite element calculations performed at Wyoming as part of this study [11] indicated that the apparent measured shear modulus decreased with increasing notch root radius and notch angle. Spigel reasoned that the predicted stress concentration was lower for larger notch angles, therefore measured strengths should increase with increasing notch angle. This argument might be valid for unidirectional orthotropic materials, for which the present analytical work was performed. However, Spigel's experimental results were for quasi-isotropic laminates, which had complex three-dimensional stress states at the free edges near the notch roots in the Iosipescu specimen. Comparisons between the quasi-isotropic composite shear strength measured by Spigel and stress states predicted during the first two years of the present grant are simply not valid.

Spigel conducted only limited tests on unidirectional composite materials.

Shear moduli for quasi-isotropic AS4/3502 graphite/epoxy, measured by Spigel using the Iosipescu shear test, are plotted in Figures 9 and 10. The data plotted in Figure 9 indicates the same trends as the analytical predictions of Figure 6, viz., that measured shear modulus should decrease with increasing notch root radius. Measured shear modulus versus notch angle results for quasi-isotropic graphite/epoxy from Reference [4] and aluminum from References [12] are plotted in Figure 10. Notch root radii for data plotted in Figure 10 were 1.27 mm (0.050 in). Again the measured shear moduli decreased with increasing notch angle, as was analytically modeled, and presented in Figures 7 and 8.

Another experimental investigation of the Iosipescu and Asymmetric Four-Point Bend (AFPB) shear test methods has been initiated by Abdallah, et al. [26]. In this investigation, photoelastic and Moire' interferometric techniques were used to evaluate the stress states within specimens loaded in an AFPB test fixture, and in both Wyoming versions of the Iosipescu shear test fixture. Comparisons of results using the three different test fixtures indicated that some differences in stress distributions were present. However, shear strength and shear modulus data obtained during this investigation had not yet been published at the time of the present report.

2.4 Effect of Notch Root Cracks

As noted earlier in this report, when Iosipescu shear tests were conducted on unidirectional graphite/epoxy with the fibers oriented parallel to the specimen length, cracks tended to initiate at the notch roots and to propagate parallel to the fibers [12]. The onset of this cracking tended to cause momentary drops in load during an individual test, also causing small "glitches" on the stress-strain plot. One such stress-strain plot obtained during the second year of this grant is plotted in Figure 11. The discontinuity in the stress-strain plot corresponding to the initiation of a crack at the notch root will be noted. The load (stress) in the specimen dropped momentarily, then subsequently increased. Ultimately the specimen failed due to massive

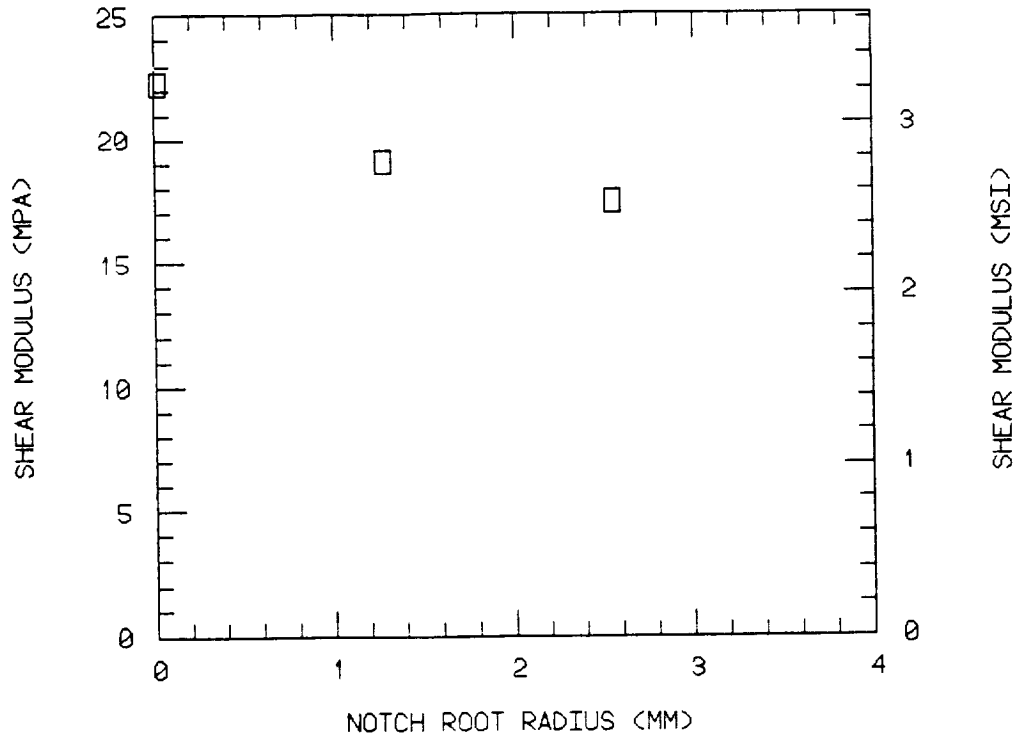

Figure 9. Measured Iosipescu Shear Moduli Versus Notch Root Radius for Quasi-Isotropic Graphite/Epoxy [4].

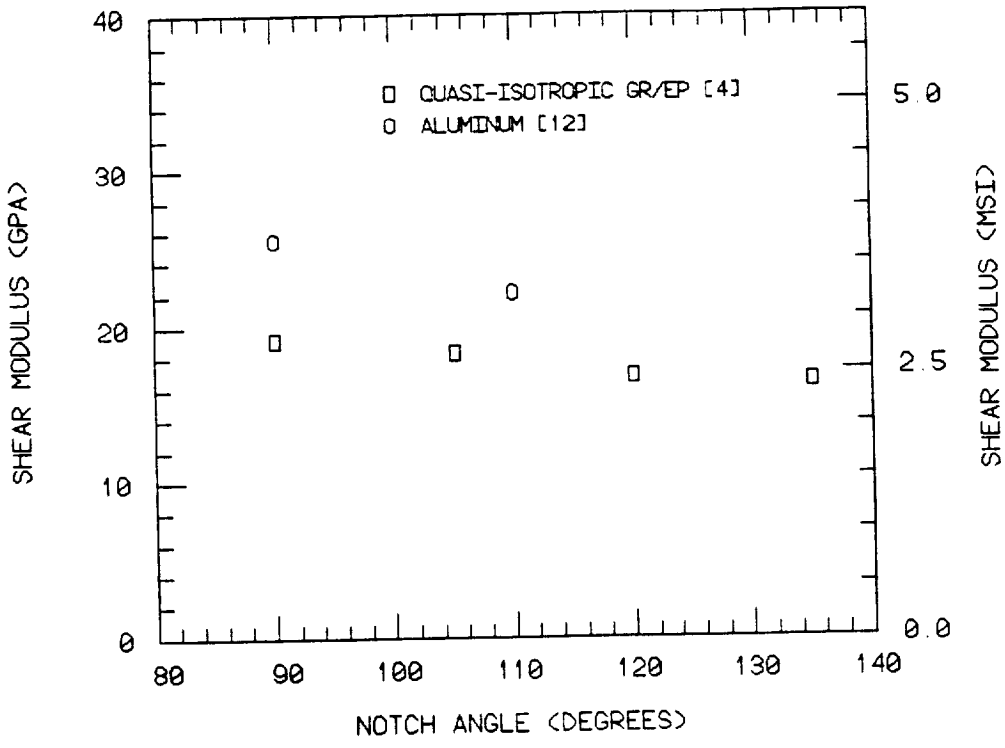

Figure 10. Measured Iosipescu Shear Moduli Versus Notch Angle for Quasi-Isotropic Graphite/Epoxy [4] and Aluminum [12].

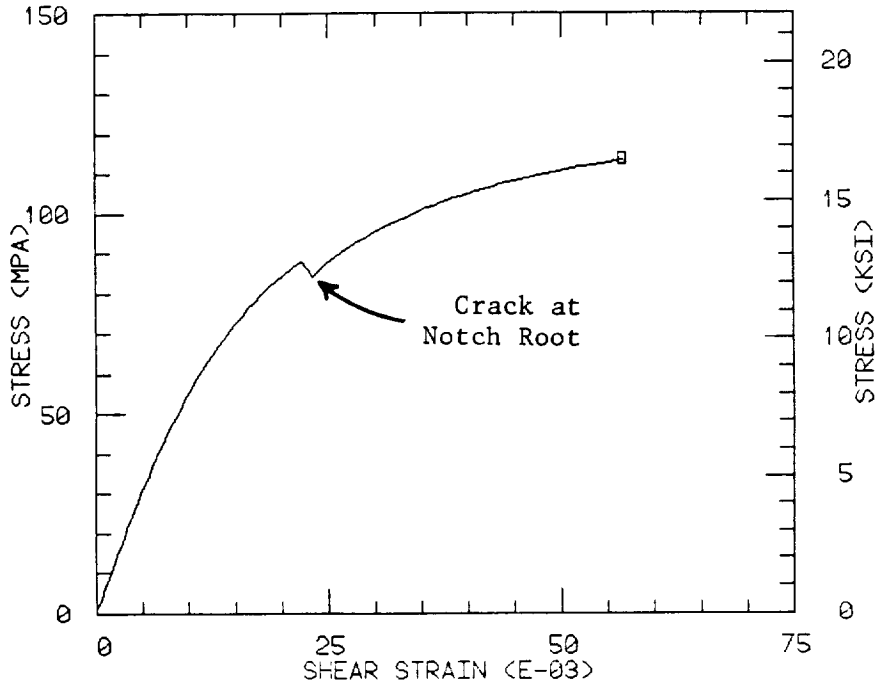

Figure 11. Iosipescu Shear Stress-Strain Plot for a Unidirectional AS4/3501-6 Graphite/Epoxy Specimen.

Figure 12. Dye Enhanced X-Radiograph of a Failed Iosipescu Shear Test Specimen of Unidirectional AS4/3501-6 Graphite/Epoxy.

shear cracking in the region between the notch roots. A dye-enhanced radiograph of one such specimen is shown in Figure 12. The two initial cracks which propagated away from the notch roots are visible. However, ultimate failure was due to cracks forming parallel to the fibers throughout the test region between the notches, as indicated.

Similar cracking was also observed by Swanson, et al., [27] who compared Iosipescu shear and torsion tube shear results for AS4/3501-6 graphite/epoxy. These authors found that shear modulus measurements from each test method agreed with each other to within one percent. Shear strength results did not agree as closely. However, there was a correspondence between failure in the torsion tubes and the stress at which the first notch root crack appeared in the Iosipescu shear tests. For this brittle material system, the onset of first cracking in the torsion test was probably catastrophic. The authors did not report ultimate (maximum) load values achieved during the Iosipescu shear tests. The definition of "shear" failure in fiber reinforced materials can be ambiguous. As deformation increases, fibers may tend to rotate and become stressed in tension. This phenomena is most apparent in tests of composites whose matrix materials have large shear strain-to-failure values. However, for the relatively brittle materials tested by Swanson, et al., and for the graphite fabric/epoxy results of Section 3, the ultimate stress attained during an individual test is probably a better representation of shear strength than the onset of cracking.

2.5 Shear Strain Measurement

There are numerous techniques for measuring shear strains, many of which have been applied to Iosipescu shear test specimens. Optical techniques such as Moire' interferometry or photoelasticity are useful for measuring the full displacement or strain fields within the test specimen, which may be very useful in the study of the test method itself. However, for routine use to measure shear properties for specific materials, the optical methods are cumbersome.

Strain gages oriented at 45° to the line of shear have probably been the most often used shear transducers in Iosipescu shear testing. Strain gages are relatively easy to use, with practice, and are quite reliable under normal test conditions. The common strain gage rosette

used for Iosipescu shear testing at the University of Wyoming consists of two strain gages oriented at ±45°, to the specimen length, as shown in Figure 13. This particular shear gage rosette is approximately 1.57 mm x 2.92 mm (0.062 in x 0.115 in), with two 350 ohm strain gages oriented at ±45° wired in a half bridge configuration. However, strain gages are expensive, and time-consuming to mount. They also may not perform well on organic matrix composites subjected to elevated temperature or wet environments. Finally, the full scale shear strain range is limited.

Prior to the present study, an attempt was made to find an alternative method for measuring shear strains in Iosipescu shear tests. A standard strain gage extensometer was modified to measure the relative (shear) displacement across the shear region [10,12]. This transducer initially appeared to be quite promising as a replacement for strain gages on each individual test specimen. The transducer was primarily used to measure shear strains during Iosipescu shear tests of Sheet Molding Compounds (SMC) materials [10]. However, test results were very sensitive to the manner in which the extensometer was clamped to the test specimen. Sullivan, et al., [3] tried a similar shear strain measurement using a transducer they fabricated, and also reported erratic results. No details of this transducer were provided although presumably it was similar to the one used at Wyoming.

It was demonstrated analytically during the second year of this grant [12] that measurement of the relative displacement across the shear region should provide an accurate representation of the shear strain. The variability in shear strain measurements made with the modified extensometer was thought to be an attachment problem. Therefore, during this present third-year research, a new mechanism for attaching an extensometer was designed, built, and tested. The major objective of this design effort was to provide an easily operated extensometer attachment device that would not be unduly sensitive to the manner in which it was installed by the test operator. As in the previous design, this newer version of a modified extensometer indexes at points on both sides of center in the uniform shear region of the test specimen. One half of the extensometer is attached to the left side of this shear region, and the other half is attached to the right side

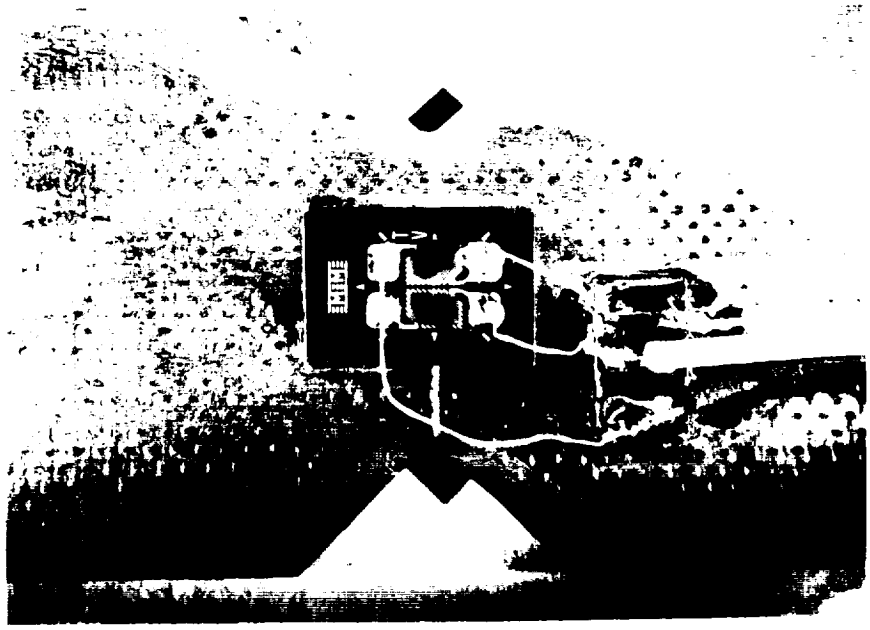

Figure 13. Strain Gage Rosette Bonded to an Iosipescu Shear Specimen of AS4/3501-6 Graphite/Epoxy.

of the shear region. Photographs of this modified extensometer are shown in Figures 14 and 15. In Figure 14 the transducer is shown in its open position, permitting installation of the test specimen. In Figure 15 the transducer is in its use position. Points on the ends of the extensometer arms are held against the front face of the test specimen by a small adjustable compression spring. The extensometer is mounted such that it is free to rotate and vertically translate with the test specimen as necessary.

To test the modified extensometer shear transducer, Iosipescu shear tests were performed during which the modified extensometer and a strain gage rosette were used simultaneously. The modified extensometer was attached to the front face of the test specimen, as shown previously in Figure 15. The strain rosette was bonded to the back face of the test specimen. These Iosipescu shear tests were conducted using test specimens of unidirectional graphite/epoxy, aluminum, and plexiglas, to provide a range of shear stiffnesses. Results for one such test, on an aluminum test specimen, are plotted in Figure 16. As can be seen in Figure 16, the shear stress-shear strain plots for both transducer types are similar in appearance. The modified extensometer provides a shear strain measurement to specimen failure at approximately 15.5 percent shear strain, while the strain gage rosette itself failed at approximately 5.8 percent shear strain, as expected. However, the shear moduli as calculated from the initial slopes of the shear stress-shear strain plots are quite different. The shear modulus measured with the strain gage rosette is 28.7 GPa (4.16 Msi), while the shear modulus measured with the modified extensometer is 17.9 GPa (2.59 Msi), i.e., a factor of 1.6 too low. In fact, the shear moduli measured with the modified extensometer were less than the shear moduli obtained from strain gage data for all tests conducted. Furthermore, the results were quite variable, and an unacceptable amount of hysteresis was present in the measurements.

Variability in the initial tests of the device was thought to be due to slippage between the modified extensometer and the test specimen. Various attachment heads were built for the extensometer. The first configuration used four needle points pressed to the face of the test specimen. Two points were attached to each arm of the extensometer.

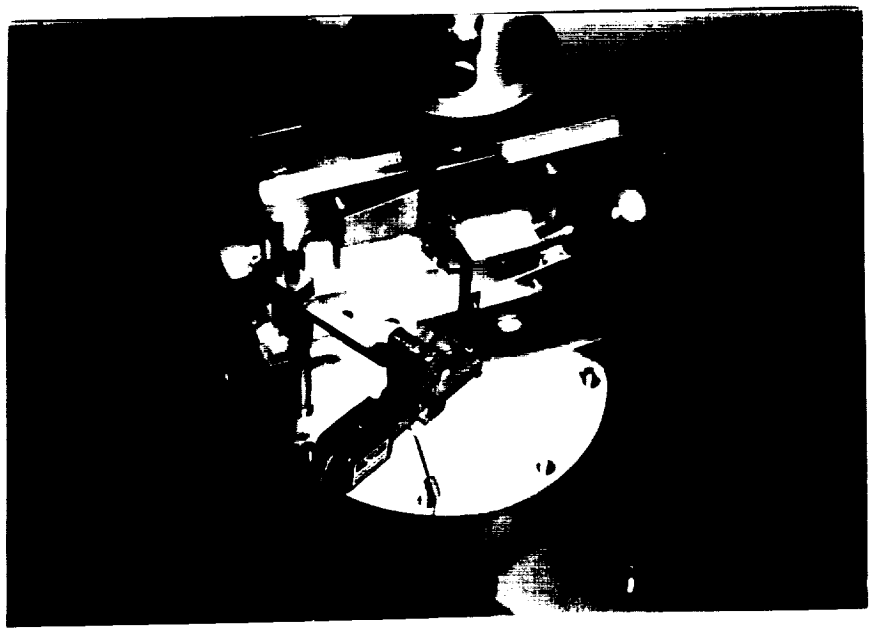

Figure 14. Modified Extensometer Shear Strain Transducer in the Open or Load Position.

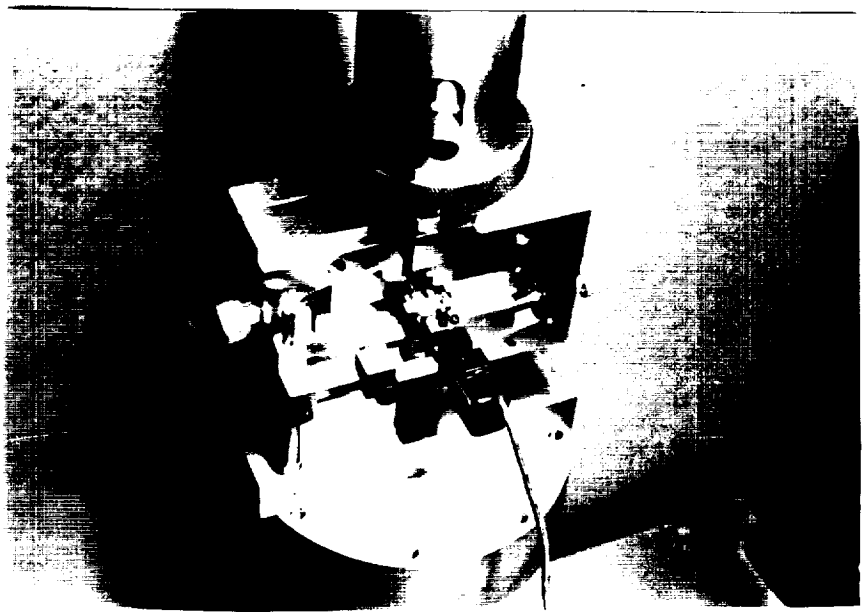

Figure 15. Modified Extensometer Shear Strain Transducer in the Closed or Ready Position.

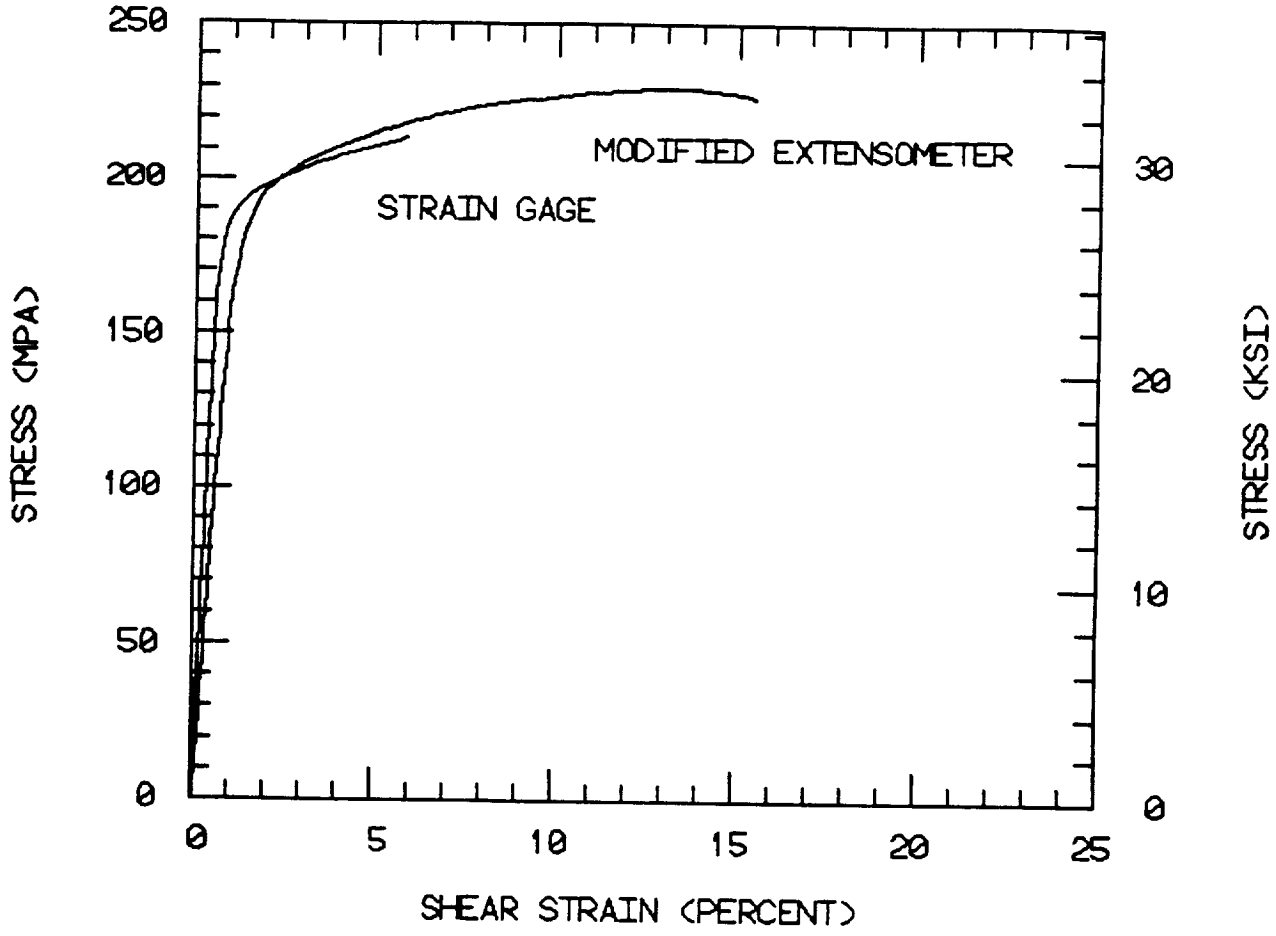

Figure 16. Iosipescu Shear Stress-Strain Plot for an Aluminum Test Specimen Instrumented with a Strain Gage Rosette and the Modified Extensometer Shear Strain Transducer.

specimen surface evenly. Therefore, one point was removed; three points always make even contact. There was some improvement in performance, but slippage between the extensometer and the test specimen still occurred too frequently. Finally, in an effort to improve stability, small knife edges were substituted for the needle points. The knife edges were much more rigid than the needle points, which had a tendency to flex. However, tests with the knife edge contacts produced results similar to those previously obtained. Finally, a series of tests were conducted in which a fast curing adhesive was used to bond the knife edges to the specimen, ensuring they would not slip. Loads were cycled, remaining below the yield strengths of the test specimens. Considerable hysteresis still occurred in the modified extensometer shear strain data. However, this hysteresis was not present in the strain gage rosette data. Furthermore, variations of 15 percent or more were still present in the modified extensometer strain data between successive loading cycles on the same test specimen. Virtually no variation was present in the strain gage data.

Reasons for the data variability and hysteresis are not presently understood. Perhaps some unrecognized restraint in the device is causing an extraneous bending or twisting of the extensometer resulting in false readings. Even though slippage was eliminated as a possible cause by bonding the knife edges to the specimen, there were still variations in successive loadings of the same test specimen.

An alternative method of measuring shear strains with an extensometer is to measure the extension along a line at 45° to the shear region, as is done with the shear rosette shown previously in Figure 13. A test region of reasonable size could be monitored, e.g., 1.5 mm (0.06 in) square. This is approximately the size of the shear strain rosette currently used. For a shear strain γ of 0.05, the magnitude of the normal strain at 45° to the shear line of action is

$$|\epsilon| = \frac{\gamma}{2} = 0.025$$

assuming the two normal strains as measured by a strain gage rosette are of equal magnitude, differing only in sign. The measurable extension along the 45° line is the strain times the length of the line, viz.,

0.054 mm (0.0021 in). The relative shear displacement measured across the shear region by the modified extensometer tested during the present program is the shear strain times the length of the side of the square area monitored. Thus, the displacement measured with the present modified extensometer is 0.076 mm (0.003 in), which is slightly larger than the 45° diagonal displacement, but of the same order of magnitude. Both displacements are small, pushing the resolution capabilities of conventional strain gage extensometers.

Theoretically it should be possible to calculate the shear strain from extension measurements along just one 45° diagonal. But it has been noted by the present authors that strains measured at ±45° often differ from each other. However, while there may be significant variations in magnitude between the +45° normal strain and the -45° normal strain, the computed shear strains are quite consistent from test to test. The variations between +45° and -45° normal strain readings might be caused by a very small misalignment of the strain rosette, or small load introduced components of normal strain. For consistent shear strain measurement, normal strains should thus be measured at both +45° and -45° to the line of shear. From a practical standpoint, this may be difficult to do with an extensometer, even a biaxial extensometer.

At this point, use of the modified extensometer still cannot be recommended. Further study of shear strain measurement techniques is planned, including examination of other potential sensors. In the meantime, strain gage rosettes are available as an accurate, proven technique for measuring shear strains during an Iosipescu shear test. As was just discussed, it is recommended that two-element strain rosettes be used to measure strains on both the +45° and the -45° diagonal lines rather than using a single strain gage on just one diagonal.

2.6 Summary Remarks

Agreement has been shown to exist between the finite element analyses performed as part of this grant and analyses conducted by other investigators. Furthermore, these analyses correctly predict trends in shear modulus as a function of notch geometry variations, as verified by recent experimental shear measurements. Data from these analyses were used to guide the Iosipescu shear test fixture design particularly in

positioning the inner loading points. The analyses have also demonstrated that the stress state obtained with an Iosipescu shear test specimen is truly pure shear in the test region, and that the test is a viable method of measuring both shear strength and shear modulus of isotropic and anisotropic materials.

Considerable effort has gone into the study of this test method by the present authors as well as by other investigators in the composites community. Arguments have often been focused on detailed comparisons between notch geometries, or differences in stress states between Iosipescu and AFPB loading configurations. While these examinations are of course important, they must not overshadow the basic utility of the test method. It has been clearly demonstrated that reliable engineering data for shear properties of materials can be measured. Test specimens are easily prepared and can be tested using equipment commonly available in mechanical testing laboratories. Whether one particular fixture is more or less useful depends greatly on the number and type of specimens to be tested and the availability of test material. In an evaluation of shear test methods conducted by Lee and Munro using a decision analysis technique [12], they concluded that overall, the Iosipescu shear test method was the most practical technique currently available for testing composite materials.

SECTION 3
GRAPHITE FABRIC/EPOXY SHEAR PROPERTIES

3.1 Materials and Specimens

A major objective of this third-year grant was to generate in-plane and interlaminar shear properties of four graphite fabric/epoxy composite materials. Ten different laminated panels were fabricated by NASA-Langley, portions of which were sent to the University of Wyoming for shear properties characterization. All shear test specimens were machined at the University of Wyoming. Material data, including weave geometry, ply orientations, and fiber volumes are summarized in Table 1, this information being taken from Reference [28]. The constituent materials consisted of Union Carbide T300 graphite fiber and Fiberite 934 epoxy resin. The graphite yarn was woven into four different fabrics, viz., an Oxford weave, a 5-harness satin weave, an 8-harness satin weave, and a plain weave with auxiliary warp yarns.

The Oxford, 5-harness, and 8-harness fabrics were laid up as orthogonal panels of two different thicknesses, consisting of 8 and 16 plies of fabric and as 24-ply quasi-isotropic laminates. The warp direction of the fabric was assumed to be the principal (0°) material direction and was therefore designated as the 1-axis. The fill direction was designated as the 2-axis with the 3-axis perpendicular to the plane of the fabric. Thus an in-plane shear loading, designated as τ_{12}, represents a shear loading in a plane perpendicular to the warp or 1-direction, parallel to the fill or 2-direction. For the quasi-isotropic panels, the 1-direction was assumed to correspond to the axial or x-direction of the panel, parallel to the warp direction of the 0° plies.

The 8-ply panels were nominally 2.0 mm (0.08 in.) thick, and tested in in-plane (τ_{12} and τ_{21}) shear loadings only. The 16-ply panels were nominally 4.1 mm (0.16 in.) thick. Both in-plane (τ_{12} and τ_{21}) and interlaminar (τ_{13} and τ_{23}) shear tests were performed on these panels. In order to achieve a sufficient thickness of material from which interlaminar test specimens could be cut, three layers of these 16-ply panels were bonded together in the manner discussed in Appendix A. Thus, the overall height (width) of these interlaminar shear test specimens

TABLE 1

PANEL PARAMETERS FOR T300*/934 GRAPHITE FABRIC/EPOXY LAMINATES [28]

Fabric Weave Pattern	Panel No.	Layup Orientation	No. of Fabric Plies	Fiber Volume Percent
Oxford HMF 2319/34**	1	Orthogonal	8	64.5
	2	Orthogonal	16	59.4
	3	Quasi-Isotropic	24	63.3
5-Harness Satin HMF 371/34**	4	Orthogonal	8	64.2
	5	Orthogonal	16	63.7
	6	Quasi-Isotropic	24	66.9
8-Harness Satin HMF 2320/34**	7	Orthogonal	8	64.6
	8	Orthogonal	16	63.0
	9	Quasi-Isotropic	24	65.6
Plain Weave Auxiliary Warp	18	Orthogonal	12	53.5

*Designation of Union Carbide Corporation
**Designation of Fiberite Corporation

was nominally 13 mm (0.5 in). Further discussion of Iosipescu interlaminar shear test specimen preparation is included in Appendix A.

The 24-ply quasi-isotropic panels were nominally 6.4 mm (0.25 in) thick. In-plane (τ_{12} and τ_{21}) as well as interlaminar (τ_{13} and τ_{23}) shear tests were conducted on these laminates. As the thicknesses of these panels were sufficient, only a single laminate thickness was used for interlaminar shear test specimen preparation. No stacking and bonding of layers was done to fabricate the quasi-isotropic interlaminar shear test specimens.

The auxiliary warp fabric was nominally an 18x18 (18 yarns/inch) plain weave fabric, with three additional warp yarns per inch added on 5 mm (0.2 in.) spacings. These additional yarns produced ridges in the fabric which mesh with those in adjacent fabric plies when the multiple-ply orthogonal lay up panels are fabricated. It was hoped that this meshing would increase the interlaminar toughness as well as the interlaminar shear strength of the composite material due to a mechanical locking effect. Polished cross sections of the auxiliary warp panel are shown in Figure 17. Figure 17a shows a view perpendicular to the warp direction. The nested warp fiber ridges should be visible in this view. However, no regularly repeating nested ridges appeared in any of the examined specimens, typified by Figure 17a. A cross-sectional view perpendicular to the fill yarns is shown in Figure 17b. This confused appearing structure was typical of the fill direction cross sections examined. It is difficult to see a regular appearing nested ridge structure in Figure 17. A different viewing technique may be necessary. Both in-plane and interlaminar shear tests were conducted on this nominally 7.1 mm (0.28 in) thick panel. Interlaminar shear specimens from this panel consisted of a single laminate thickness.

All in-plane (τ_{12} or τ_{21}) test specimens were 76 mm (3 in) long and 19 mm (0.75 in) wide, with thicknesses equal to the panel thicknesses. For the interlaminar (τ_{13} or τ_{23}) shear tests, the height dimension of the specimen was dictated by the thickness of the panel from which the specimen was cut, consisting of three bonded layers of Panel Numbers 2, 5 and 8, and single layers of Panel Numbers 3, 6, 9, and 18. For all specimens, both in-plane and interlaminar, 90° notches were ground to a depth equal to 22 percent of the overall specimen height. Notch root

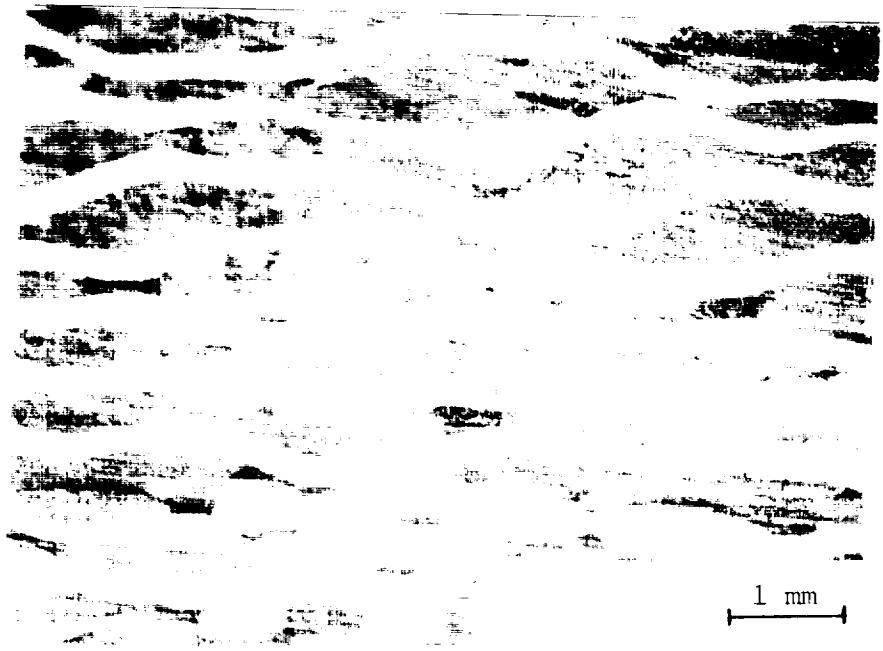

a) Plane Perpendicular to the Warp Direction.

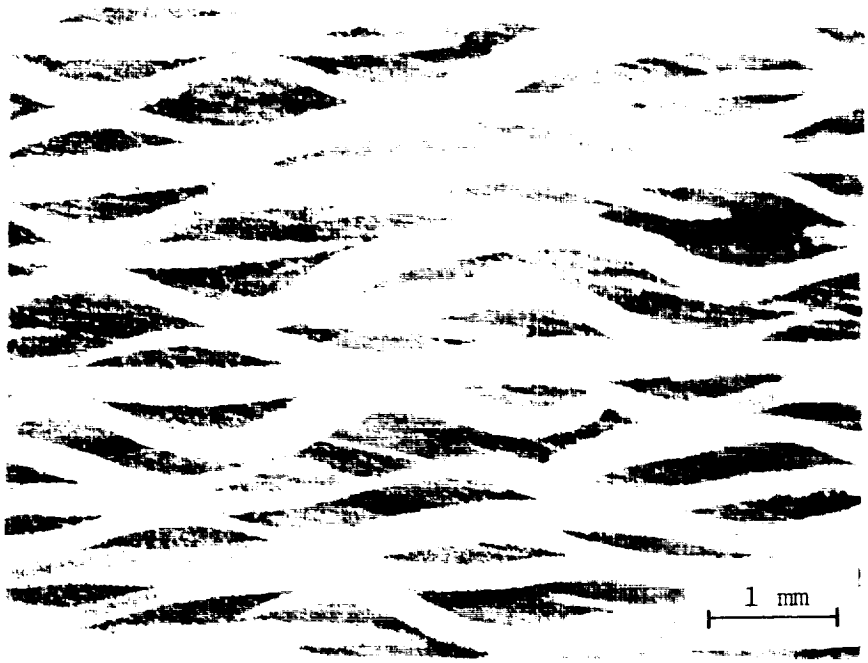

b) Plane Perpendicular to the Fill Direction.

Figure 17. Polished Cross Sections of the Auxiliary Warp Material, Panel 18.

radii were approximately 1.3 mm (0.05 in). All specimens were instrumented with a two-gage shear rosette, Micro-Measurements EA06-062-350, as previously shown in Figure 13.

3.2 In-plane Shear Test Results

Average in-plane (τ_{12} or τ_{21}) shear strengths and shear moduli for all ten panels tested during this third-year effort are listed in Table 2. Each value in Table 2 represents average results from at least three, and more typically five, shear test specimens. Individual shear strengths and shear moduli from each test are listed in Appendix B. Shear stress versus shear strain and shear stress versus fixture displacement plots for each group of tests are also included in Appendix B.

As was previously discussed in Section 2 of this report, the definition of shear failure may become somewhat ambiguous when measuring shear properties of fiber reinforced materials. During the second year of this research grant, shear strengths were defined as the stress value at which the slope of the stress-strain plot abruptly decreased, as opposed to a strength based on ultimate load. In an effort to minimize ambiguity, shear strength values reported in this document were calculated from the maximum load attained during the test. In order to compare these third-year shear strength results with those strengths obtained during the second year of the grant, strength values from the preceding year shear testing are also included in Table 2. In order to make comparisons meaningful, the shear strengths from the previous year were recalculated based on maximum load attained. Thus the values reported here in Table 2 for in-plane shear strengths from the previous year tend to be higher than those reported in Reference [12]. However, the difference is small, less than 10 percent in most cases.

In-plane shear test results reported in Table 2 are grouped by weave geometry. Thus, one can compare the effect of weave geometry on shear performance of the orthogonal layup material. The in-plane shear strengths and shear moduli of the quasi-isotropic panels are also listed in Table 2. In-plane shear strengths and shear moduli for these quasi-isotropic laminates, Panel Numbers 3, 6, and 9, tend to be much greater than comparable values for the orthogonal layup panels. This

TABLE 2

AVERAGE IN-PLANE IOSIPESCU SHEAR STRENGTHS AND SHEAR MODULI FOR T300/934 GRAPHITE FABRIC/EPOXY COMPOSITES

Fabric Weave Pattern	Panel No.	Test Orientation	Strength (MPa)	Strength (ksi)	Modulus (GPa)	Modulus (Msi)
Oxford	1	12	110	15.9	5.6	0.81
		21	111	16.1	5.7	0.83
	2	12	120	17.4	5.0	0.72
		21	114	16.5	5.0	0.72
	Previous Year [12]*	12	108	15.7	4.5	0.65
		21	112	16.2	5.0	0.72
	3	12	244	35.3	14.0	2.03
		21	231	33.5	14.0	2.04
5-Harness	4	12	117	16.9	5.5	0.80
		21	131	19.0	5.4	0.78
	5	12	129	18.7	5.0	0.73
		21	132	19.2	5.0	0.73
	Previous Year [12]*	12	122	17.7	5.7	0.83
		21	129	18.7	5.4	0.78
	6	12	252	36.5	13.9	2.01
		21	246	35.7	14.3	2.08
8-Harness	7	12	121	17.5	5.5	0.79
		21	132	19.1	5.6	0.81
	8	12	146	21.2	5.1	0.75
		21	137	19.8	5.3	0.76
	Previous Year [12]*	12	141	20.5	5.3	0.77
		21	138	20.1	5.2	0.76
	9	12	266	38.6	14.7	2.13
		21	252	36.7	15.1	2.19
Auxiliary Warp	18	12	117	16.9	3.9	0.56
		21	102	14.9	3.4	0.50

*Strength values from [12] have been recalculated, based on maximum load attained.

was, of course, expected due to the presence of fibers oriented at ±45° to the shear stress direction.

In order to more easily visualize these data for comparative purposes, the average in-plane shear strengths and shear moduli for all panels are plotted in Figures 18 through 21. Average in-plane shear strengths for the orthogonal panels are plotted in Figure 18, with the corresponding shear modulus values plotted in Figure 19. Average in-plane shear strengths and shear moduli for the quasi-isotropic laminates are plotted in Figures 20 and 21, respectively. Values are grouped by panel number, which are listed on the abscissas of the plots.

As can be seen in Figure 18, for any particular panel the in-plane (τ_{12} and τ_{21}) shear strengths are nearly equal, as would be expected. The τ_{12} shear strength for Oxford weave Panel Number 1 is 110 MPa (15.9 ksi) while the τ_{21} shear strength for the same panel is 111 MPa (16.1 ksi). The largest in-plane shear strength difference was noted for Panel Number 18, the auxiliary warp fabric, which had an average τ_{12} shear strength of 117 MPa (16.9 ksi) and a τ_{21} shear strength of 102 MPa (14.9 ksi), a difference of approximately 12 percent. Theoretical considerations would dictate that due to the symmetry of the stress tensor the values should be equal. The 12 percent difference was not too severe given variations between results from the individual tests (see Table B10).

Similar comparisons may be made for the shear moduli values plotted in Figure 19. Again, the G_{12} and G_{21} values for any given laminate are very similar. Average G_{12} and G_{21} values for the Oxford weave Panel Number 2 were identical at 5.0 GPa (0.72 Msi). The G_{12} and G_{21} shear moduli for 5-harness satin weave Panel Number 5 are also identical. None of the G_{12} in-plane shear modulus values measured during this present year of the grant differed from the corresponding G_{21} shear modulus values for the same laminate by more than 3 percent.

Greater variations are present in data from the previous year of testing. This variability in the averaged data stems from larger variations in the individual specimen data [12]. Overall, the shear strengths and shear moduli plotted in Figures 18 and 19 and listed in Table 2 are consistent in that the τ_{12} and τ_{21} shear properties for a

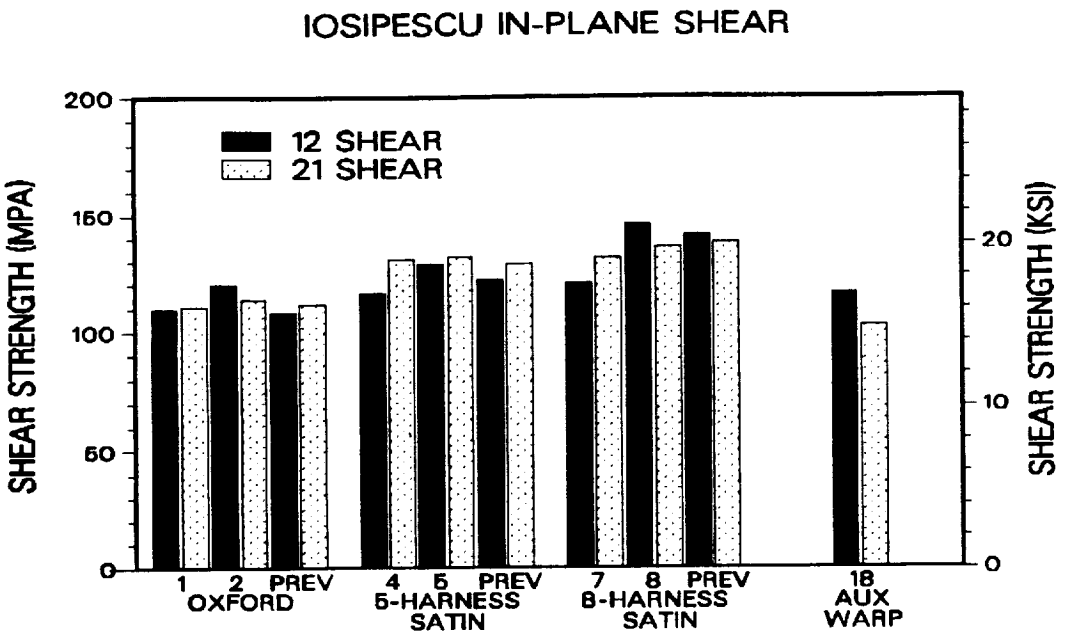

Figure 18. Average In-plane Iosipescu Shear Strengths for Orthogonal Layup T300/934 Graphite Fabric/Epoxy Laminates.

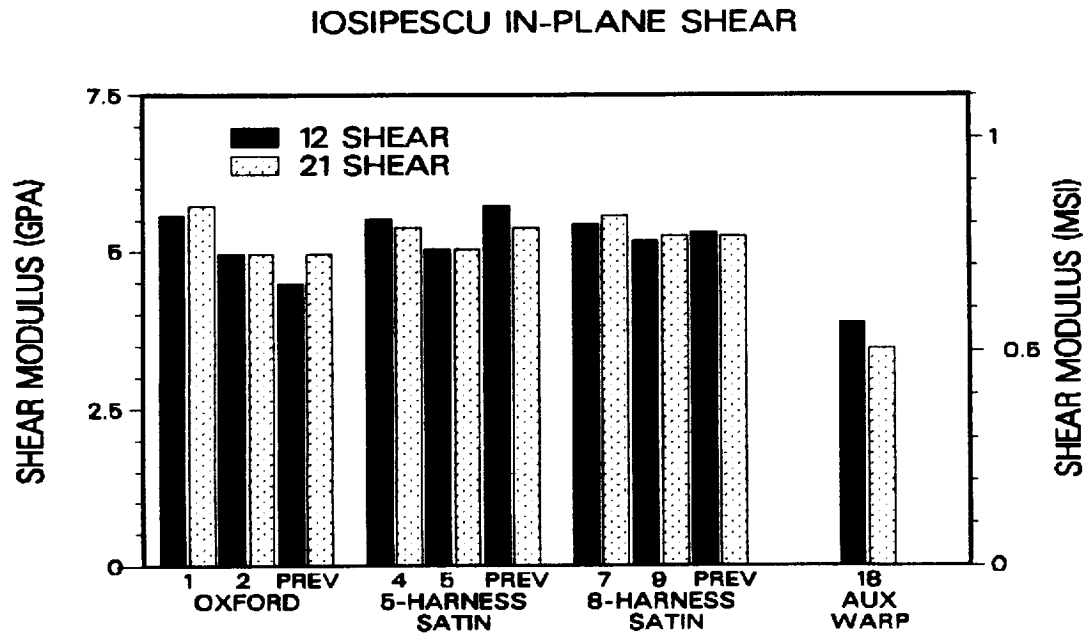

Figure 19. Average In-plane Iosipescu Shear Moduli for Orthogonal Layup T300/934 Graphite Fabric/Epoxy Laminates.

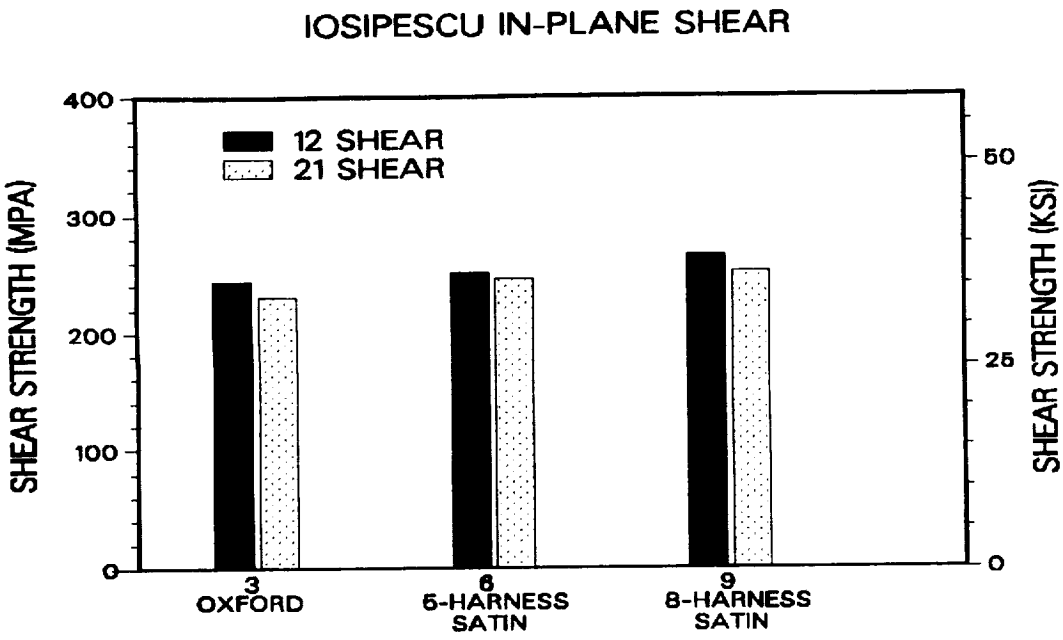

Figure 20. Average In-plane Iosipescu Shear Strengths for Quasi-isotropic Layup T300/934 Graphite Fabric/Epoxy Laminates.

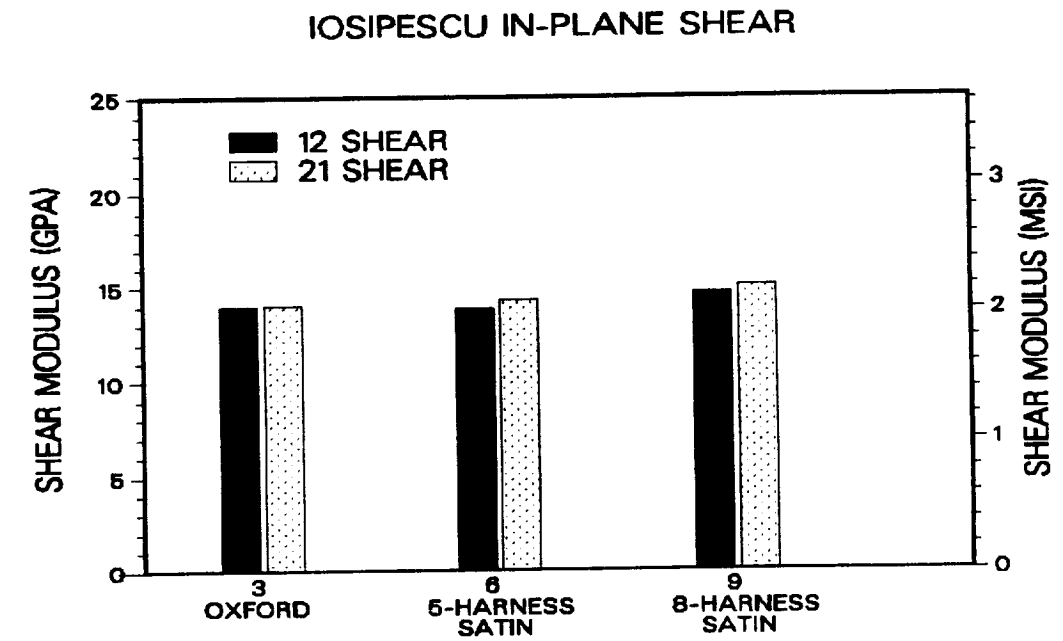

Figure 21. Average In-plane Iosipescu Shear Moduli for Quasi-isotropic Layup T300/934 Graphite Fabric/Epoxy Laminates.

given laminate are virtually equal, within the scatter of individual specimen measurements.

Observations similar to those made for the orthogonal layup panels are also valid for the in-plane shear strengths and shear moduli of the quasi-isotropic laminates plotted in Figures 20 and 21, respectively. The average τ_{12} shear strength of the 5-harness satin weave Panel Number 6 is 252 MPa (36.5 ksi) and the corresponding τ_{21} shear strength for the same laminate is 246 MPa (35.7 ksi), a difference of only 6 percent. The shear strength percent differences for Panel Numbers 3 and 9 are even less. Shear modulus symmetry is also apparent for these three quasi-isotropic laminates, as plotted in Figure 21 and listed in Table 2.

Other shear property comparisons can be made from Figures 18 through 21 for panels of the same weave geometry. Only minor differences in average shear strength exist among the Oxford weave orthogonal layup Panel Numbers 1 and 2 and similar data from the previous year. The average in-plane shear strength of all the orthogonal Oxford weave material is 112 MPa (16.3 ksi). The maximum average measured in-plane strength is 120 MPa (17.4 ksi) and the minimum average measured in-plane shear strength is 108 MPa (15.7 ksi).

Average in-plane shear modulus values for the Oxford weave material, plotted in Figure 19, are somewhat more scattered than the corresponding shear strength numbers. Even so, the average shear modulus values for the Oxford weave material are similar among the different panels. The average in-plane shear modulus of all the orthogonal Oxford weave material is 5.1 GPa (0.74 Msi). The maximum average measured in-plane shear modulus is 5.6 GPa (0.81 Msi) and the minimum is 4.5 GPa (0.65 Msi), as listed in Table 2.

The shear property data for the 5-harness satin and 8-harness weave materials exhibit similar behavior. The mean in-plane shear strength of the 5-harness satin weave material is 127 MPa (18.4 ksi) and the mean in-plane shear modulus is 5.3 GPa (0.77 Msi). The mean shear strength for the 8-harness satin weave material is 136 MPa (19.7 ksi); the mean shear modulus is 5.3 GPa (0.77 Msi).

Comparing the in-plane shear properties among the four different weave geometries, it is obvious in Figures 18 and 19 that the Oxford, 5-harness, and 8-harness fabric composites are very similar. A slight

increase in in-plane shear strength in going from Oxford weave to 5-harness to 8-harness satin weave fabrics is indicated. The average in-plane shear modulus values for the Oxford, 5-harness satin, and 8-harness satin weave fabrics are approximately equal. The in-plane shear strengths for the quasi-isotropic laminates, plotted in Figure 20, also increase slightly in going from Oxford to 5-harness to 8-harness satin weave geometries. The in-plane shear moduli for the quasi-isotropic laminates plotted in Figure 21 are about equal.

The plain weave auxiliary warp material (Panel Number 18) is obviously weaker and less stiff in in-plane shear than the other three fabrics. The average in-plane shear strength of Panel Number 18 is 110 MPa (15.9 ksi) and the average in-plane shear modulus is 3.7 GPa (0.53 Msi). One possible explanation for these lower shear properties could be due to the lower fiber volume, viz., 53.5 percent as indicated in Table 1. The other laminates tested during this third-year effort all had fiber volumes near or greater than 60 percent. However, the fiber volumes of laminates tested during the previous year were between 54.8 and 56.7 percent [12]. These slightly lower fiber volumes of the previous year laminates did not appear to degrade the in-plane shear properties of the Oxford, 5-harness, or 8-harness satin weave materials compared to the data measured for higher fiber volume laminates this present year. The lower in-plane shear properties of the auxiliary warp material are more likely related to the weave geometry. The tighter plain weave pattern may have degraded the performance of the graphite yarns.

3.3 Interlaminar Shear Test Results

Average interlaminar (τ_{13} and τ_{23}) shear test results are listed in Table 3 and plotted in Figures 22 and 23. Individual test results as well as shear stress-shear strain and stress-displacement plots are included in Appendix B. Interlaminar shear strengths were calculated from ultimate loads. Results from the previous year of testing [12] are repeated in this report. Interlaminar shear strengths listed for the previous year's testing have been recalculated, based on ultimate load rather than the first abrupt slope change in the stress strain plot.

TABLE 3

AVERAGE INTERLAMINAR IOSIPESCU SHEAR STRENGTHS AND SHEAR MODULI FOR T300/934 GRAPHITE FABRIC/EPOXY COMPOSITES

Fabric Weave Pattern	Panel No.	Test Orientation	Strength (MPa)	Strength (ksi)	Modulus (GPa)	Modulus (Msi)
Oxford	2	13	76	11.0	4.7	0.68
		23	74	10.6	3.9	0.57
	3	13	61	8.9	3.9	0.57
		23	57	8.3	3.6	0.52
	Previous Year [12]*	13	57	8.3	3.4	0.49
		23	49	7.1	4.6	0.67
5-Harness	5	13	75	10.9	4.2	0.61
		23	75	10.9	3.8	0.55
	6	13	59	8.5	4.0	0.58
		23	59	8.5	3.5	0.51
	Previous Year [12]*	13	56	8.1	3.5	0.51
		23	55	7.9	3.4	0.49
8-Harness	8	13	76	11.0	3.4	0.49
		23	71	10.2	3.5	0.50
	9	13	63	9.1	3.9	0.57
		23	56	8.1	3.7	0.53
	Previous Year [12]*	13	57	8.3	2.8	0.40
		23	50	7.3	3.6	0.52
Auxiliary Warp	18	13	63	9.1	4.4	0.64
		23	38	5.5	3.1	0.45

*Strength values from [12] have been recalculated, based on maximum load attained.

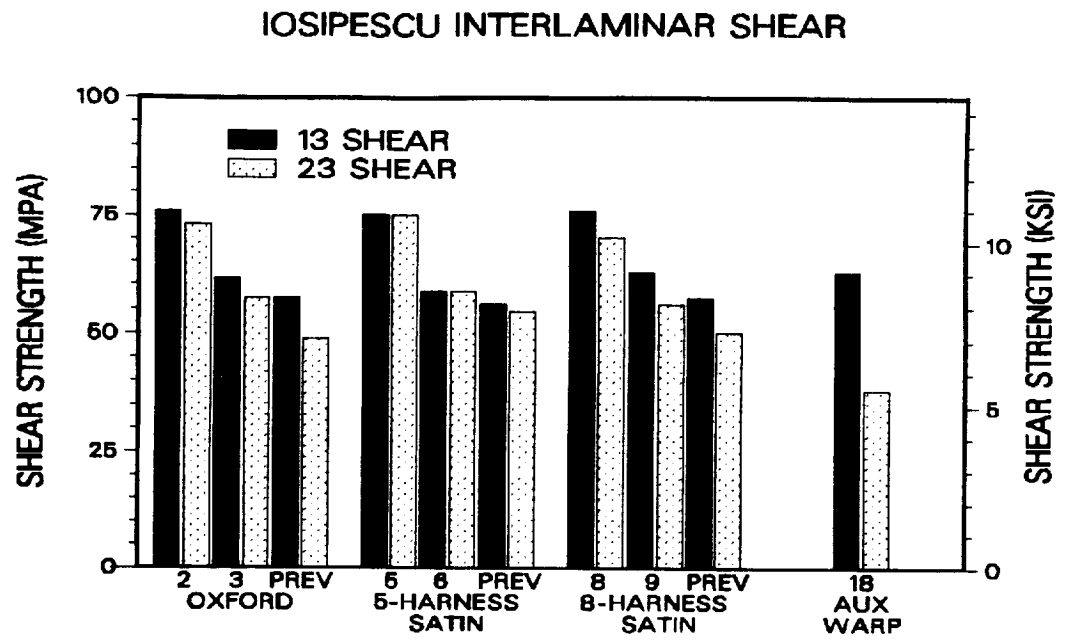

Figure 22. Average Interlaminar Iosipescu Shear Strengths for T300/934 Graphite Fabric/Epoxy Laminates.

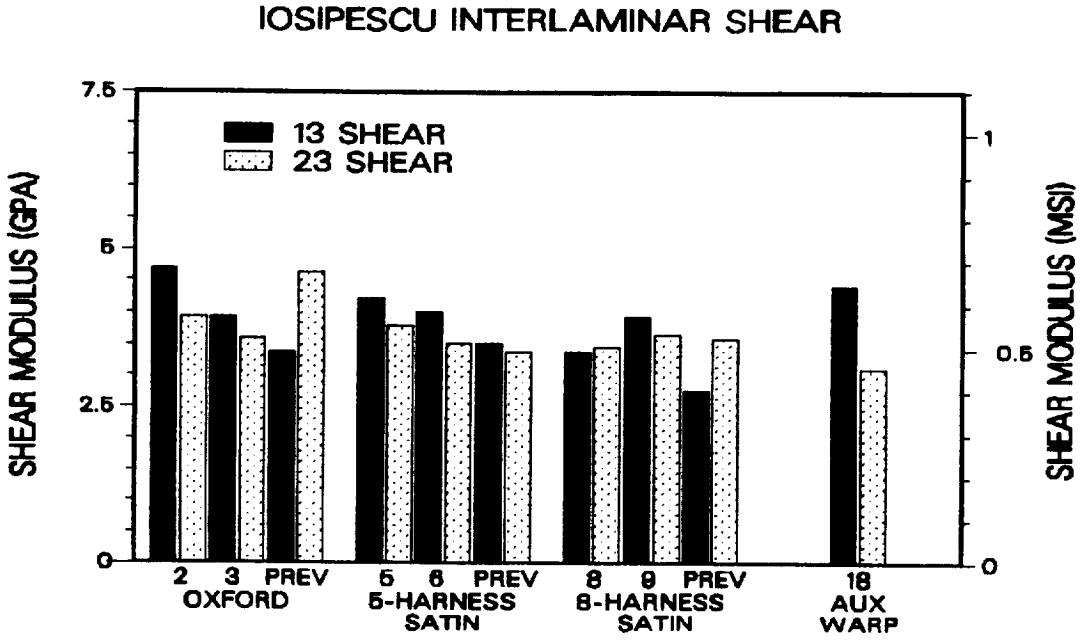

Figure 23. Average Interlaminar Iosipescu Shear Moduli for T300/934 Graphite Fabric/Epoxy Laminates.

Thus the interlaminar shear strength values listed in Table 3 and plotted in Figure 22 are all calculated in a consistent manner.

Shear stress symmetry would dictate that τ_{13} and τ_{31} shear response be equal. Similarly, the τ_{23} and τ_{32} shear behavior should also be equal. There need not be similarity between τ_{13} and τ_{23} shear response. Indeed, significant interlaminar shear differences should be expected for the auxiliary warp panel, where the mechanical locking effect of the nested auxiliary warp yarns are directionally dependent.

Overall, the Oxford, 5-harness, and 8-harness weave interlaminar shear properties did not significantly differ between the τ_{13} and τ_{23} shear planes for an individual laminate. However, in comparing the shear properties plotted in Figures 22 and 23 for panels of different ply orientations, it can be seen that the orthogonal layup panels of the Oxford, 5-harness, and 8-harness weave materials, Panel Numbers 2, 5, and 8, respectively, were consistently stronger and stiffer under interlaminar shear loading than were the quasi-isotropic laminates, Panel Numbers 3, 6, and 9. Interlaminar shear properties measured during the previous year appeared to be even lower. Interlaminar shear properties may have been lower for the quasi-isotropic panels due to the difference in the way the individual plies nested together during laminate fabrication. It is possible that the ±45° plies and the 0°/90° plies were separated by more matrix materials, producing an interlaminar interface which was weaker than the interface between two orthogonal layup plies. The orthogonal layup Panel Numbers 2, 5, and 8 were consistently stronger than the quasi-isotropic Panel Numbers 3, 6, and 9.

Interlaminar shear properties measured during the previous year were consistently lower than the corresponding shear properties measured during this present year for Panels 2, 5, and 8. Interlaminar Iosipescu shear test specimens of orthogonal laminates for both years consisted of materials layers bonded together to achieve a desired thickness. The test procedures and instrumentation were identical. However, two differences between the orthogonal layup tests of this present year and those of the previous year did exist. First, the panels of the previous year had lower fiber volumes, viz., 55 to 57 percent [12], as compared to the 60 to 69 percent fiber volumes of Panel Numbers 2, 5, and 8

listed in Table 1. The lower fiber volumes of panels tested during the previous year may have influenced the measured interlaminar shear response. A second difference between specimens from the previous year and the present interlaminar shear specimens was that the previous year's shear tests were performed with 110° notch angles, while shear tests performed during the present year were conducted using 90° notch angles. However, this same difference in notch angle was also present for the in-plane shear results plotted in Figures 18 and 19, where no significant difference was observed between the previous year's data and that from the present year. It would appear that the differences in fiber volumes were probably the more significant effect in explaining interlaminar shear property variations. However, fiber volume variations did not appear to affect in-plane shear properties as was discussed earlier. Panels exhibiting lower fiber volumes may have contained slightly thicker interlaminar resin rich regions or slightly degraded interlaminar bonds. Thus the interlaminar shear properties were lower for panels with lower fiber volumes. In-plane shear properties were affected to a much lesser degree as the in-plane shear response is less dependent on the interlaminar region.

A final comparison between fabric types can be made for the interlaminar shear data of Figures 22 and 23. Again, little significant difference in interlaminar shear strength or shear modulus exists among the Oxford, 5-harness, and 8-harness weave materials. The τ_{13} interlaminar shear properties of the auxiliary warp material also compares quite favorably with the shear properties of the other three fabric laminates. However, the τ_{23} interlaminar shear properties of the auxiliary warp material are significantly lower than for the other three weave geometries.

3.4 In-plane and Interlaminar Shear Failure Modes

In-plane shear failures in the orthogonal layup Oxford weave panels occur both parallel and perpendicular to the warp direction. Fine networks of cracks parallel to both the 1 (warp) and 2 (fill) directions are apparent in both the τ_{12} and τ_{21} orthogonal layup Oxford weave test specimens, as shown in Figure 24. The failures shown in Figure 24 are

typical of the in-plane shear failures for the Oxford weave specimens from Panel Numbers 1 and 2.

In-plane shear failures in the orthogonal layup 5-harness satin weave material occur in a direction perpendicular to the warp yarns and parallel to the fill yarns, as can be seen in Figure 25. In Figure 25a, a failed τ_{12} shear test specimen, the primary failure mode is parallel to a line between the notch roots. Thus, the cracks are parallel to the loading direction. The vertical cracks shown in Figure 25a are parallel to the 2 or fill direction of the fabric. Cracks in the τ_{21} shear specimen, depicted in Figure 25b are perpendicular to a line between the notches, perpendicular to the τ_{21} plane. Thus, the horizontal cracks in Figure 25b are also perpendicular to the 1 (warp) and parallel to the 2 (fill) directions. The orthogonal layup 5-harness satin weave materials, Panel Numbers 4 and 5, all have this preferred in-plane shear failure mode parallel to the 2 or fill direction. It will be noted in Figure 25, however, that there are also cracks propagating perpendicular to the fill direction, parallel to the warp fibers.

In-plane shear failures for the orthogonal layup 8-harness satin weave materials were similar to those of the 5-harness satin weave material as shown in Figure 26. Again the dominant cracking occurs parallel to the 2 or fill direction, i.e., vertical cracks in Figure 26a and horizontal cracks in Figure 26b. However, shear cracks parallel to the warp direction are also present in both Figures 26a and 26b, similar to those shown in Figure 25.

Failure modes in the quasi-isotropic laminates were similar for all three weave geometries, viz., the Oxford, 5-harness, and 8-harness weave fabric laminates. In these test specimens, the outer 45° ply tended to buckle outward due to compression loading parallel to either its warp or fill yarns. Failures representative of all quasi-isotropic in-plane shear test specimens are shown in Figure 27. This outward buckling usually caused the strain gage to fail, followed quickly by total failure of the test specimen. Failures for the Oxford weave quasi-isotropic Panel Number 3 are shown in Figure 27. In-plane shear failures in the 5-harness and 8-harness satin weave quasi-isotropic laminates, Panel Numbers 6 and 9, were very similar.

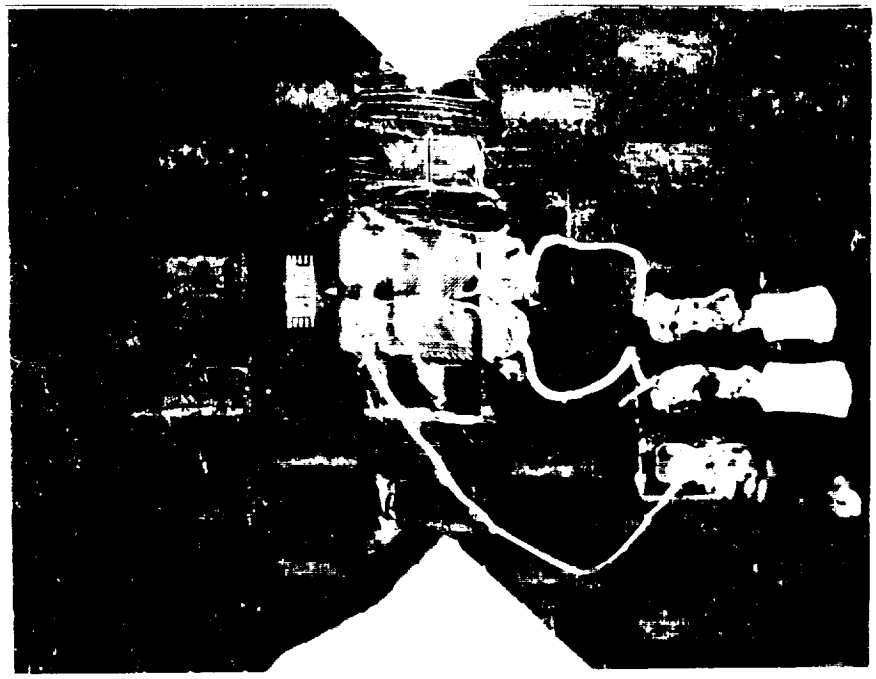

a) In-plane (12) Shear Test.

b) In-plane (21) Shear Test.

Figure 24. Typical Failures of In-plane Iosipescu Shear Test Specimens of Orthogonal Layup Oxford Weave T300/934 Graphite Fabric/Epoxy Laminates.

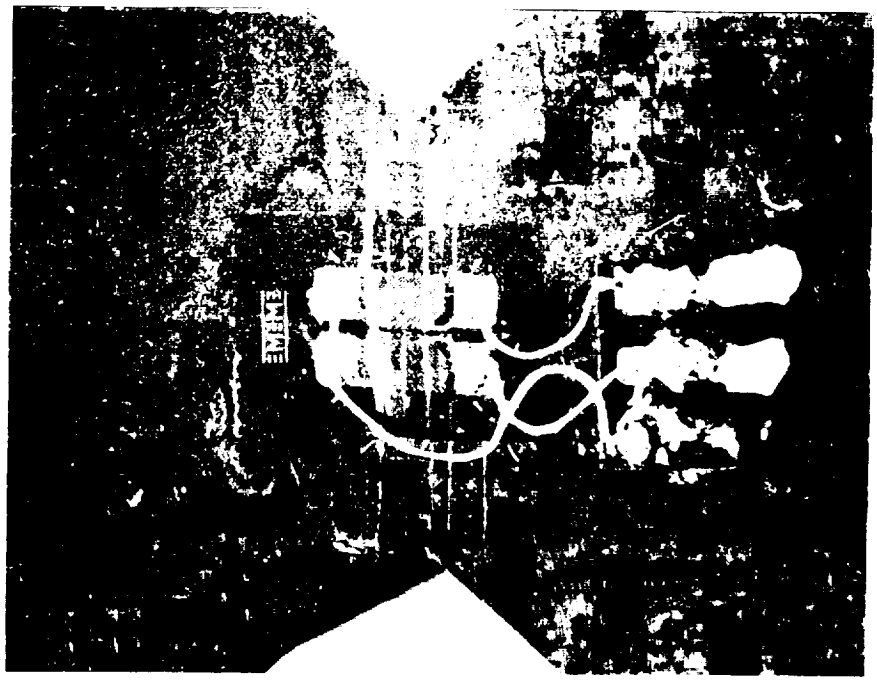

a) In-plane (12) Shear Test

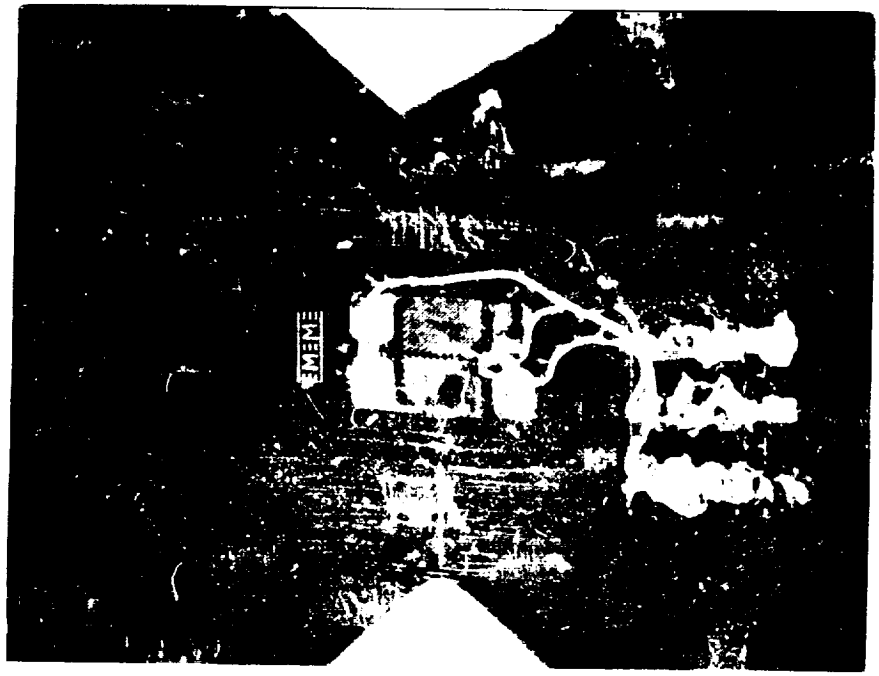

Figure 25. Typical Failures of In-plane Iosipescu Shear Test Specimens of Orthogonal Layup 5-Harness Satin Weave T300/934 Graphite Fabric/Epoxy Laminates.

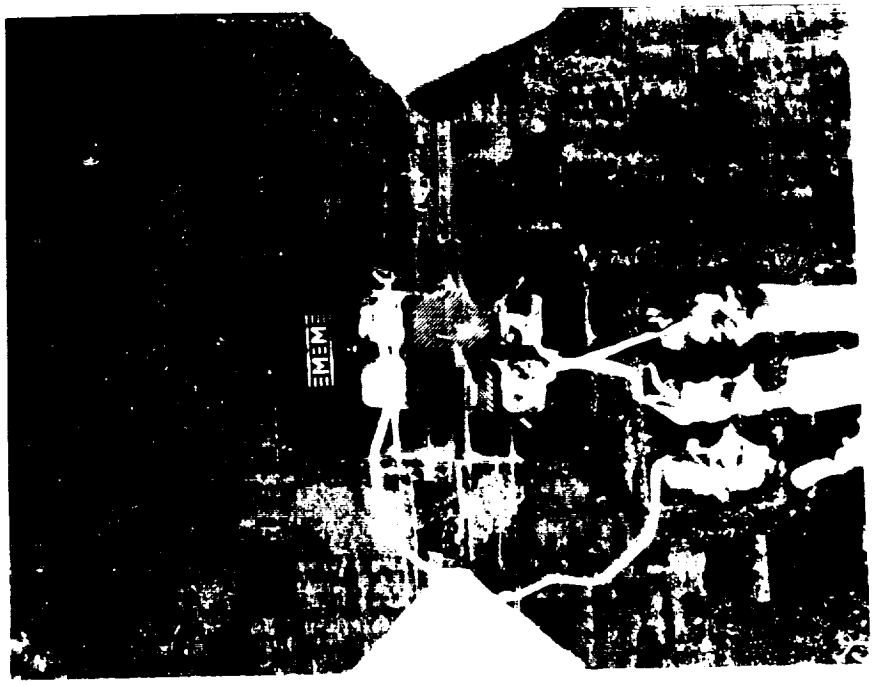

a) In-plane (12) Shear Test

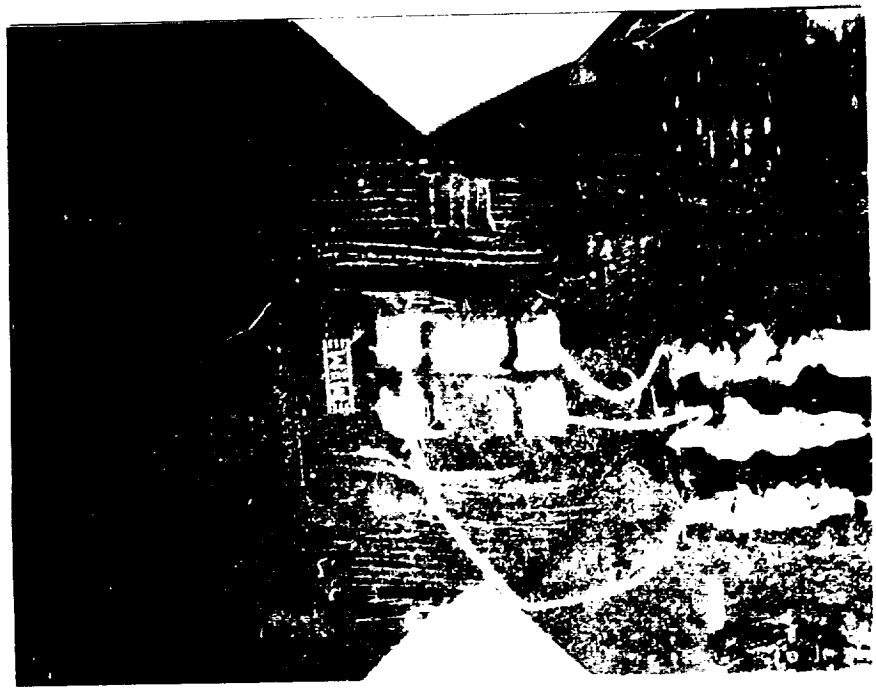

b) In-plane (21) Shear Test

Figure 26. Typical Failures for In-plane Iosipescu Shear Test Specimens of Orthogonal Layup 8-Harness Satin Weave T300/934 Graphite Fabric/Epoxy Laminates.

a) In-plane (12) Shear Test.

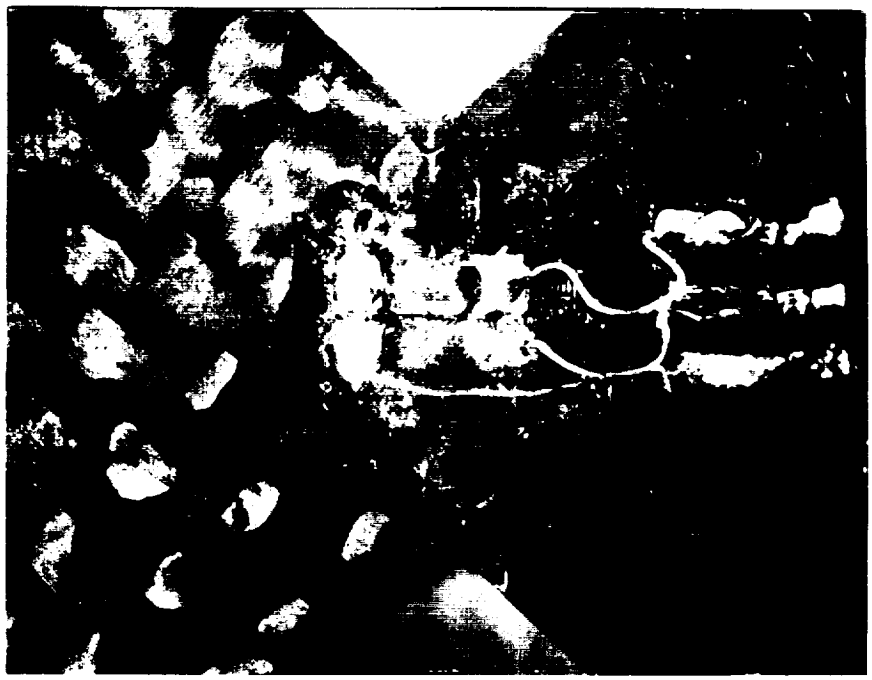

b) In-plane (21) Shear Test.

Figure 27. Typical Failures of In-plane Iosipescu Shear Test Specimens of Quasi-Isotropic Layup Oxford Weave T300/934 Graphite Fabric/Epoxy Laminates.

Failure cracks in all of the interlaminar (τ_{13} and τ_{23}) shear tests were always parallel to the plane of the laminate, i.e. on interlaminar planes. Cracks in the failed 13 interlaminar shear test specimens were parallel to the 1 or warp direction, and cracks in the failed τ_{23} shear test specimens were parallel to the 2 or fill direction, as shown in Figures 28 and 29. The failed specimen shown in Figure 28 is a τ_{13} interlaminar shear test specimen from the quasi-isotropic Oxford weave Panel Number 3. Note the cracks emanating from the notch roots, propagating horizontally in the photograph. Also note the horizontal shear crack in the center of the test specimen between the notch roots. Similar cracks were noted for the τ_{13} interlaminar shear test specimen from the orthogonal layup 5-harness satin weave Panel Number 5 shown in Figure 29.

The interlaminar test specimen shown in Figure 28 was cut from one laminate thickness. The specimen shown in Figure 29 was cut from three bonded laminate thicknesses of Panel Number 5. Note that two of the cracks evident in Figure 29 were along these bond lines. However, other cracks were also present within the center laminate thickness. As the specimen shown in Figure 28 was cut from only one laminate thickness, the cracks were of course all within that one thickness. The interlaminar shear failures depicted in Figures 28 and 29 are fully representative of all interlaminar shear failures observed during this research.

Overall, few differences in either in-plane or interlaminar shear response were observed among the Oxford, 5-harness, or 8-harness weave fabric laminates. There was a slight increase in the in-plane shear strength going from the Oxford to the 8-harness satin weave geometry. Slight differences in in-plane failure mode were also observed. Interlaminar shear failures were always on interlaminar planes.

Figure 28. Typical Failure of Interlaminar Iosipescu Shear Test Specimens of Quasi-Isotropic Layup Oxford Weave T300/934 Graphite Fabric/Epoxy Laminates.

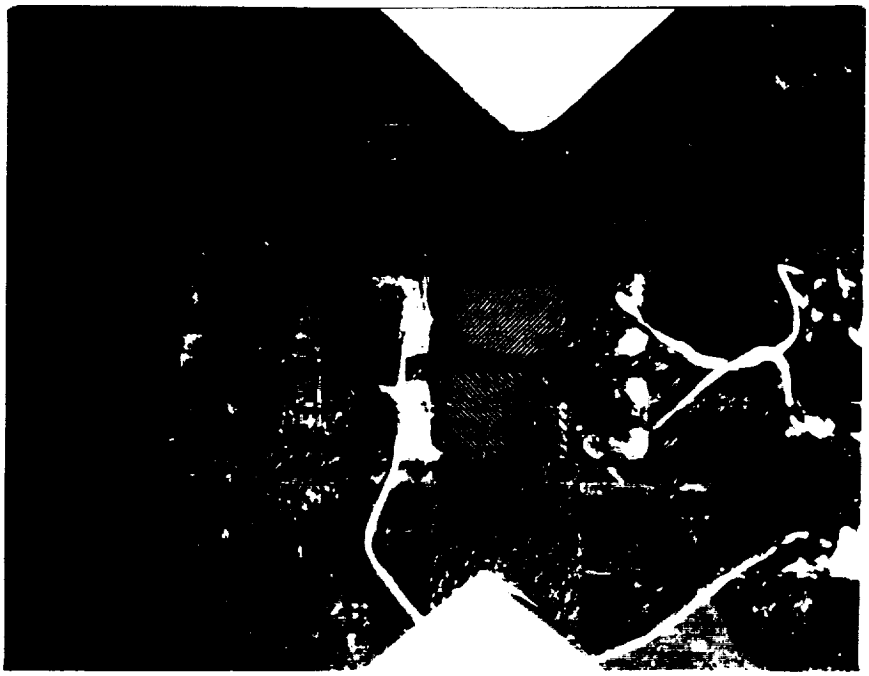

Figure 29. Typical Failure of Interlaminar Iosipescu Shear Test Specimens of Orthogonal Layup 5-Harness Satin Weave T300/934 Graphite Fabric/Epoxy Laminates.

SECTION 4
CONCLUSION

Double edge notch shear test methods, viz., the Iosipescu, AFPB, and Arcan versions, have been studied extensively. In particular, during the period of this NASA grant, the Iosipescu shear test method as used at the University of Wyoming was modeled via finite elements. The test fixture was totally redesigned and rebuilt. Finally, the in-plane and interlaminar shear properties of three T300/934 graphite fabric/epoxy composite materials were fully characterized. Shear properties for a fourth, plain weave auxiliary warp fabric, composite were also studied.

Finite element analyses performed during the first and second years of this grant period demonstrated the potential usefulness of the Iosipescu shear test method in characterizing composite materials. A minor design problem involving the positioning of the inner loading points (faces) of the first Wyoming test fixture was identified and corrected. The edge notch geometry was also modeled. It was found that the depth of the notches was not critical as long as it was in the range of 20-25 percent of the overall specimen height, reconfirming Iosipescu's original design.

The root radius of the notch was found to significantly affect test results. Sharp notch root radii induced shear stress concentrations at the notch root in (orthotropic) composites. As the radius of the notch root was increased, the shear stress concentration was reduced. However, this stress concentration was also found to depend on the degree of orthotropy of the material being tested. For highly orthotropic laminates this stress concentration could be reduced, but not eliminated.

Notch angle was found to influence results also. Specimens modeled with notch angles greater than 90° exhibited lower stress concentrations at the notch root and lower apparent shear moduli.

While all of these variations in notch configuration did influence results, the degree of influence was relatively small. Most notch geometry variations did not affect overall shear stress-strain response by more than 10 to 20 percent at most. The Iosipescu shear test can thus

be routinely used, using a standard notch geometry and specimen size, if desired.

The Wyoming version of the Iosipescu shear test fixture was redesigned to reposition the inner loading points. An effort was also made to correct some of the features which made the earlier test fixture configuration inconvenient to use. First, a clamping mechanism involving screw driven sliding wedges was incorporated into each fixture half. This mechanism was installed to ensure specimens would fit snugly within the fixture. Since the fixture is now adjustable, the close dimensional tolerances on specimen height previously required have been eliminated.

A second change made in the test fixture was to increase the size of the test specimen. A larger specimen size makes installation of shear strain instrumentation much easier. The new fixture is more open, making specimen installation and viewing during a test less difficult.

Other changes included incorporating the previously separate centering tool as an integral part of the left (fixed) fixture half. This was done to eliminate the need for a "third" hand while trying to install test specimens. Also, a linear ball bushing is now used to support the movable fixture half. This was done to remove the lubrication requirements for the test fixture. Binding in this bearing should not be a problem.

It should be noted that the guiding design concept for this test fixture was production testing. The full characterization of the shear properties of a particular composite material, viz., both in-plane and interlaminar shear properties for several different environments, requires many tests. The current Iosipescu shear fixture was designed to permit rapid testing of large numbers of specimens if desired. Furthermore, these specimens do not require extensive fabrication, e.g., special handling or end tabs.

Finally, the usability of the Iosipescu shear test method to characterize the in-plane and interlaminar shear properties of graphite fabric/epoxy laminates was demonstrated. In-plane and interlaminar shear moduli, shear strengths, and shear stress-shear strain plots were obtained for four different graphite fabric/epoxy composite materials.

The Iosipescu shear test is currently being studied by the American Society for Testing and Materials (ASTM) for round-robin testing and future standardization.

REFERENCES

1. Walrath, D. E. and Adams, D. F., "The Iosipescu Shear Test as Applied to Composite Materials," Experimental Mechanics, Vol. 23, No. 1, March 1983, pp. 105-110.

2. Lee, S., and Munro, M., "In-plane Shear Properties of Graphite Fiber/Epoxy Composites for Aerospace Applications: Evaluation of Test Methods by the Decision Analysis Technique," Aeronautical Note NAE-AN22, NRC No. 23778, Mechanical Engineering Department, University of Ottawa, Ottawa, Canada, October 1984.

3. Sullivan, J. L., Kao, B. G., and Van Oene, H., "Shear Properties and a Stress Analysis Obtained from Vinyl-ester Iosipescu Specimens," Experimental Mechanics, Vol. 24, No. 3, September 1984, pp. 223-232.

4. Spigel, B. S., "An Experimental and Analytical Investigation of the Iosipescu Shear Test for Composite Materials," M. S. Thesis, Old Dominion University, August 1984.

5. Arcan, M. and Goldenberg, N., "On a Basic Criterion for Selecting a Shear Testing Standard for Plastic Materials," (In French) ISO/TC 61-WG 2 SP. 171, Burgenstock-Switzerland, 1957.

6. Goldenberg, N., Arcan, M. and Nicolau, E., "On the Most Suitable Specimen Shape for Testing Shear Strength of Plastics," International Symposium on Plastics Testing and Standardization, ASTM STP 247, American Society for Testing and Materials, 1958, pp. 115-121.

7. Arcan, M., Hashin, Z. and Voloshin, A., "A Method to Produce Uniform Plane-stress States with Applications to Fiber-reinforced Materials," Experimental Mechanics, Vol. 18, No. 4, 1978, pp. 537-666.

8. Iosipescu, N., "New Accurate Procedure for Single Shear Testing of Metals," Journal of Materials, Vol. 2, No. 3, September 1967, pp. 537-666.

9. Slepetz, J. M., Zagaeski, T. F. and Novello, R. F., "In-plane Shear Test for Composite Materials," Report No. AMMRC TR 78-30, Army Materials and Mechanics Research Center, Watertown, Massachusetts, July 1978.

10. Adams, D. F. and Walrath, D. E., "Iosipescu Shear Properties of SMC Composite Materials," Composite Materials: Testing and Design (Sixth Conference), ASTM STP 787, 1982, pp. 19-33.

11. Walrath, D. E. and Adams, D. F., "Analysis of the Stress State in an Iosipescu Shear Test Specimen," Report No. UWME-DR-301-102-1, Department of Mechanical Engineering, University of Wyoming, June 1983.

12. Walrath, D. E. and Adams, D. F., "Verification and Application of the Iosipescu Shear Test Method," Report No. UWME-DR-401-103-1, Department of Mechanical Engineering, University of Wyoming, June 1984.

13. Place, T. R., Private Communication, Aeronutronic Division, Ford Aerospace and Communication Corporation, Newport Beach, CA, 1974.

14. Walrath, D. E. and Adams, D. F., "Damage Mechanisms/Failure Mechanics of Carbon-Carbon Composite Materials," Report UWME-DR-904-101-1, Composite Materials Research Group, Department of Mechanical Engineering, University of Wyoming, September 1979.

15. Walrath, D. E. and Adams, D. F., "Test Methods Development for 3D Cylindrical-Weave Carbon-Carbon Composite Materials," Report UWME-DR-104-104-1, Composite Materials Research Group, Department of Mechanical Engineering, University of Wyoming, September 1981.

16. Odom, E. M. and Adams, D. F., "Axial Test Methods Development for 3D Cylindrical-Weave Carbon-Carbon Composite Materials," Report UWME-DR-301-104-1, Composite Materials Research Group, Department of Mechanical Engineering, University of Wyoming, November, 1983.

17. Walrath, D. E. and Adams, D. F., "Shear Strength and Modulus of SMC-R50 and XMC-3 Composite Materials," Report UWME-DR-004-105-1, Department of Mechanical Engineering, University of Wyoming, March 1980.

18. Walrath, D. E., and Adams, D. F., "Static and Dynamic Shear Testing of SMC Composite Materials," Report UWME-DR-004-103-1, Department of Mechanical Engineering, University of Wyoming, May 1980.

19. Zimmerman, R. S. and Adams, D. F., "Mechanical Properties Testing of Candidate Polymer Matrix Materials for Use in High Performance Composites," Report UWME-DR-401-104-1, Department of Mechanical Engineering, University of Wyoming, August 1984.

20. Davis, S. J. and Adams, D. F., "Thermal Deformation of Various Composite Material Ski Constructions," SAMPE Journal, Vol. 18, No. 3, May/June 1982, pp. 8-16.

21. Bergner, Jr. H. W., Davis, Jr. J. G. and Herakovich, C. T., "Analysis of Shear Test Method for Composite Laminates," Report VPI-E-77-14, Virginia Polytechnic Institute and State University, April 1977.

22. Herakovich, C. T. and Bergner, Jr. H. W., "Finite Element Stress Analysis of a Notched Coupon Specimen for In-plane Shear Behavior of Composites," Composites, July 1980, pp. 149-154.

23. Marloff, R. H., "Finite Element Analysis of Biaxial Stress Test Specimen for Graphite/Epoxy and Glass Fabric/Epoxy Composites," Composite Materials: Testing and Design (Sixth Conference), ASTM STP 787, 1982, pp. 34-49.

24. Monib, M. M. and Adams, D. F., "Three-Dimensional Elastoplastic Finite Element Analysis of Laminated Composites," Report UWME-DR-001-102-1, University of Wyoming, Department of Mechanical Engineering, November 1980.

25. Adams, D. F., Ramkumar, R. L. and Walrath, D. E., "Analysis of Porous Laminates in the Presence of Ply Drop-offs and Fastener Holes," Northrop Technical Report NOR 84-113, Naval Air Systems Command Contracts N00019-82-C-0156 and N00019-82-C-0063, May 1984.

26. Abdallah, M. G., Gardiner, D. S., and Gascoigne, H. E., "An Evaluation of Graphite/Epoxy Iosipescu Shear Specimen Testing Methods with Optical Techniques," Proceedings of the 1985 SEM Spring Conference on Experimental Mechanics, Las Vegas, Nevada, June 1985, pp. 833-843.

27. Swanson, S. R., Messick, M., and Toombes, G. R., "Comparison of Torsion Tube and Iosipescu In-plane Shear Test Results for Graphite/Epoxy," Report No. UTEC ME 84-065, Department of Mechanical and Industrial Engineering, University of Utah, 1984.

28. Deaton, J. W., Funk, J. G., and Lubowinski, S. J. "Characterization of Three Graphite/Epoxy 2-D Composite Fabrics," NASA TM-86342, 1985.

APPENDICES

APPENDIX A

IOSIPESCU SHEAR TEST PROCEDURES

A.1. Test Fixture

The University of Wyoming's current version of the Iosipescu shear test fixture was designed to test flat specimens nominally 7.62 cm (3 in) long, 1.91 cm (0.75 in) wide, and up to 1.27 cm (0.5 in) thick. The test fixture is shown in Figures A1 and A2. This test fixture is used in a testing machine set up in a compression loading mode. The fixture can be inserted between two flat compression platens. However, it is usually more convenient to attach the right fixture half to the upper testing machine load surface using the center hole provided in the fixture. An example adaptor for this purpose is also shown in Figure A1. This fixture has been loaded to 22 kN (5000 lbs) applied force without damage to the fixture.

The right (movable) fixture half moves on a linear ball bushing and a hardened steel post as shown on Figure A2. The fit of the linear ball bushing on the post may be adjusted via the set screw marked in Figure A2. Caution must be taken to not overtighten this set screw, however. Overtightening will result in binding of the linear ball bushing on the post and possible damage to the ball bushing.

A specimen alignment tool has been incorporated into the test fixture as shown in Figure A3. When preparing to adjust the clamping wedges, the alignment tool is lifted to index on the lower notch of the test specimen.

Machine drawings of this test fixture are included as Figures A4 through 10. All parts are fabricated from low carbon cold rolled steel with the exception of the linear bushing and post. These items are manufactured by Thompson Industries, Manhasset, New York, and may be purchased from any of their distributors.

The Iosipescu shear fixture, as shown in Figure A1, was designed to test specimens nominally 1.91 cm (0.75 in) wide. The wedge clamp blocks allow approximately 1 mm (0.04 in) variation on that height. Only light clamping is required, to ensure that no specimen rotation takes place within the fixture during a test. Narrower specimens may be tested by using thicker wedges, changing the height dimension of the wedge in Figure A5.

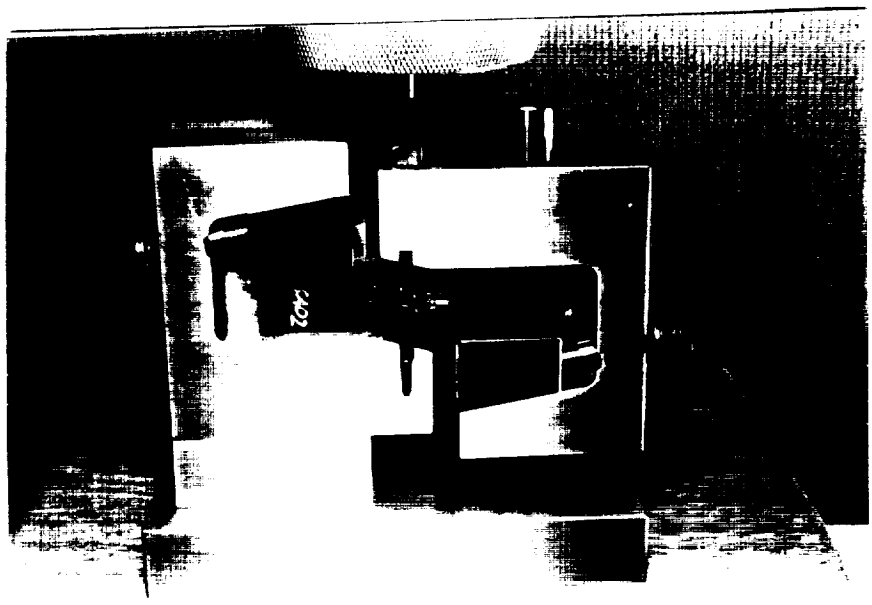

Figure A1. Iosipescu Shear Test Fixture, Front View.

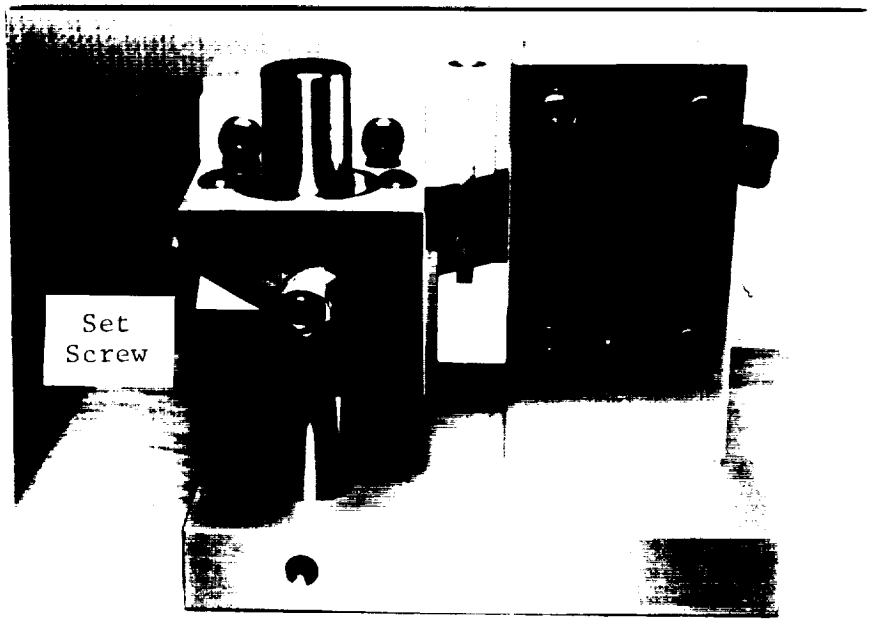

Figure A2. Iosipescu Shear Test Fixture, Rear View.

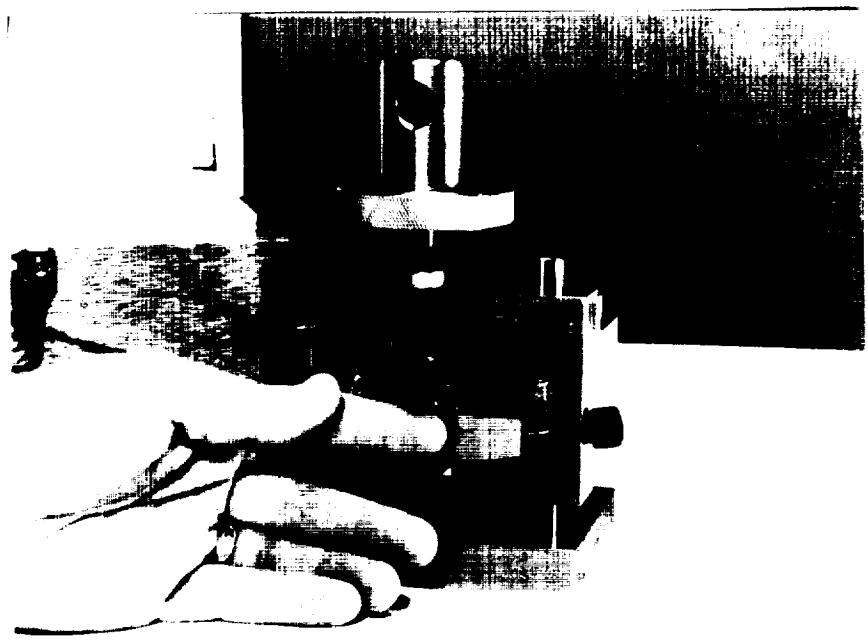

Figure A3. Alignment Tool Used During Specimen Installation.

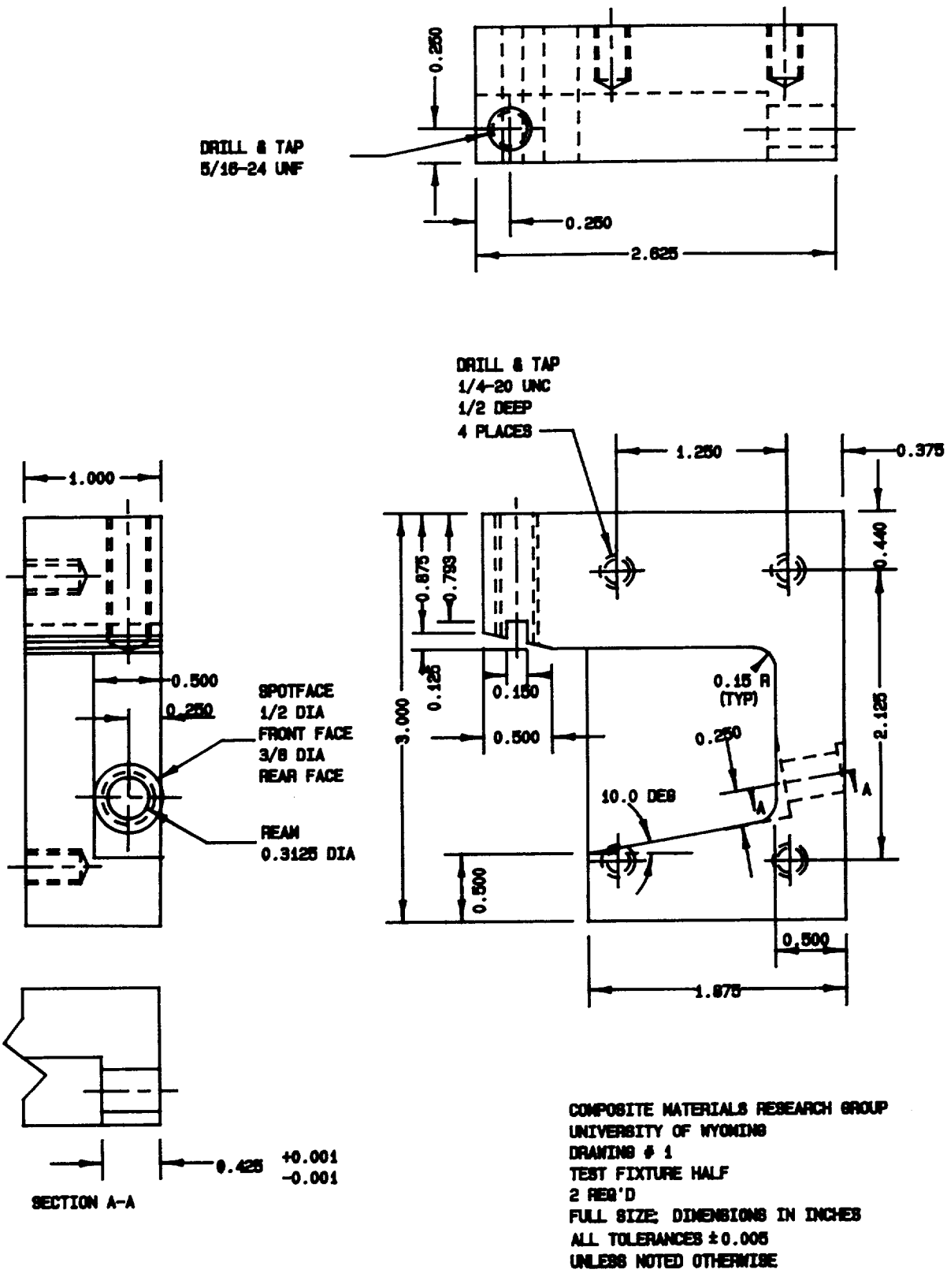

Figure A4. Iosipescu Shear Test Fixture Half.

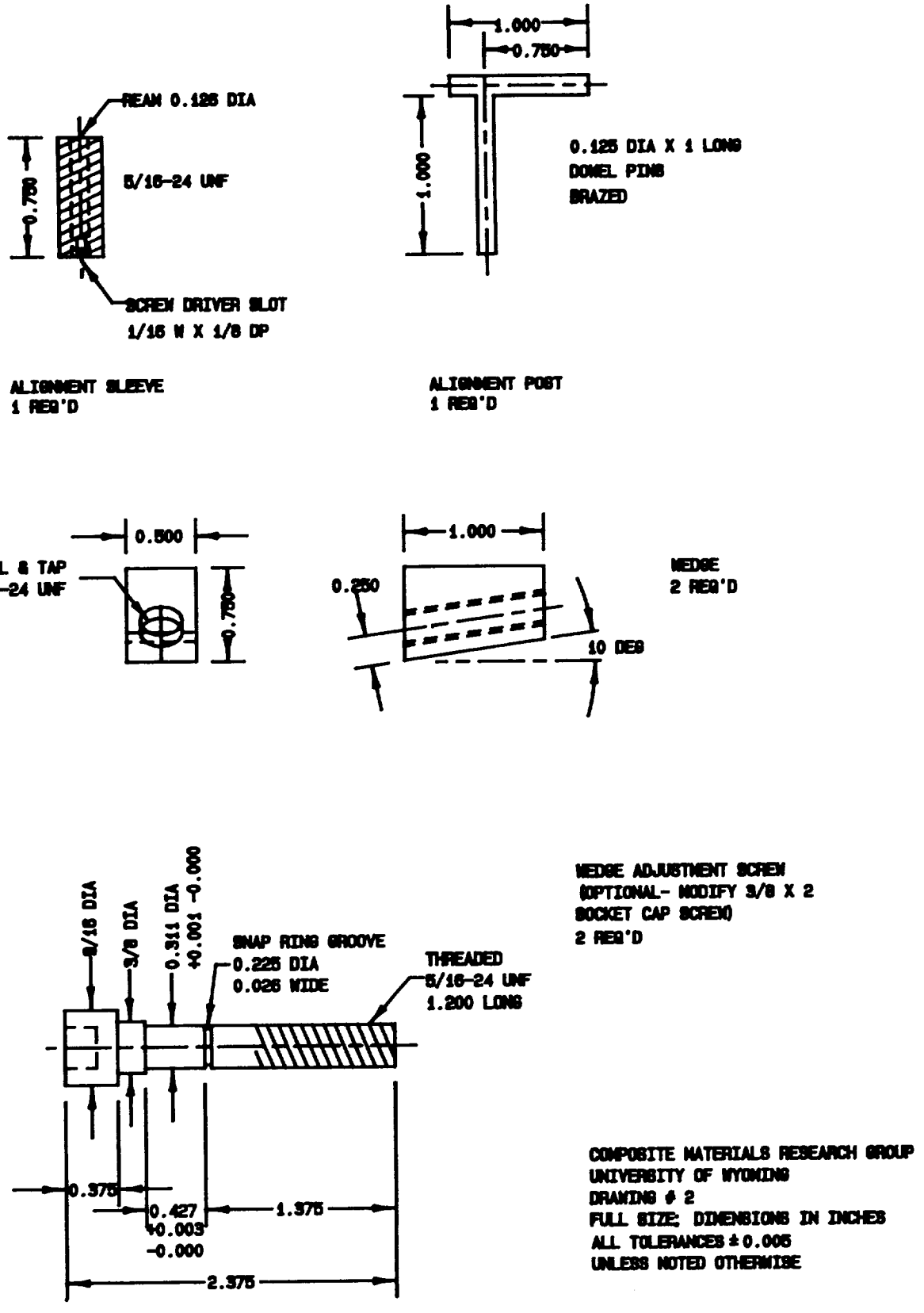

Figure A5. Iosipescu Shear Test Fixture Alignment Tool Assembly and Clamp Assembly.

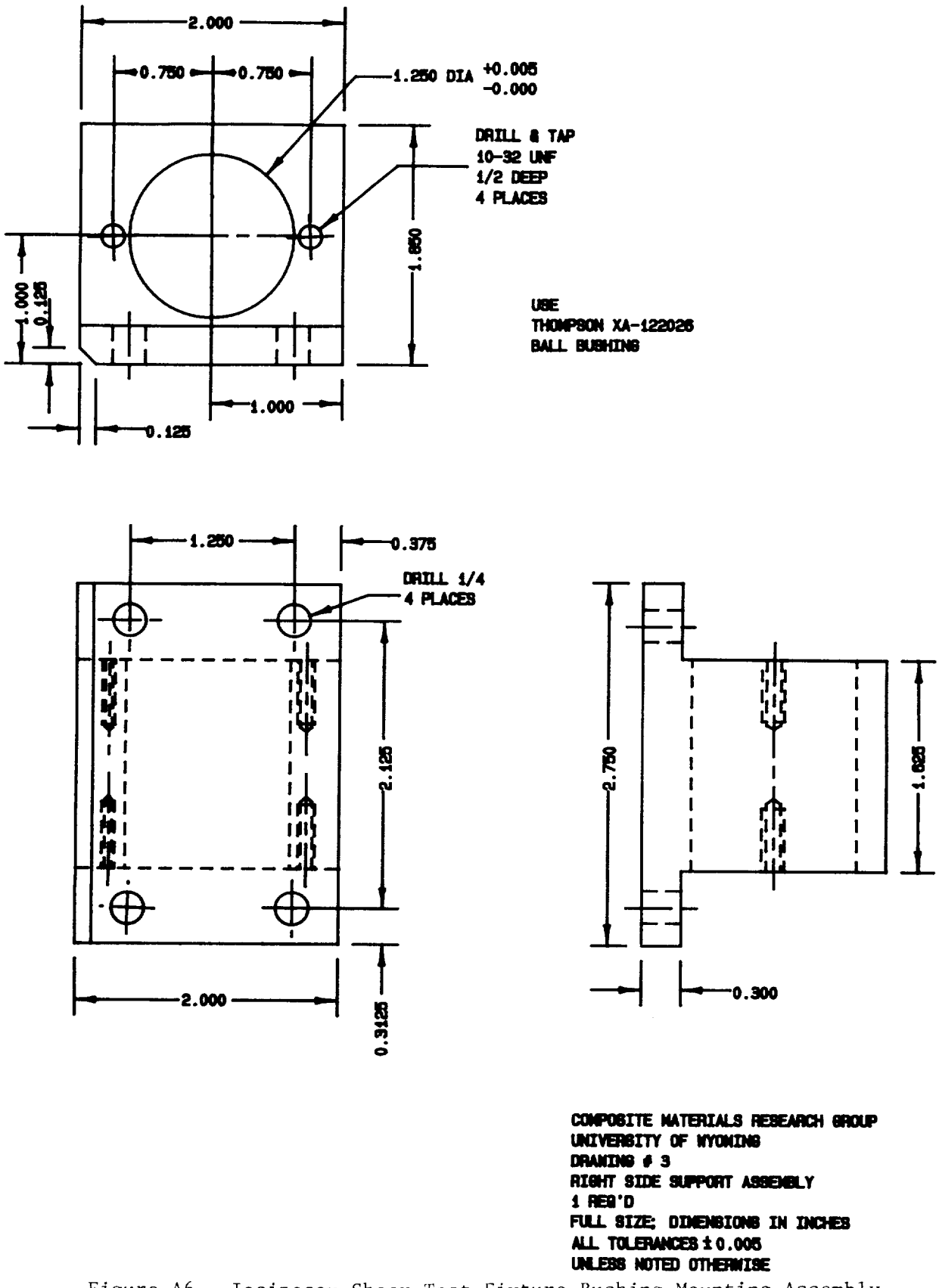

Figure A6. Iosipescu Shear Test Fixture Bushing Mounting Assembly.

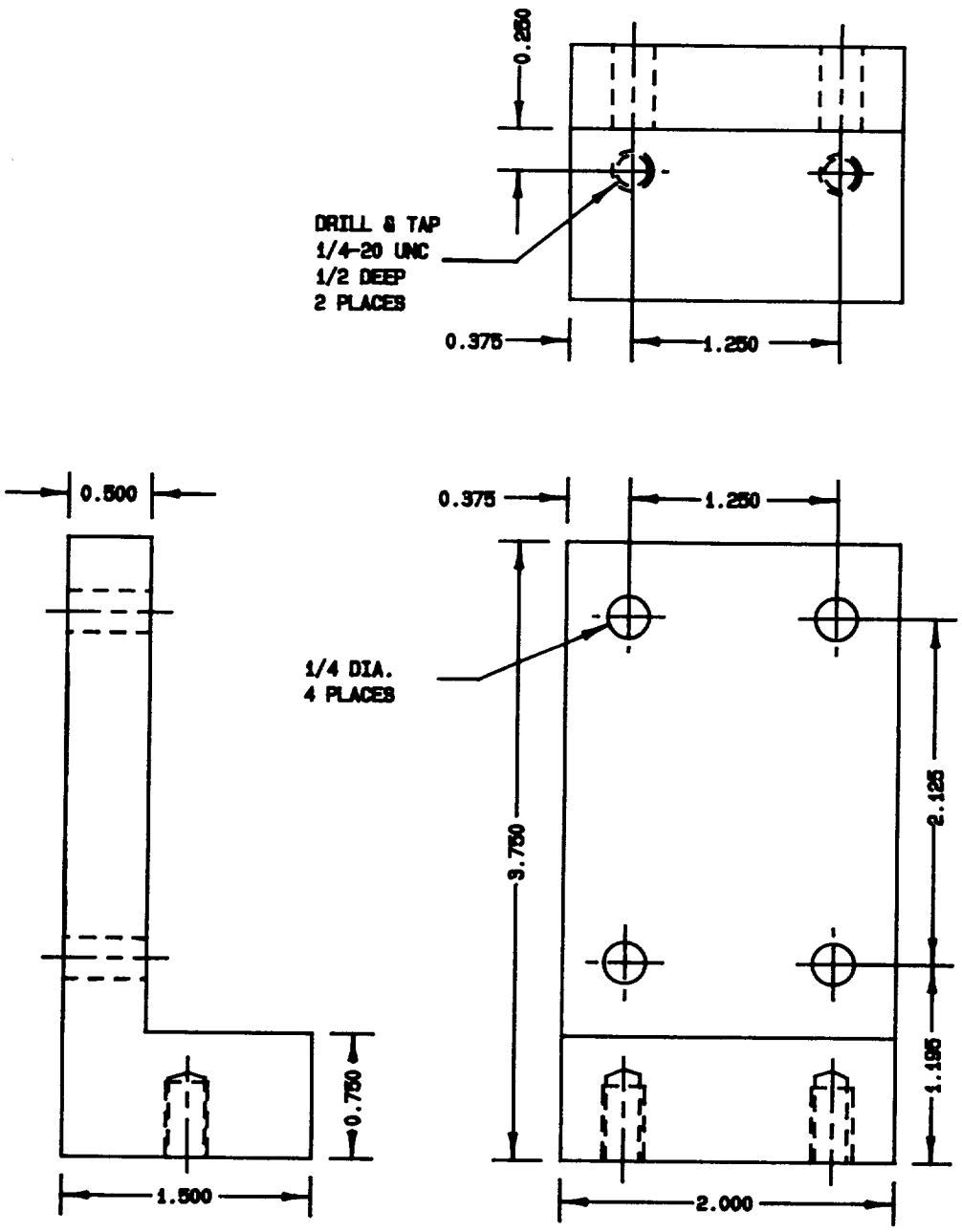

COMPOSITE MATERIALS RESEARCH GROUP
UNIVERSITY OF WYOMING
DRAWING # 4
LEFT SIDE SUPPORT
1 REQ'D
FULL SIZE; DIMENSIONS IN INCHES
ALL TOLERANCES ± 0.005
UNLESS NOTED OTHERWISE

Figure A7. Iosipescu Shear Test Fixture Fixed Half Mounting Bracket.

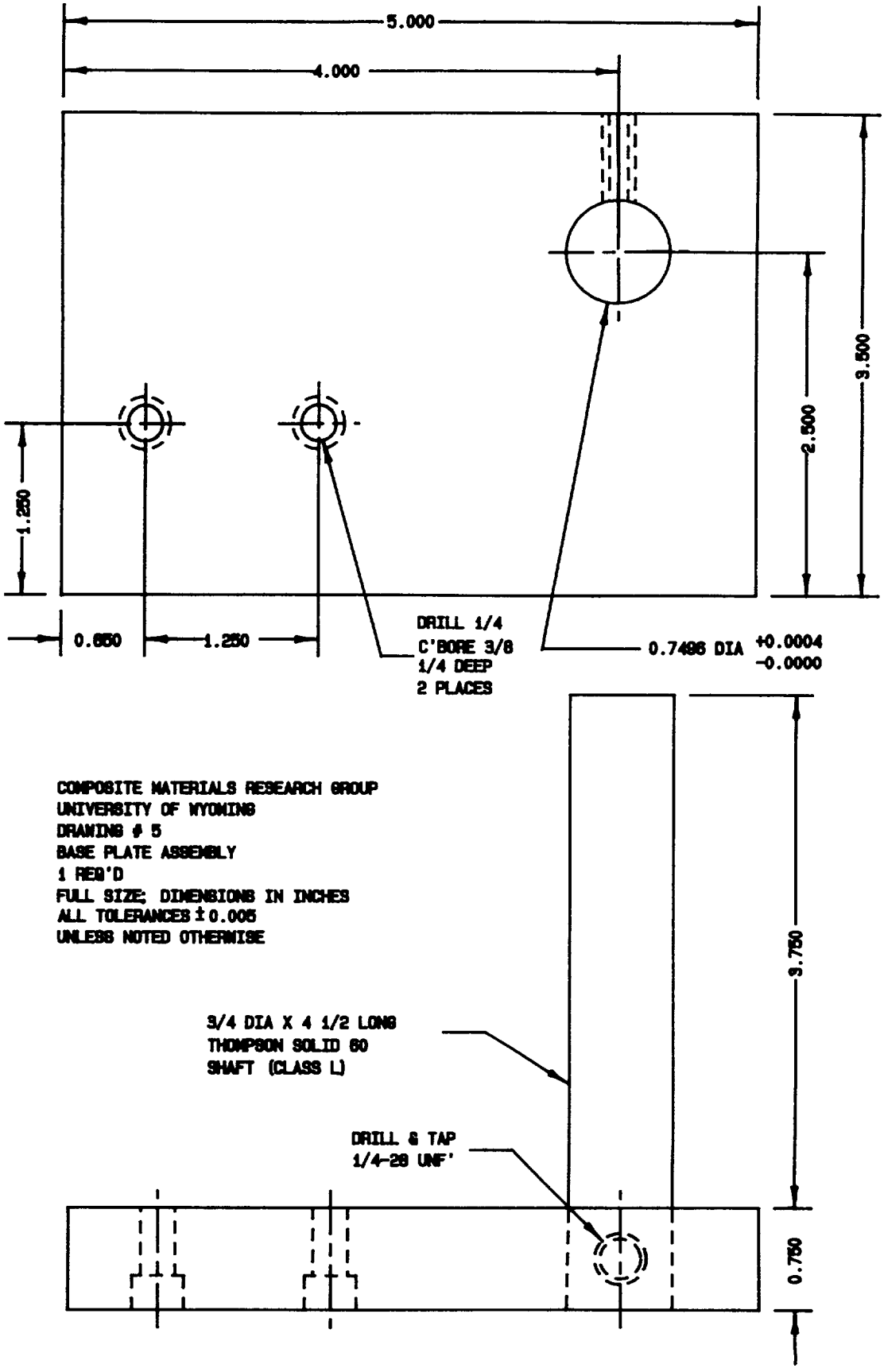

Figure A8. Iosipescu Shear Test Fixture Base and Post Assembly.

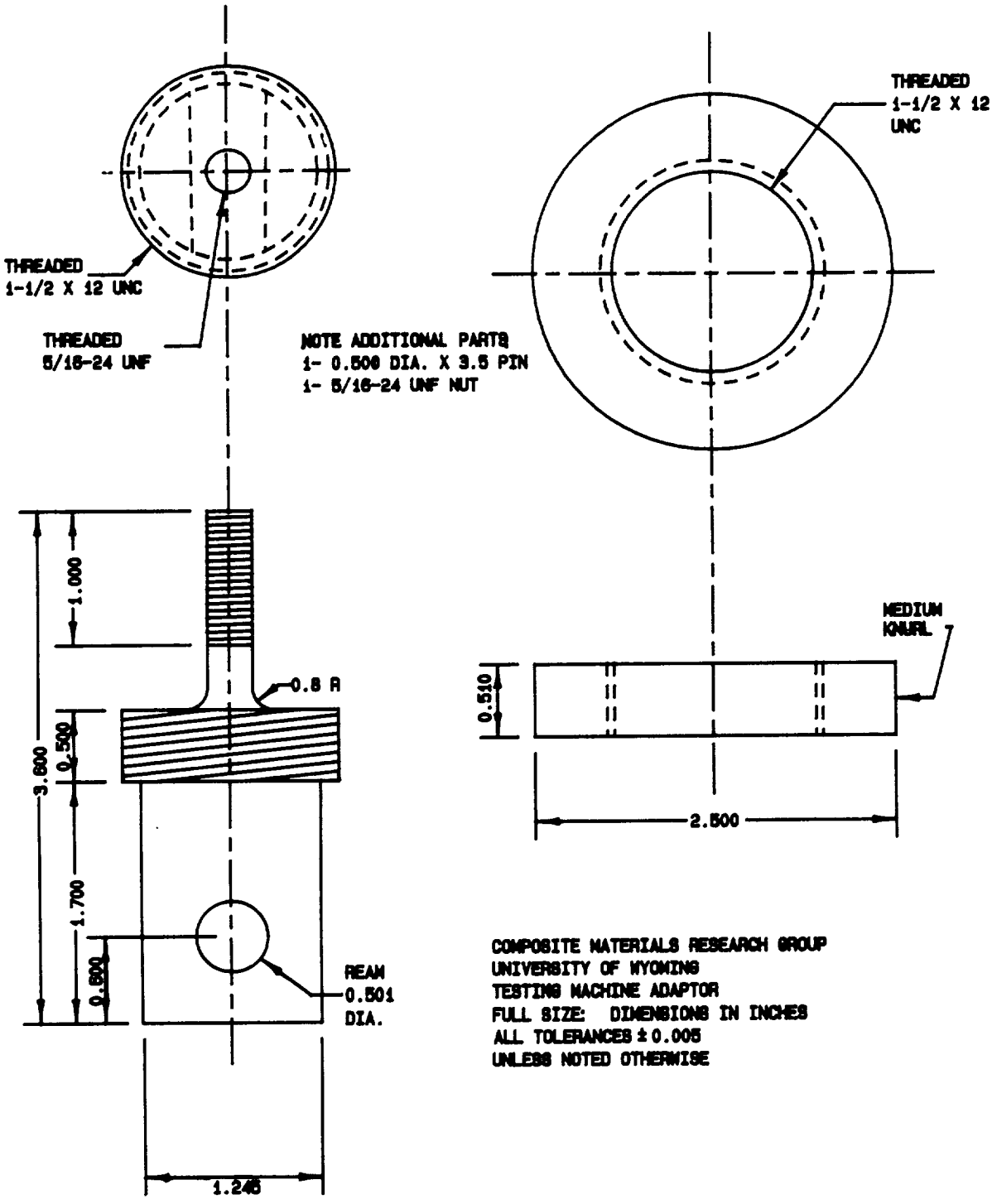

Figure A9. Iosipescu Shear Fixture Loading Adaptor.

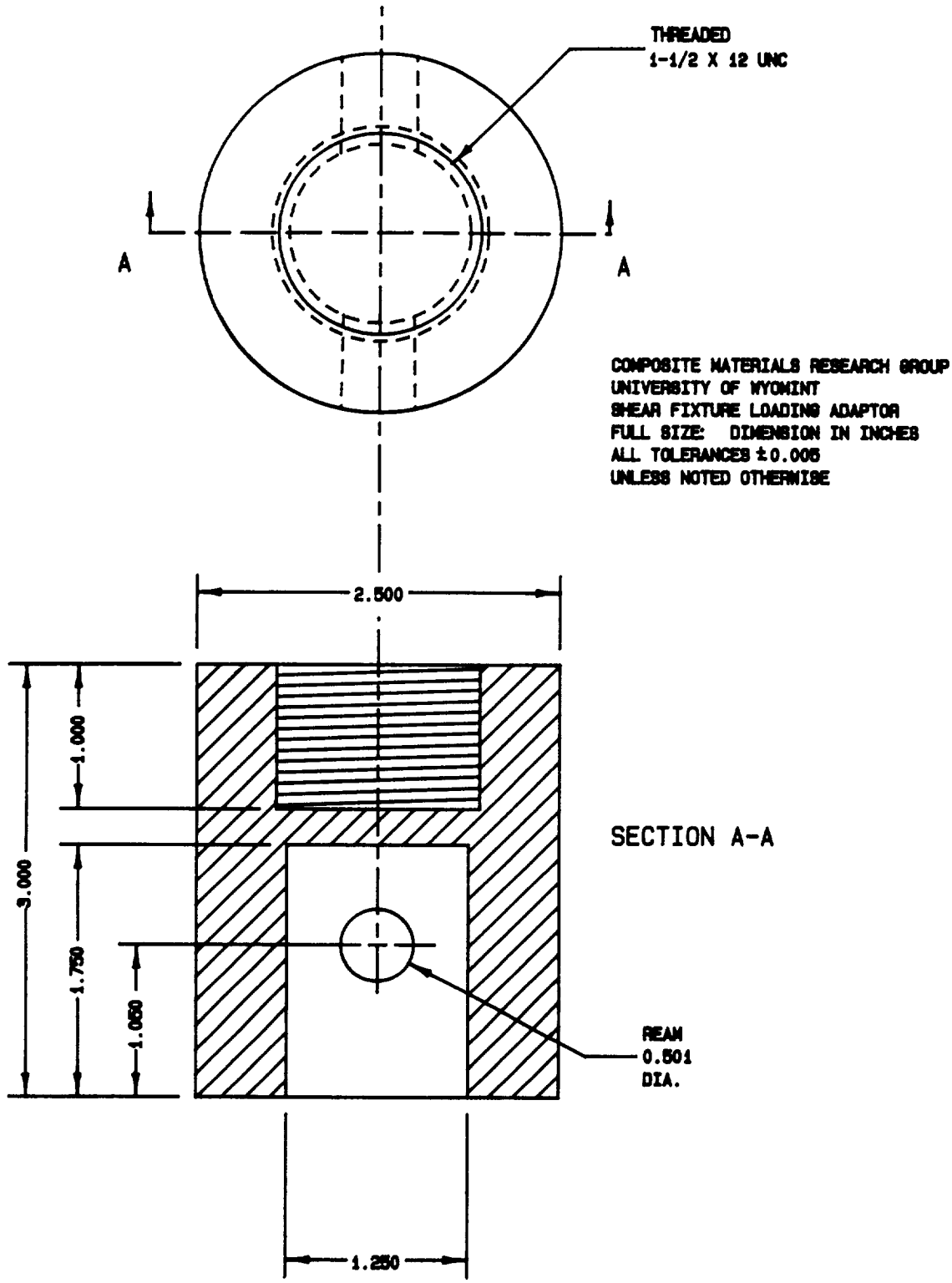

Figure A10. Iosipescu Shear Fixture Testing Machine Adaptor.

A.2. Test Specimen Fabrication

Iosipescu shear specimens for use with the present test fixture should nominally be 7.62 cm (3 in) long, 1.91 cm (0.75 in) and of any thickness up to 1.27 cm (0.5 in) thick, as shown in Figure A11. Very thin specimens may be tested, but care must be taken to ensure that compressive buckling does not occur. These specimens can be stiffened (away from the test region) by bonding tabs or backup plates to the front and back faces of the specimen.

Composite specimens are typically cut at the University of Wyoming with diamond abrasive tooling; metal specimens are normally prepared using conventional metal-working tools. Notches are ground in the composite specimens using a 60-grit abrasive wheel in a standard surface or tool grinder. This wheel is dressed to grind the prescribed notch angle and root radius shown in Figure A11. Care must be taken to avoid delaminating specimens during notch grinding. Stacking and clamping specimens in the tool grinder vise have been found to be effective. The specimens provide mutual edge support to each other during notch grinding. Notches are usually cut in metal specimens with a 90° angle milling cutter, with the desired notch root radius ground onto the cutter.

Shear tests may be performed with the Iosipescu shear test fixture in any of the six material shear planes. It is conventional to define a material coordinate system where the 1-coordinate is parallel to the principal in-plane material direction, the 2-coordinate is the second in-plane axis, and the 3-coordinate is perpendicular to the plane of the plate. The shear stress is then defined as being applied in the plane perpendicular to the first coordinate axis, in the direction parallel to the second coordinate axis. Therefore 12 and 21 are the in-plane shear components, while the interlaminar shear components are denoted 13, 31, 23, and 32. Specimens to impose any one of these four interlaminar shear components can be fabricated from a thin composite laminate by stacking and bonding sufficient layers of the composite to obtain the desired specimen as indicated in Figure A12. An in-plane 12 or 21 specimen is simply cut from a material plate, as also shown in Figure A12. The specimen type depicted in Figure A12b can be very fragile, potentially producing poor results for brittle material systems. The specimen type

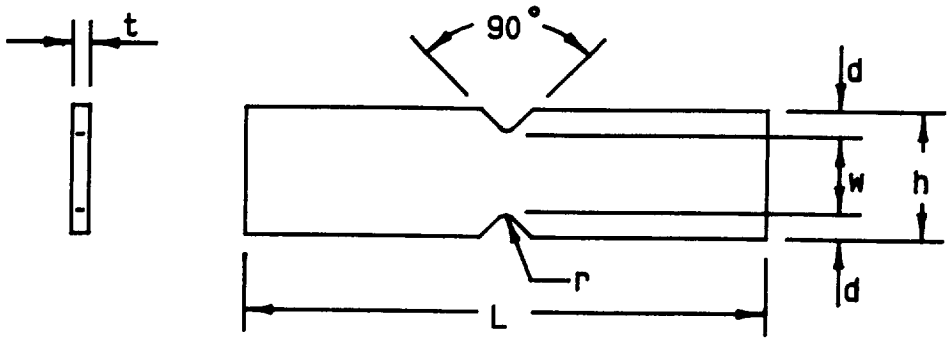

Figure A11. Iosipescu Shear Test Specimen.

t = 12.7 mm (0.5 in) maximum
h = 19.1 mm (0.75 in)
d = 4.3 mm (0.17 in)
L = 76 mm (3 in)
r = 1.3 mm (0.05 in) minimum

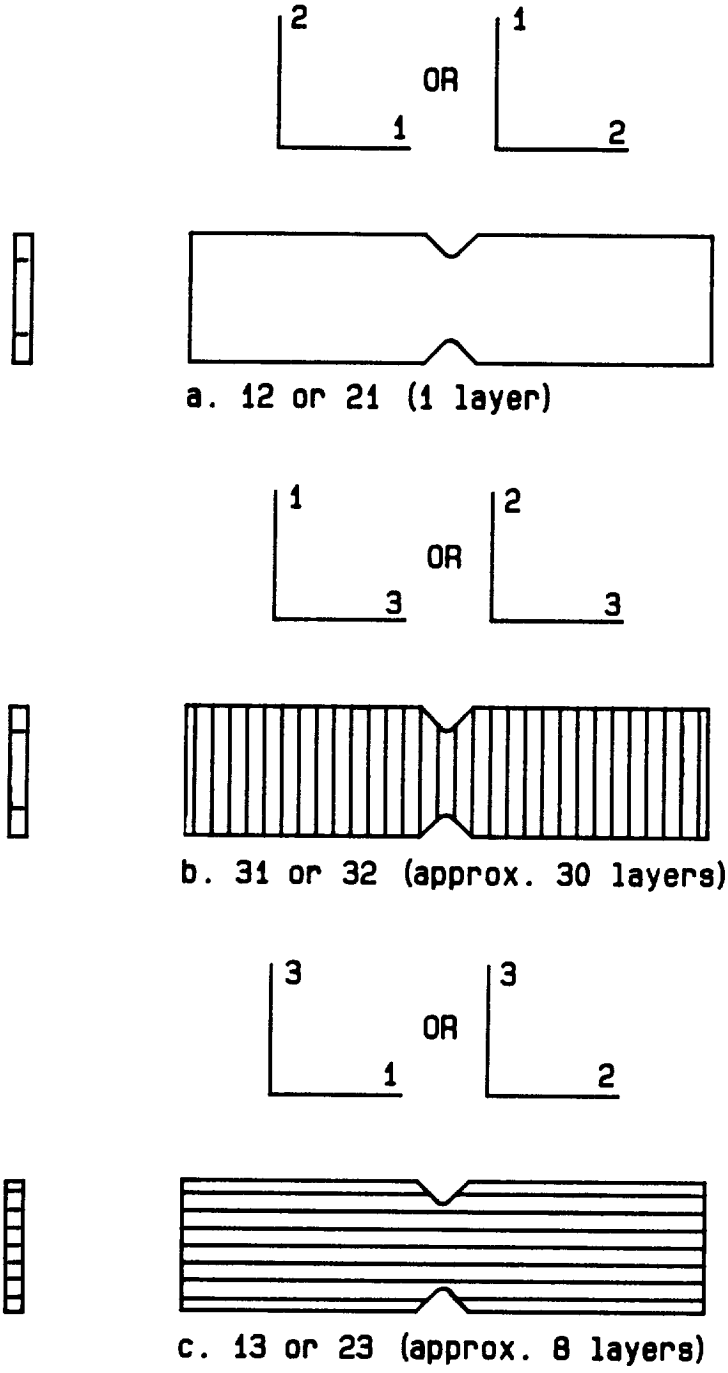

Figure A12. Possible Iosipescu Shear Test Specimen Configurations.

of Figure A12c is then preferred. As previously noted, narrower specimens may be tested if different clamping wedges are used.

A.3 Shear Instrumentation

To measure shear strains, specimens may be instrumented with a strain gage rosette incorporating two strain gages oriented at ±45°, as indicated in Figure A13. The specific strain gage rosette shown in Figure A13 consists of two 350-ohm strain gages, Micro Measurements Number EA06-062TV-350. The gages may be wired as individual channels in quarter bridge circuits, or as a single channel in a half bridge configuration. This particular strain gage rosette has a maximum shear strain range of approximately 6 percent. It is recommended that two-element strain gage rosettes be used rather than a single strain gage oriented at either +45° or -45°.

A.4 Test Procedures

The specimen is centered in the test fixture using the lift-up alignment tool to index on the lower specimen notch. The wedge clamps can then be tightened to hold the specimen firmly in place. These clamps need only be tightened "finger tight". The purpose of the wedges is to prevent the specimen from rotating during a test. Excessive tightening oft hew edge clamps is not necessary or desirable. A wrench is not required to tighten the wedges.

Tests may be performed at any desired loading rate. A convenient quasi-static rate is 2 mm/min (0.08 in/min). Cyclic loading may also be conducted, making appropriate provisions for attaching the fixture base in the test machine, if necessary.

Shear stress is calculated by dividing the applied load P by the specimen cross-sectional area between the notch tips, (see Figure A1), i.e.,

$$\tau = \frac{P}{wt} \quad .$$

Ultimate shear strength is not necessary calculated from the maximum force attained during loading. During and after actual shear failure, the reinforcing fibers in a composite material may reorient, subsequently bearing some portion of the applied force in a tensile

Figure A13. Iosipescu Shear Test Specimen Instrumented with a Strain Gage Rosette.

mode. This reorientation is more likely to occur in composites with matrix materials which are very nonlinear in shear. The point at which this happens can usually be determined from a load (stress) versus displacement plot. The point at which the stress-displacement plot abruptly changes slope is the point at which shear failure occurred. Test results must thus be carefully examined.

APPENDIX B

IOSIPESCU SHEAR PROPERTIES OF T300/934 GRAPHITE FABRIC/EPOXY COMPOSITES

TABLE B1

SHEAR STRENGTH AND SHEAR MODULUS OF ORTHOGONAL LAYUP OXFORD WEAVE T300/934 GRAPHITE/EPOXY COMPOSITE, PANEL NO. 1

Test Orientation	Specimen No.	Strength (MPa)	Strength (ksi)	Modulus (GPa)	Modulus (Msi)
12	1	111	16.1	5.4	0.79
	2	110	16.0	5.5	0.80
	3	115	16.7	5.4	0.78
	4	107	15.5	5.9	0.85
	5	105	15.2	5.7	0.83
	Average	110	15.9	5.6	0.81
	Std. Dev.	4	0.6	0.2	0.03
21	1	114	16.6	5.1	0.74
	2	112	16.3	6.1	0.89
	3	112	16.2	4.6*	0.67*
	4	108	15.6	5.5	0.80
	5	109	15.8	6.0	0.87
	Average	111	16.1	5.7	0.83
	Std. Dev.	3	0.4	0.5	0.07

*not included in average

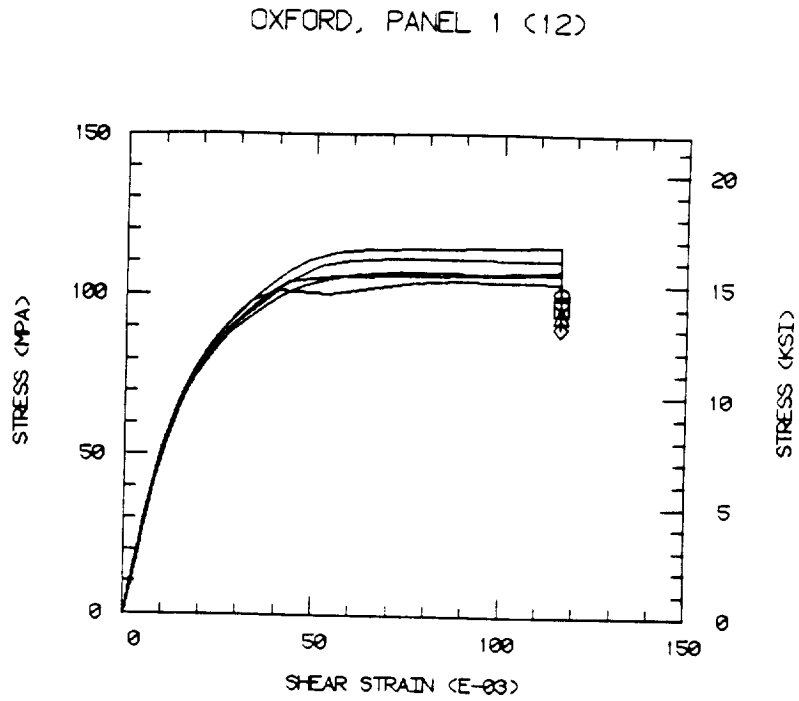

a. Stress-Strain Plot

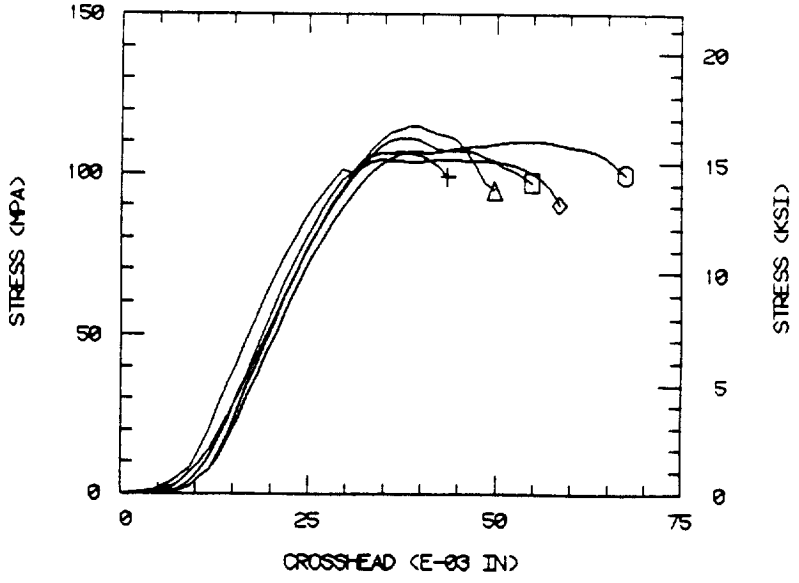

b. Stress-Displacement Plot

Figure B1. In-plane (12) Iosipescu Shear Stress-Strain and Stress-Displacement Plots for Orthogonal Layup Oxford Weave T300/934 Graphite/Epoxy Composite, Panel No. 1.

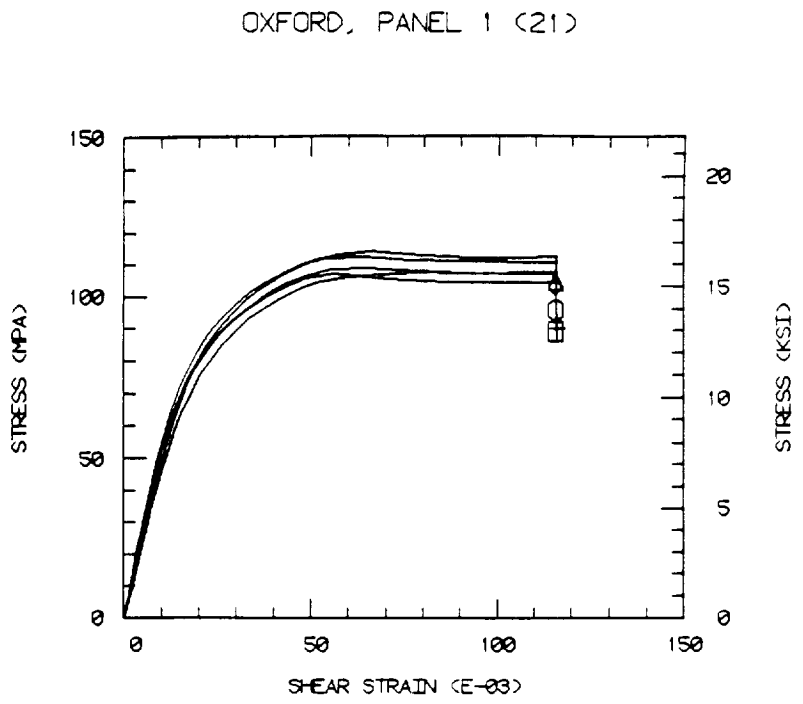

a. Stress-Strain Plot

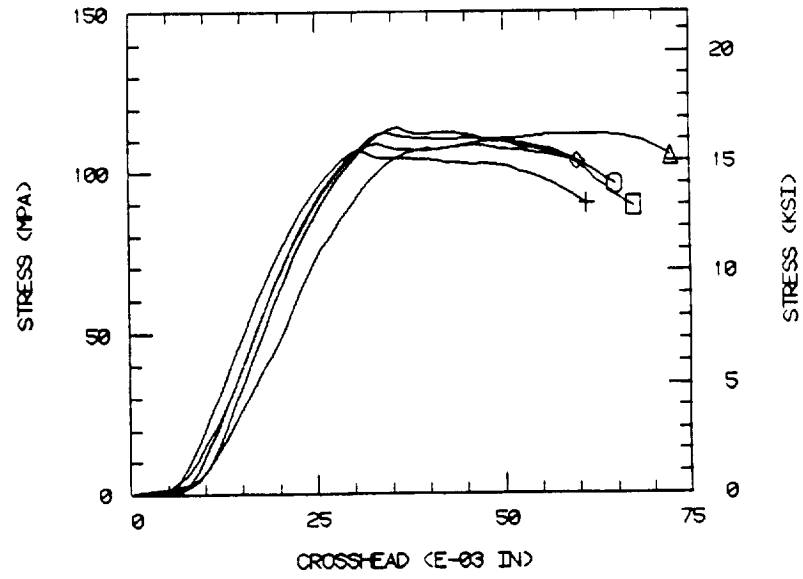

b. Stress-Displacement Plot

Figure B2. In-plane (21) Iosipescu Shear Stress-Strain and Stress-Displacement Plots for Orthogonal Layup Oxford Weave T300/934 Graphite/Epoxy Composite, Panel No. 1.

TABLE B2

SHEAR STRENGTH AND SHEAR MODULUS OF ORTHOGONAL LAYUP OXFORD WEAVE T300/934 GRAPHITE/EPOXY COMPOSITE, PANEL NO. 2

Test Orientation	Specimen No.	Strength (MPa)	Strength (ksi)	Modulus (GPa)	Modulus (Msi)
12	1	111	16.1	4.6	0.66
	2	112	16.3	4.9	0.71
	3	125	18.2	5.4	0.78
	4	131	19.0	5.1	0.74
	Average	120	17.4	5.0	0.72
	Std. Dev.	10	1.4	0.3	0.05
21	1	112	16.2	5.1	0.74
	2	114	16.6	5.0	0.72
	3	107	15.5	3.2*	0.47*
	4	114	16.5	4.8	0.70
	5	123	17.8	7.9*	1.15*
	Average	114	16.5	5.0	0.72
	Std. Dev.	6	0.8	0.1	0.02
13	2	72	10.6	5.4	0.78
	3	78	11.3	4.1	0.59
	4	82	11.9	4.8	0.69
	5	74	10.7	4.4	0.64
	6	72	10.5	4.9	0.71
	Average	76	11.0	4.7	0.68
	Std. Dev.	4	0.6	0.5	0.07
23	1	72	10.5	3.9	0.57
	2	75	10.9	3.8	0.55
	3	70	10.2	4.0	0.58
	4	73	10.6	3.9	0.57
	5	75	10.9	4.1	0.59
	Average	73	10.6	3.9	0.57
	Std. Dev.	2	0.3	0.1	0.02

*not included in average

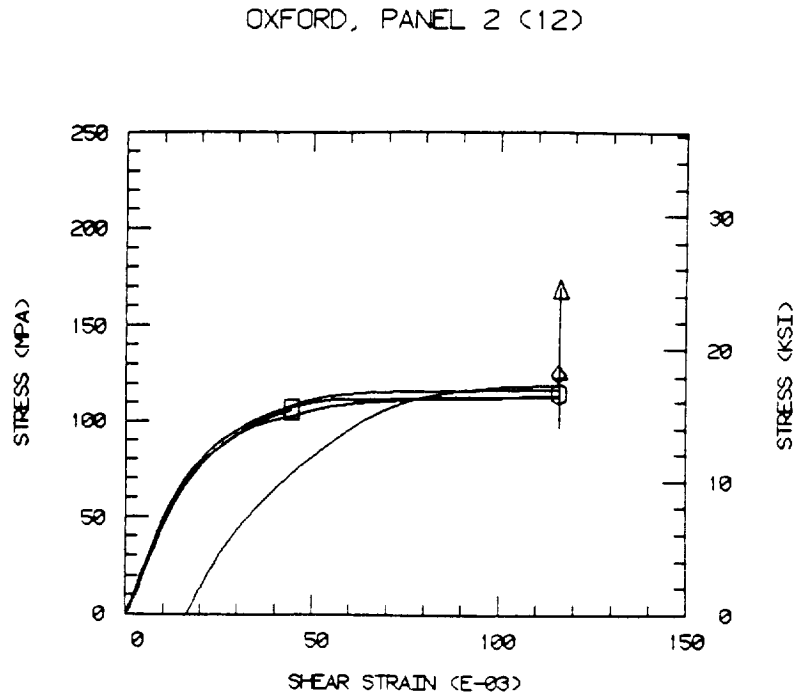

a. Stress-Strain Plot

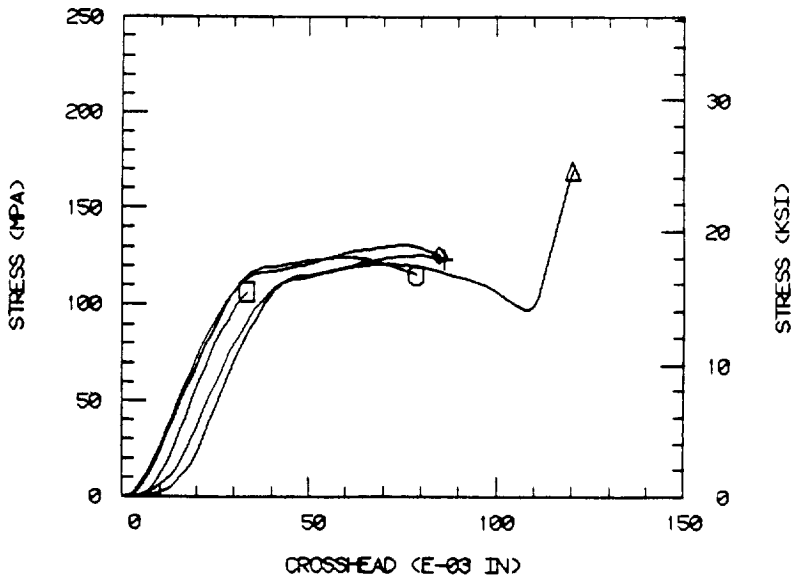

b. Stress-Displacement Plot

Figure B3. In-plane (12) Iosipescu Shear Stress-Strain and Stress-Displacement Plots for Orthogonal Layup Oxford Weave T300/934 Graphite/Epoxy Composite, Panel No. 2.

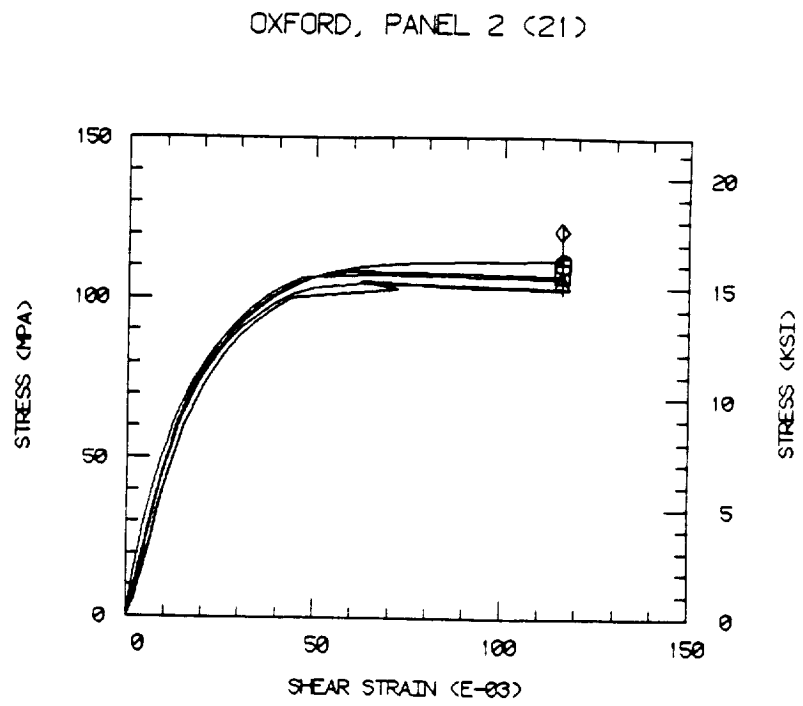

a. Stress-Strain Plot

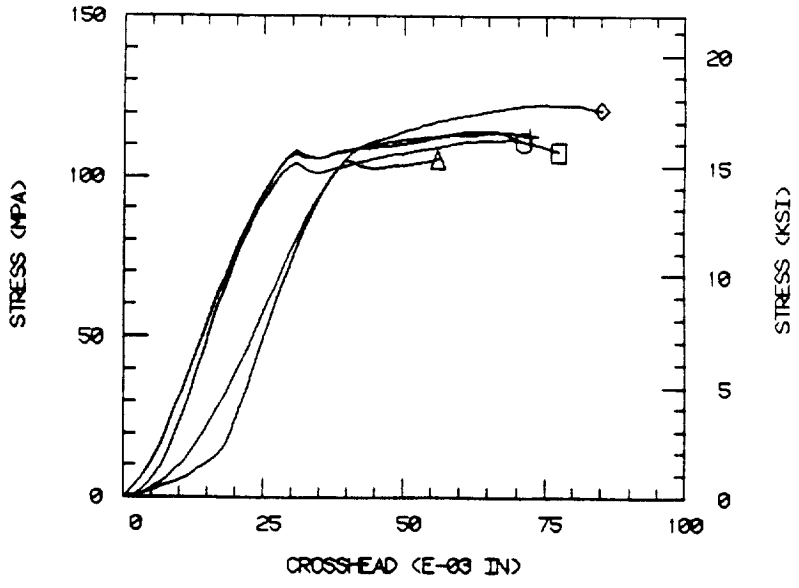

b. Stress-Displacement Plot

Figure B4. In-plane (21) Iosipescu Shear Stress-Strain and Stress-Displacement Plots for Orthogonal Layup Oxford Weave T300/934 Graphite/Epoxy Composite, Panel No. 2.

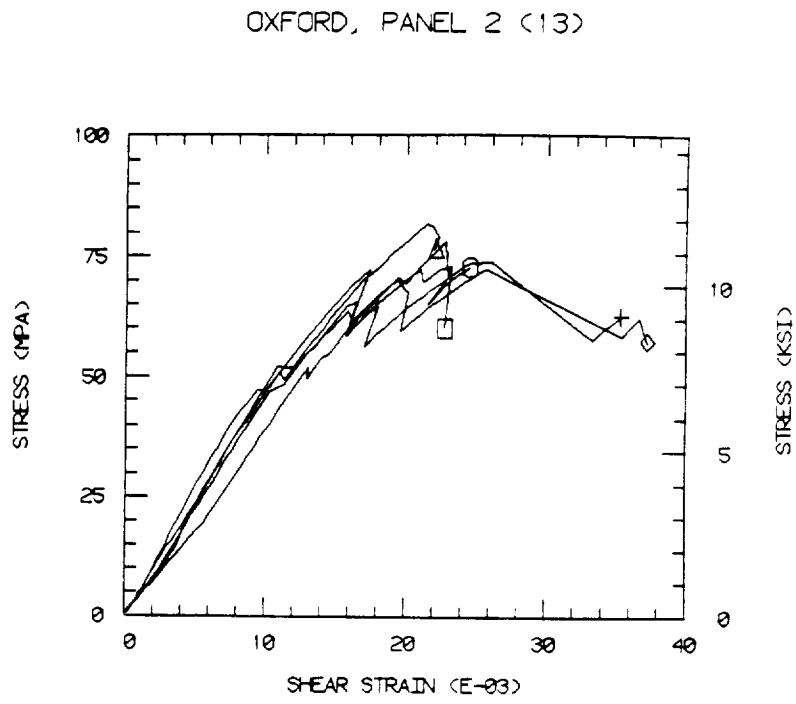

a. Stress-Strain Plot

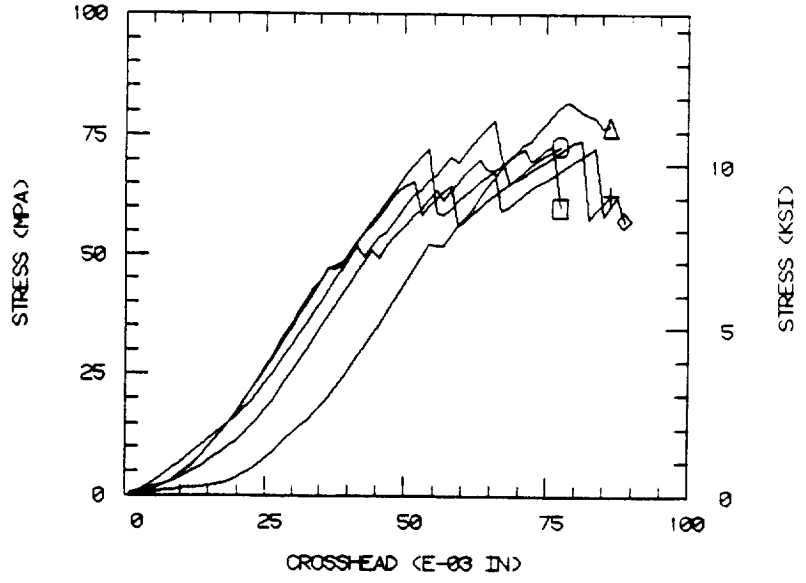

b. Stress-Displacement Plot

Figure B5. Interlaminar (13) Iosipescu Shear Stress-Strain and Stress-Displacement Plots for Orthogonal Layup Oxford Weave T300/934 Graphite/Epoxy Composite, Panel No. 2.

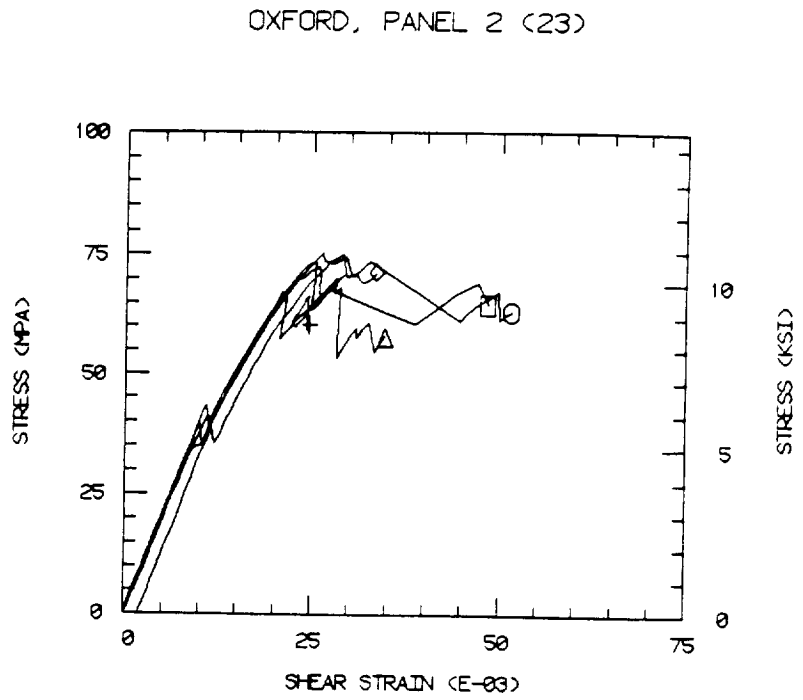

a. Stress-Strain Plot

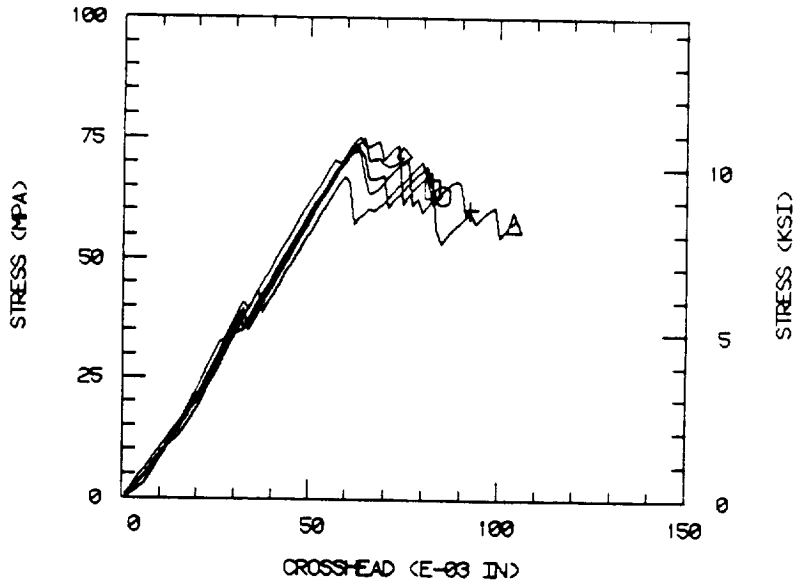

b. Stress-Displacement Plot

Figure B6. Interlaminar (23) Iosipescu Shear Stress-Strain and Stress-Displacement Plots for Orthogonal Layup Oxford Weave T300/934 Graphite/Epoxy Composite, Panel No. 2.

TABLE B3

SHEAR STRENGTH AND SHEAR MODULUS OF QUASI-ISOTROPIC LAYUP OXFORD WEAVE T300/934 GRAPHITE/EPOXY COMPOSITE, PANEL NO. 3

Test Orientation	Specimen No.	Strength (MPa)	Strength (ksi)	Modulus (GPa)	Modulus (Msi)
12	1	250	36.2	14.3	2.08
	2	258	37.4	19.7*	2.86*
	3	254	36.8	10.6*	1.54*
	4	236	34.2	13.7	1.99
	5	221	32.0	10.3*	1.50*
	Average	244	35.3	14.0	2.03
	Std. Dev.	15	2.2		
21	1	234	33.9	18.1*	2.62*
	2	228	33.0	13.1	1.91
	3	217	31.4	16.2	2.35
	4	237	34.4	13.8	2.00
	5	240	34.8	13.0	1.89
	Average	231	33.5	14.0	2.04
	Std. Dev.	9	1.4	1.5	0.21
13	1	60	8.7	3.7	0.54
	2	62	9.0	3.9	0.56
	3	43*	6.2*	4.2	0.61
	Average	61	8.9	3.9	0.57
23	1	56	8.1	3.7	0.53
	2	60	8.7	3.7	0.54
	3	56	8.1	3.4	0.49
	Average	57	8.3	3.6	0.52

*not included in average

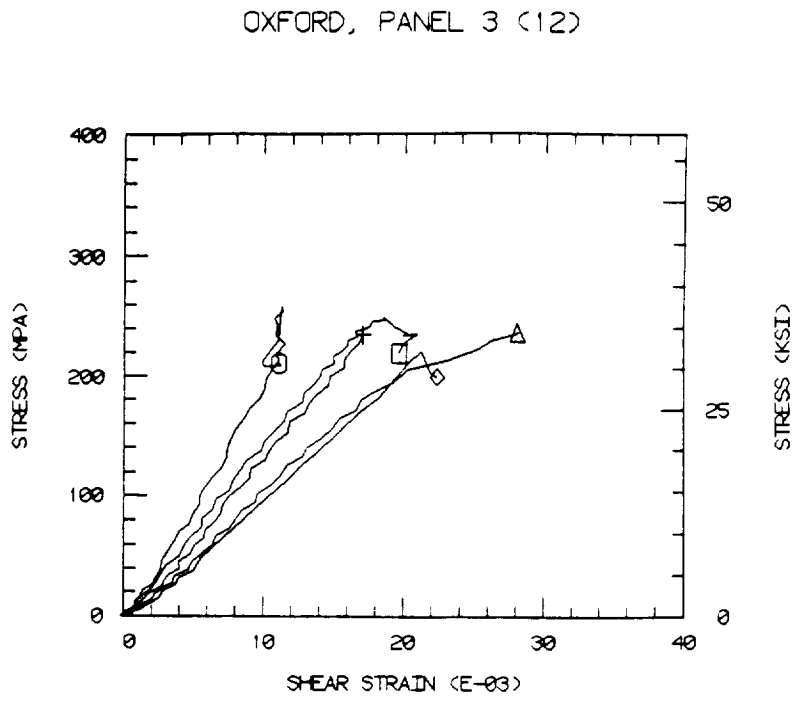

a. Stress-Strain Plot

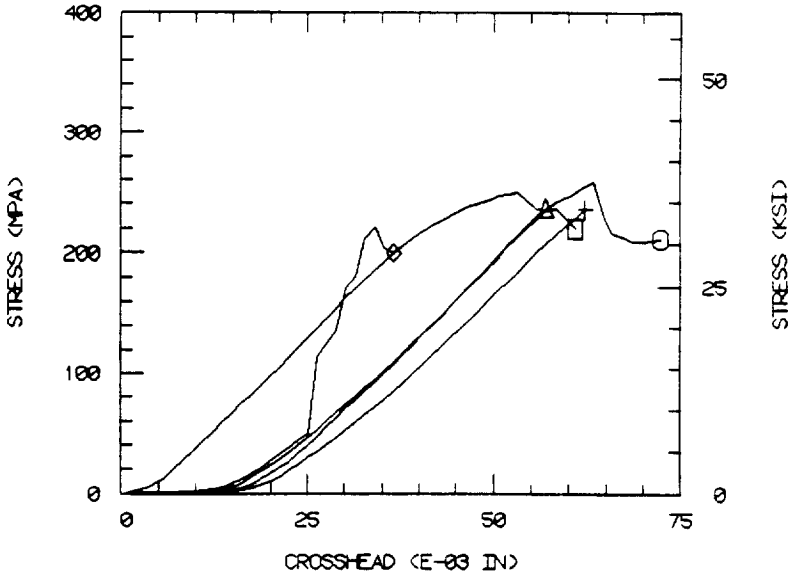

b. Stress-Displacement Plot

Figure B7. In-plane (12) Iosipescu Shear Stress-Strain and Stress-Displacement Plots for Quasi-Isotropic Layup Oxford Weave T300/934 Graphite/Epoxy Composite, Panel No. 3.

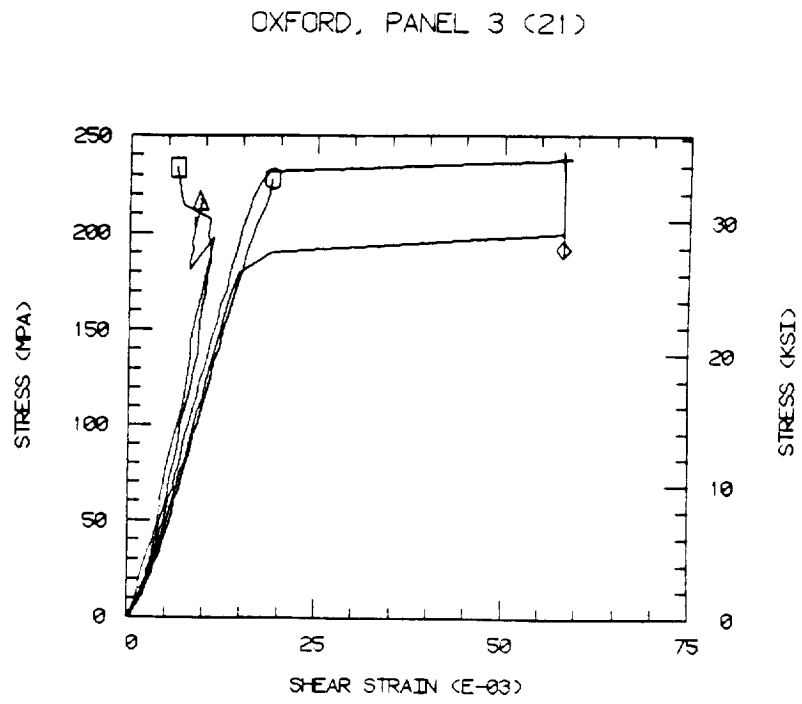

a. Stress-Strain Plot

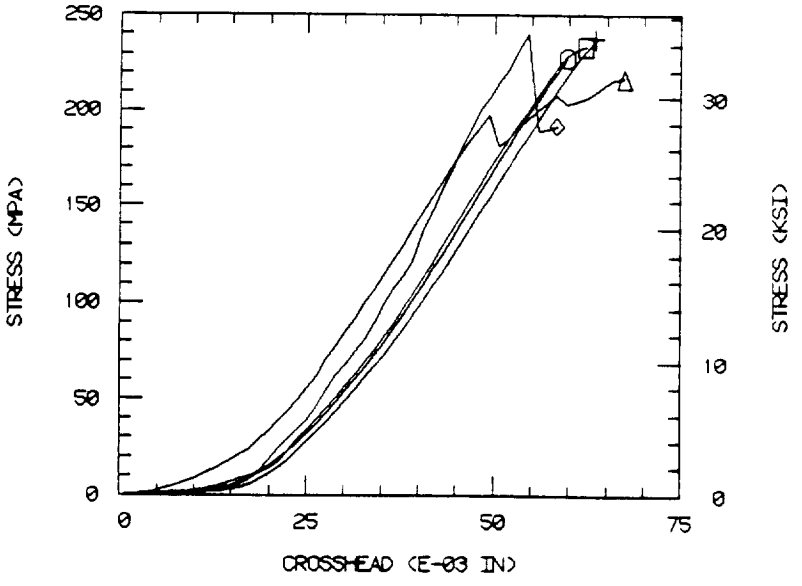

b. Stress-Displacement Plot

Figure B8. In-plane (21) Iosipescu Shear Stress-Strain and Stress-Displacement Plots for Quasi-Isotropic Layup Oxford Weave T300/934 Graphite/Epoxy Composite, Panel No. 3.

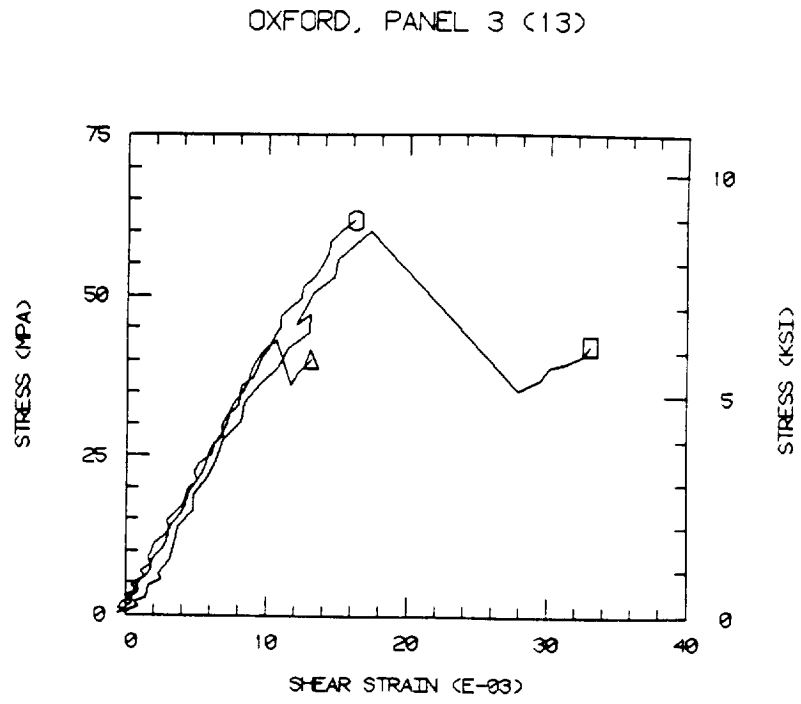

a. Stress-Strain Plot

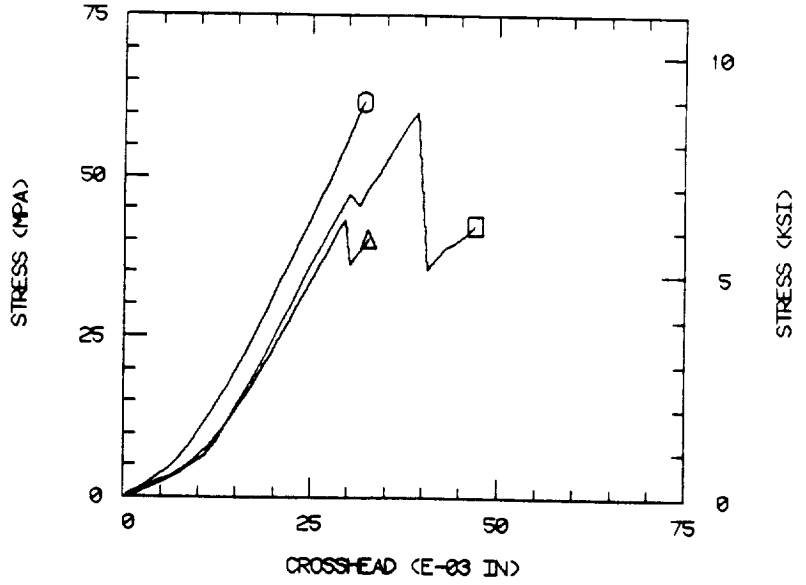

b. Stress-Displacement Plot

Figure B9. Interlaminar (13) Iosipescu Shear Stress-Strain and Stress-Displacement Plots for Quasi-Isotropic Layup Oxford Weave T300/934 Graphite/Epoxy Composite, Panel No. 3.

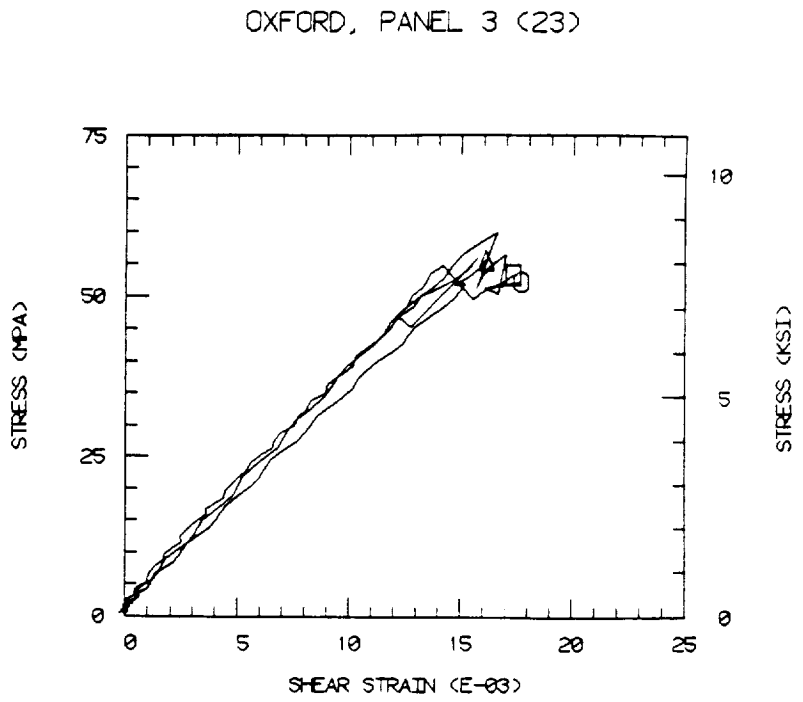

a. Stress-Strain Plot

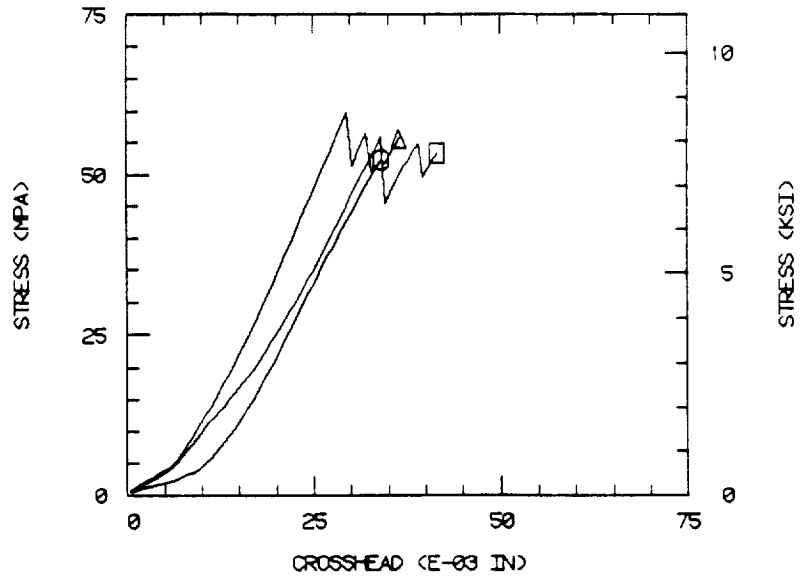

b. Stress-Displacement Plot

Figure B10. Interlaminar (23) Iosipescu Shear Stress-Strain and Stress-Displacement Plots for Quasi-Isotropic Layup Oxford Weave T300/934 Graphite/Epoxy Composite, Panel No. 3.

TABLE B4

SHEAR STRENGTH AND SHEAR MODULUS OF ORTHOGONAL LAYUP 5-HARNESS SATIN WEAVE T300/934 GRAPHITE/EPOXY COMPOSITE, PANEL NO. 4

Test Orientation	Specimen No.	Strength (MPa)	Strength (ksi)	Modulus (GPa)	Modulus (Msi)
12	1	114	16.5	5.2	0.76
	2	112	16.2	5.6	0.81
	3	115	16.7	5.7	0.83
	4	122	17.7	5.4	0.79
	5	121	17.5	5.6	0.81
	Average	117	16.9	5.5	0.80
	Std. Dev.	4	0.6	0.2	0.03
21	1	137	19.8	5.9	0.86
	2	131	19.0	5.0	0.73
	3	129	18.7	5.7	0.83
	4	123	17.9	5.1	0.74
	5	137	19.8	5.2	0.75
	Average	131	19.0	5.4	0.78
	Std. Dev.	6	0.8	0.4	0.06

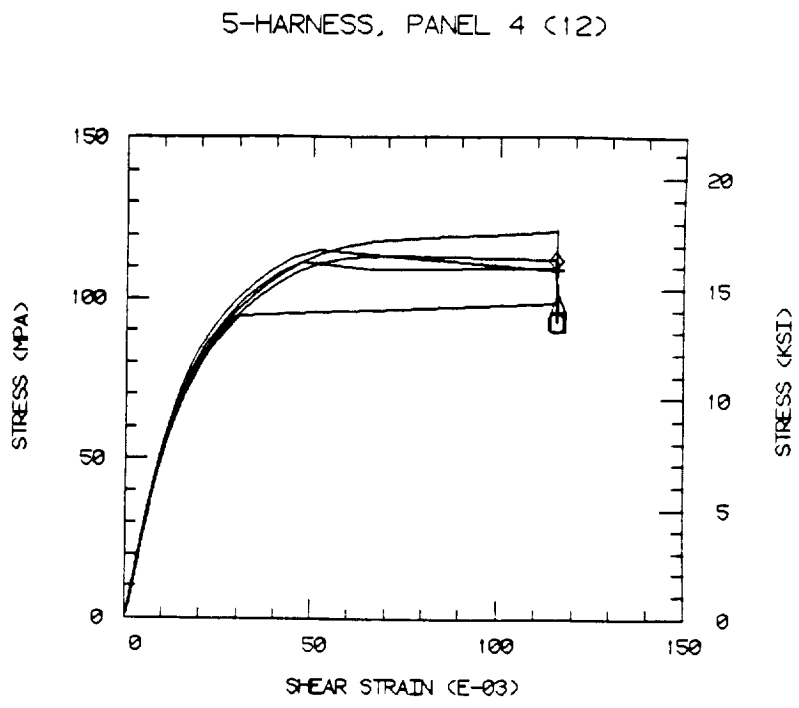

a. Stress-Strain Plot

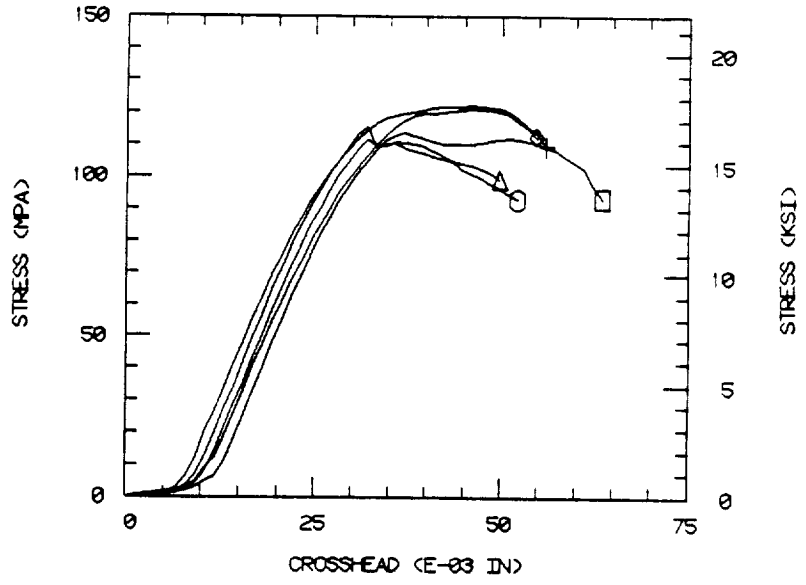

b. Stress-Displacement Plot

Figure B11. In-plane (12) Iosipescu Shear Stress-Strain and Stress-Displacement Plots for Orthogonal Layup 5-Harness Satin Weave T300/934 Graphite/Epoxy Composite, Panel No. 4.

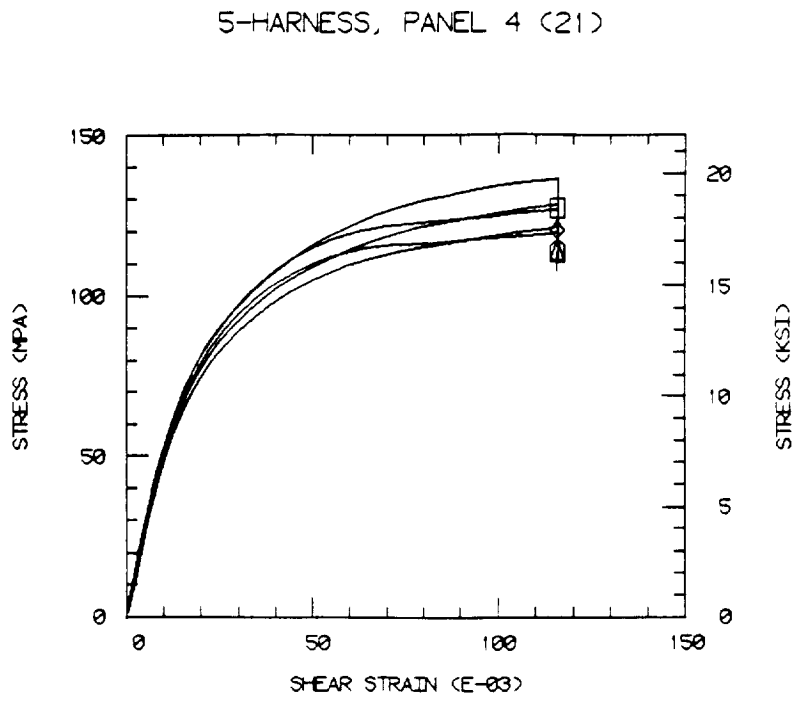

a. Stress-Strain Plot

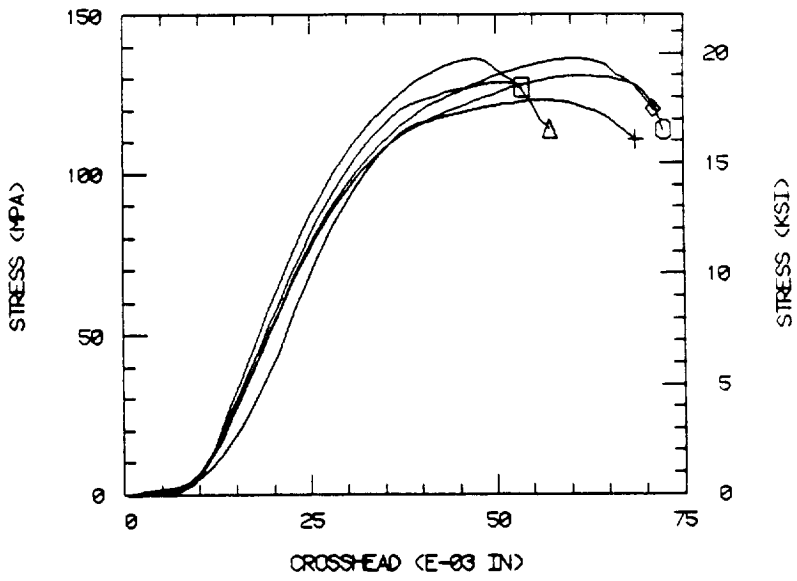

b. Stress-Displacement Plot

Figure B12. In-plane (21) Iosipescu Shear Stress-Strain and Stress-Displacement Plots for Orthogonal Layup 5-Harness Satin Weave T300/934 Graphite/Epoxy Composite, Panel No. 4.

TABLE B5

SHEAR STRENGTH AND SHEAR MODULUS OF ORTHOGONAL LAYUP 5-HARNESS SATIN WEAVE T300/934 GRAPHITE/EPOXY COMPOSITE, PANEL NO. 5

Test Orientation	Specimen No.	Strength (MPa)	Strength (ksi)	Modulus (GPa)	Modulus (Msi)
12	1	130	18.9	4.8	0.69
	2	128	18.5	5.4	0.78
	3	129	18.8	4.9	0.71
	Average	129	18.7	5.0	0.73
21	1	133	19.3	5.0	0.73
	2	137	19.8	4.9	0.71
	3	134	19.4	4.9	0.71
	4	129	18.7	5.1	0.74
	5	131	19.0	5.2	0.75
	6	131	19.0	5.0	0.72
	Average	132	19.2	5.0	0.73
	Std. Dev.	3	0.4	0.1	0.02
13	1	74	10.8	4.5	0.65
	2	77	11.1	4.5	0.65
	3	76	11.0	4.1	0.59
	4	72	10.5	3.8	0.55
	5	75	10.9	4.1	0.60
	Average	75	10.9	4.2	0.61
	Std. Dev.	2	0.2	0.3	0.04
23	1	80	11.6	3.7	0.53
	2	74	10.8	3.8	0.55
	3	68	9.8	3.6	0.52
	4	79	11.4	3.6	0.52
	5	74	10.7	4.2	0.61
	Average	75	10.9	3.8	0.55
	Std. Dev.	5	0.7	0.2	0.04

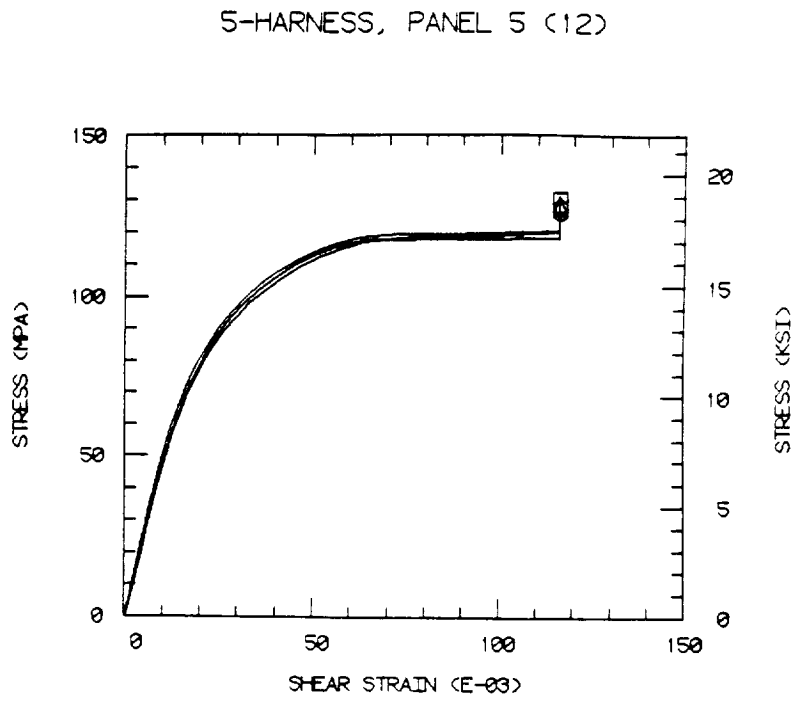

a. Stress-Strain Plot

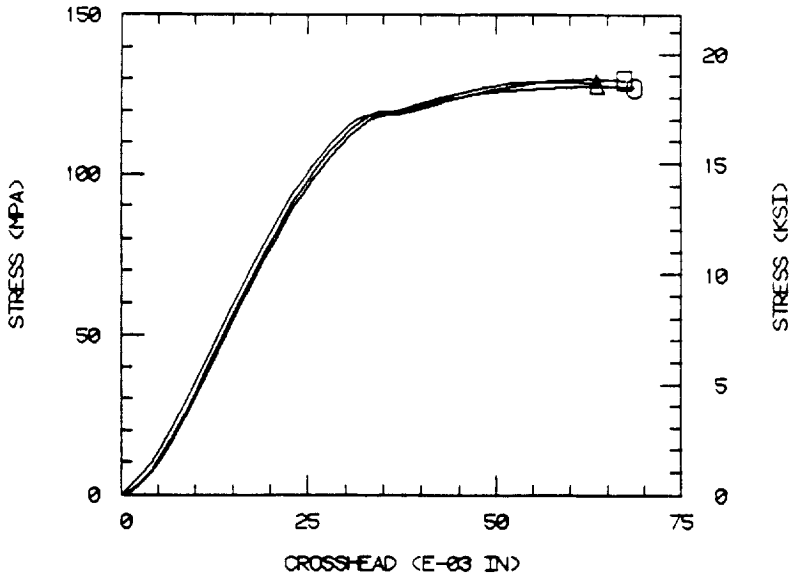

b. Stress-Displacement Plot

Figure B13. In-plane (12) Iosipescu Shear Stress-Strain and Stress-Displacement Plots for Orthogonal Layup 5-Harness Satin Weave T300/934 Graphite/Epoxy Composite, Panel No. 5.

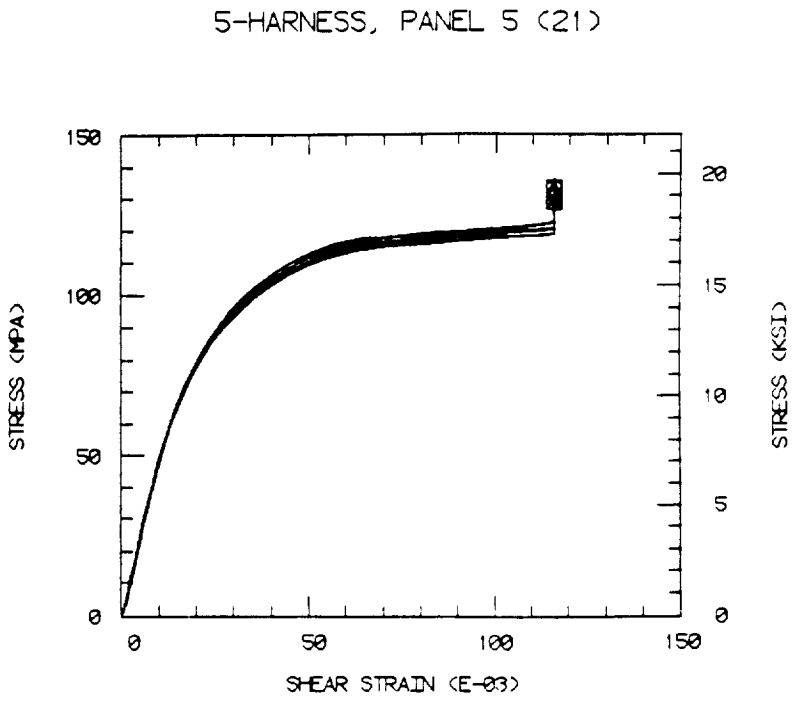

a. Stress-Strain Plot

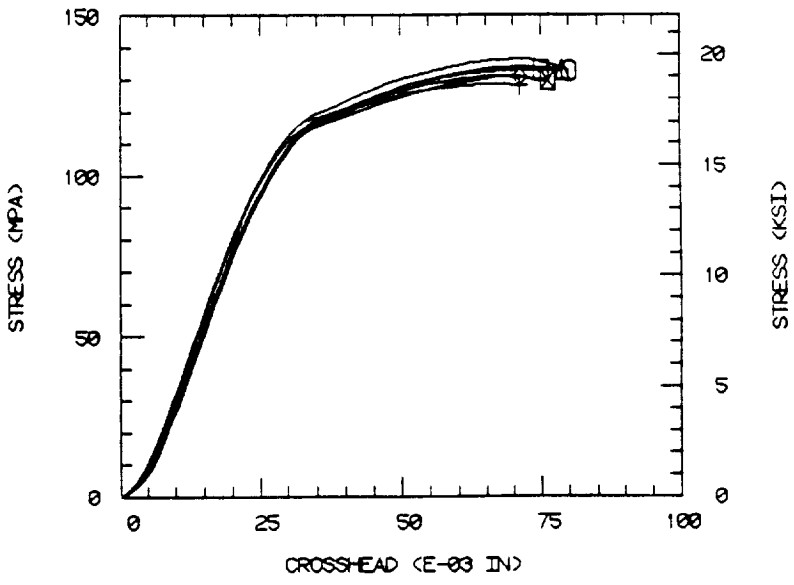

b. Stress-Displacement Plot

Figure B14. In-plane (21) Iosipescu Shear Stress-Strain and Stress-Displacement Plots for Orthogonal Layup 5-Harness Satin Weave T300/934 Graphite/Epoxy Composite, Panel No. 5.

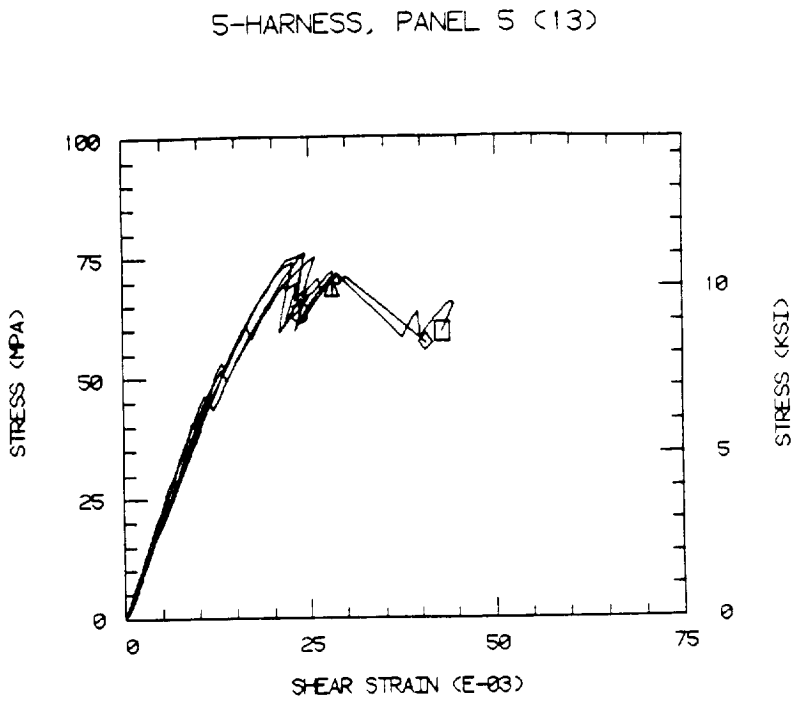

a. Stress-Strain Plot

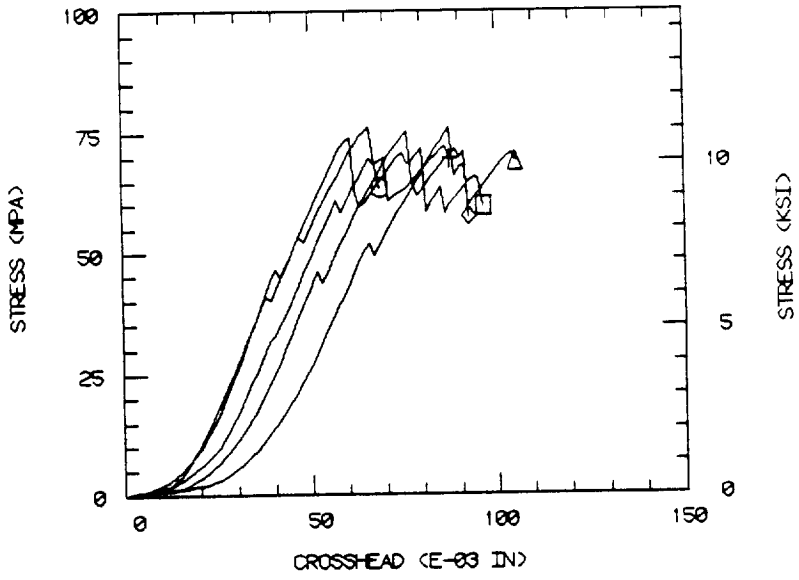

b. Stress-Displacement Plot

Figure B15. Interlaminar (13) Iosipescu Shear Stress-Strain and Stress-Displacement Plots for Orthogonal Layup 5-Harness Satin Weave T300/934 Graphite/Epoxy Composite, Panel No. 5.

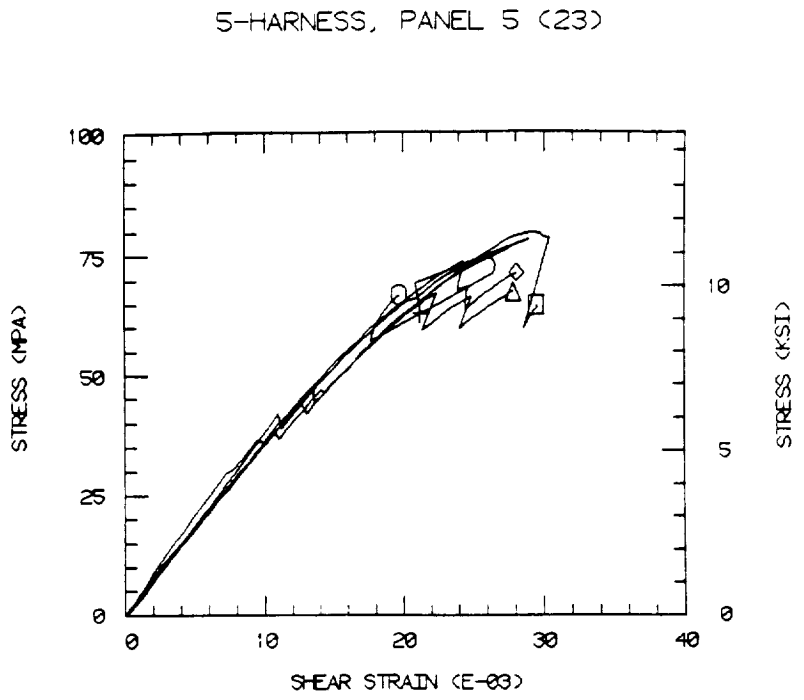

a. Stress-Strain Plot

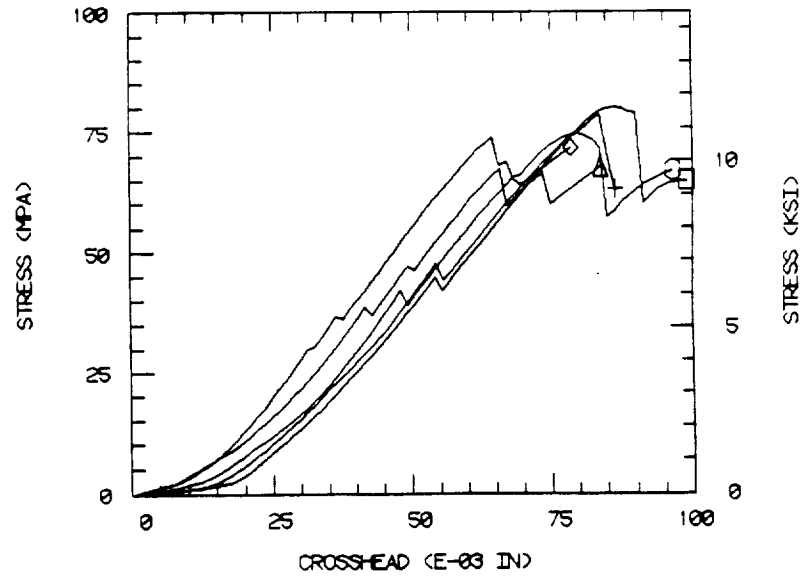

b. Stress-Displacement Plot

Figure B16. Interlaminar (23) Iosipescu Shear Stress-Strain and Stress-Displacement Plots for Orthogonal Layup 5-Harness Satin Weave T300/934 Graphite/Epoxy Composite, Panel No. 5.

TABLE B6

SHEAR STRENGTH AND SHEAR MODULUS OF QUASI-ISOTROPIC LAYUP 5-HARNESS SATIN WEAVE T300/934 GRAPHITE/EPOXY COMPOSITE, PANEL NO. 6

Test Orientation	Specimen No.	Strength (MPa)	Strength (ksi)	Modulus (GPa)	Modulus (Msi)
12	1	239	34.7	14.5	2.10
	2	223	32.4	14.1	2.04
	3	256	37.1	19.3*	2.80*
	4	273	39.6	13.4	1.94
	5	266	38.6	13.7	1.98
	Average	252	36.5	13.9	2.01
	Std. Dev.	20	2.9	0.5	0.07
21	1	285	41.3	14.5	2.10
	2	246	35.7	14.8	2.15
	3	231	33.5	15.9	2.30
	4	228	33.0	13.0	1.89
	5	241	35.0	13.4	1.95
	Average	246	35.7	14.3	2.08
	Std. Dev.	23	3.3	1.1	0.16
13	1	59	8.5	3.9	0.57
	2	48	7.0	4.0	0.58
	3	69	10.0	4.1	0.59
	Average	59	8.5	4.0	0.58
23	1	59	8.6	3.0	0.44
	2	48	7.0	2.3*	0.34*
	3	68	9.9	4.0	0.58
	Average	59	8.5	3.5	0.51

*not included in average

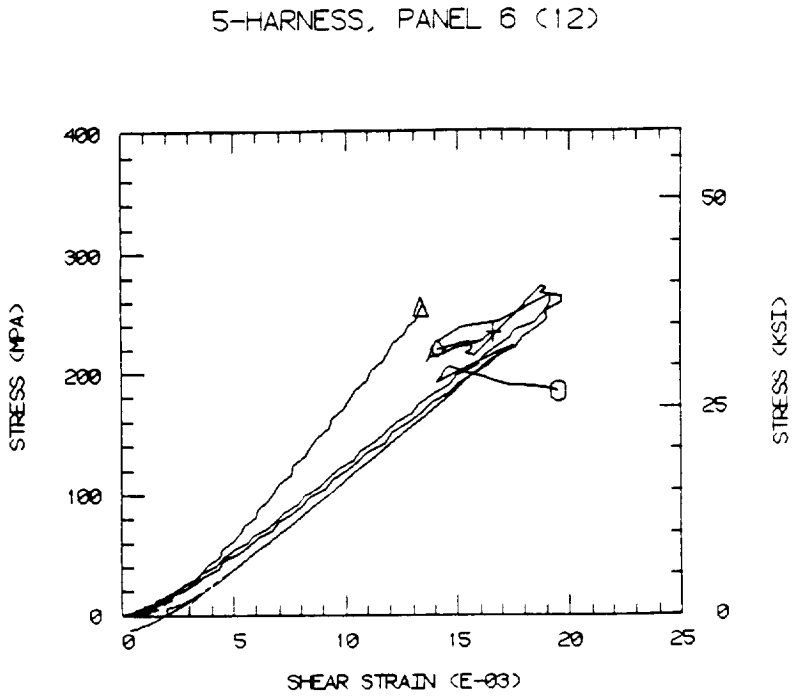

a. Stress-Strain Plot

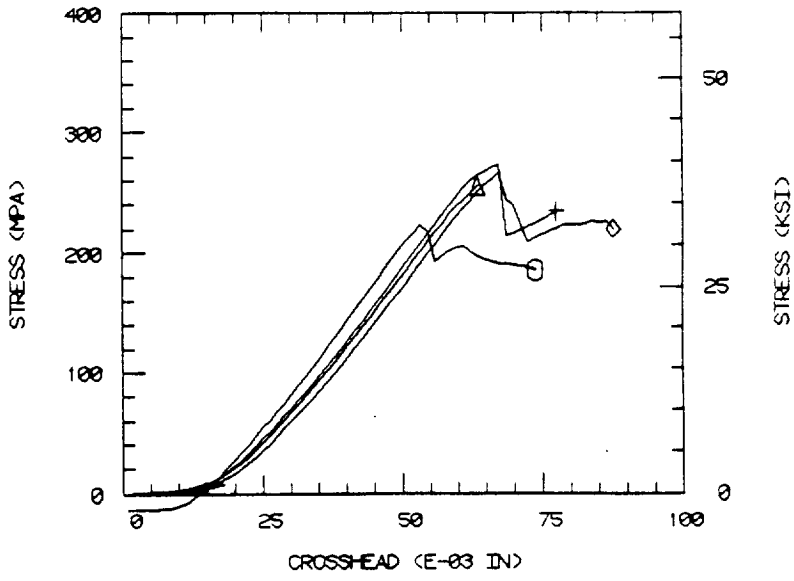

b. Stress-Displacement Plot

Figure B17. In-plane (12) Iosipescu Shear Stress-Strain and Stress-Displacement Plots for Quasi-Isotropic Layup 5-Harness Satin Weave T300/934 Graphite/Epoxy Composite, Panel No. 6.

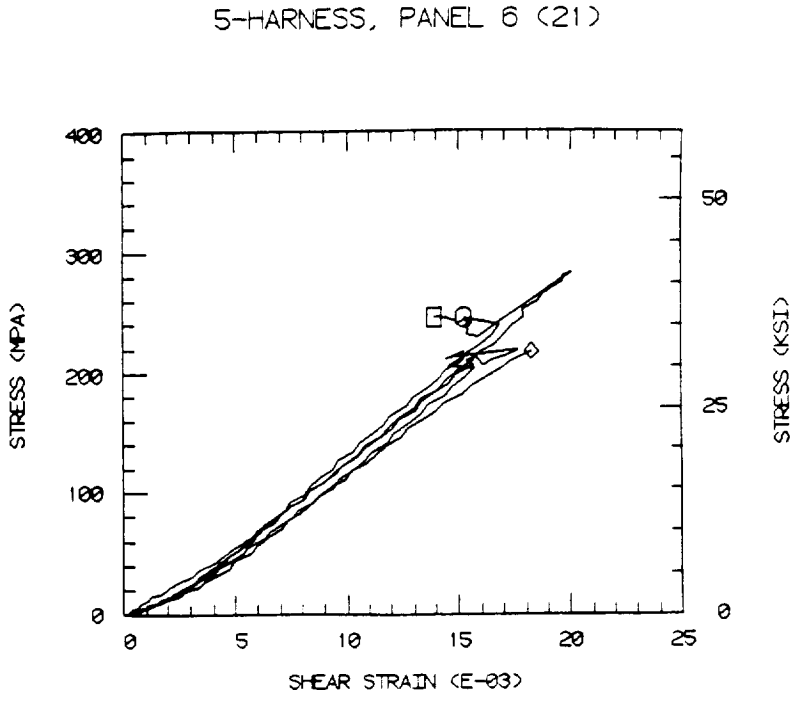

a. Stress-Strain Plot

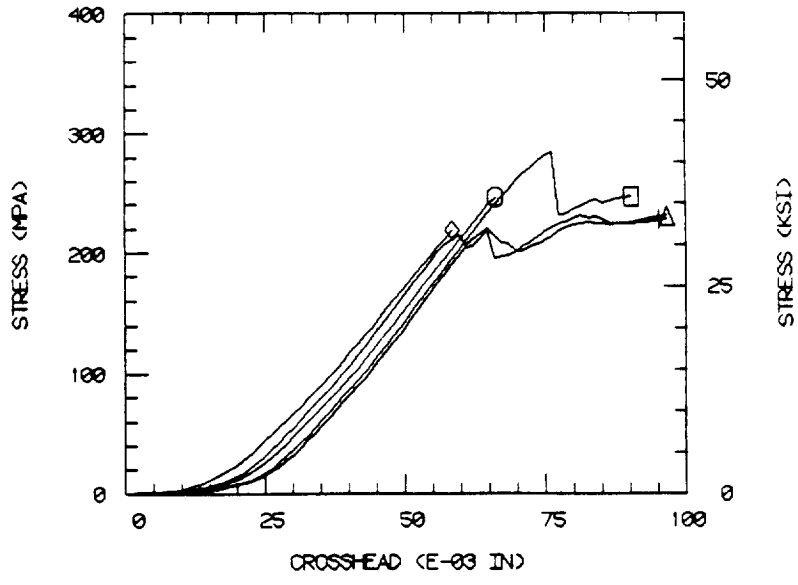

b. Stress-Displacement Plot

Figure B18. In-plane (21) Iosipescu Shear Stress-Strain and Stress-Displacement Plots for Quasi-Isotropic Layup 5-Harness Satin Weave T300/934 Graphite/Epoxy Composite, Panel No. 6.

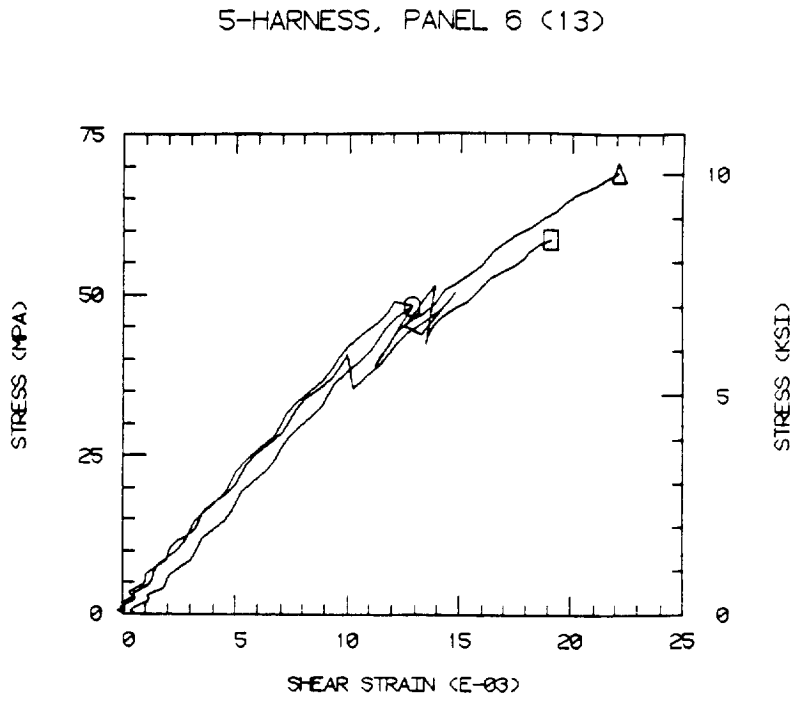

a. Stress-Strain Plot

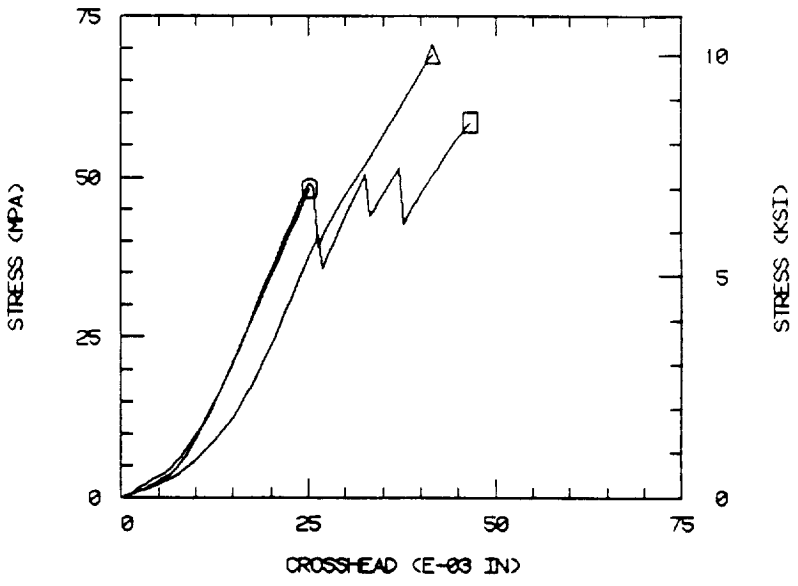

b. Stress-Displacement Plot

Figure B19. Interlaminar (13) Iosipescu Shear Stress-Strain and Stress-Displacement Plots for Quasi-Isotropic Layup 5-Harness Satin Weave T300/934 Graphite/Epoxy Composite, Panel No. 6.

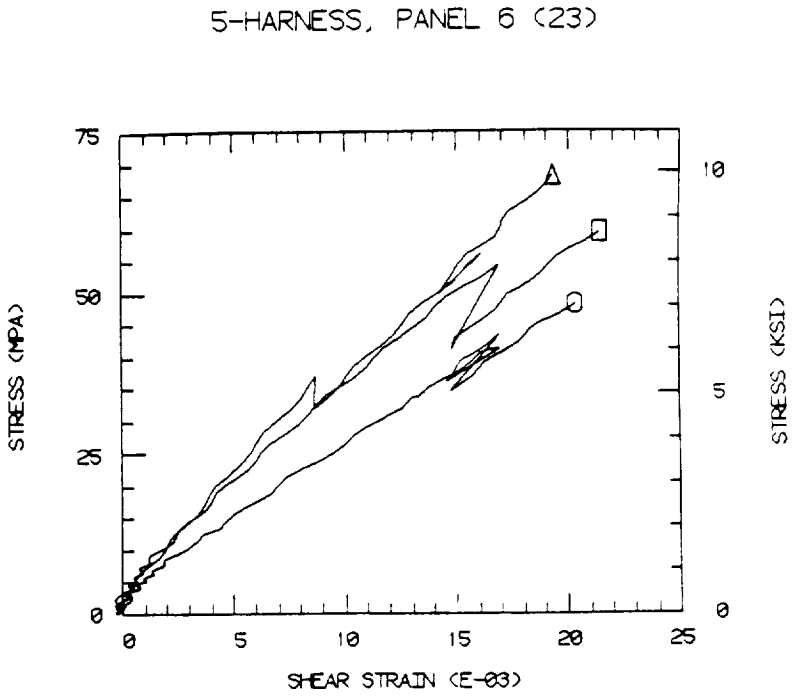

a. Stress-Strain Plot

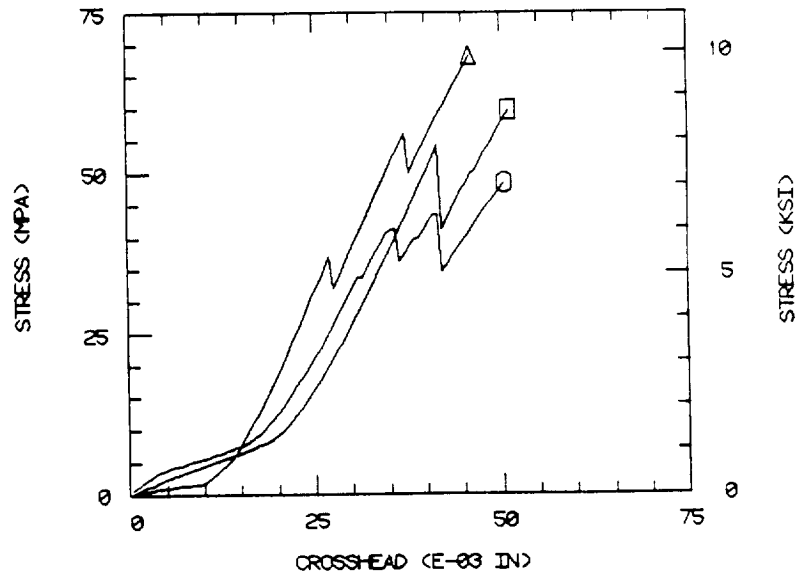

b. Stress-Displacement Plot

Figure B20. Interlaminar (23) Iosipescu Shear Stress-Strain and Stress-Displacement Plots for Quasi-Isotropic Layup 5-Harness Satin Weave T300/934 Graphite/Epoxy Composite, Panel No. 6.

TABLE B7

SHEAR STRENGTH AND SHEAR MODULUS OF ORTHOGONAL LAYUP 8-HARNESS SATIN WEAVE T300/934 GRAPHITE/EPOXY COMPOSITE, PANEL NO. 7

Test Orientation	Specimen No.	Strength (MPa)	Strength (ksi)	Modulus (GPa)	Modulus (Msi)
12	1	121	17.5	5.5	0.80
	2	127	18.4	5.4	0.78
	3	118	17.1	5.4	0.78
	4	117	16.9	5.4	0.79
	5	121	17.5	5.7	0.82
	Average	121	17.5	5.5	0.79
	Std. Dev.	4	0.6	0.1	0.02
21	1	132	19.1	5.4	0.79
	2	130	18.9	6.1	0.88
	3	130	18.9	5.5	0.80
	4	132	19.1	5.4	0.79
	5	133	19.3	5.5	0.80
	Average	132	19.1	5.6	0.81
	Std. Dev.	1	0.2	0.3	0.04

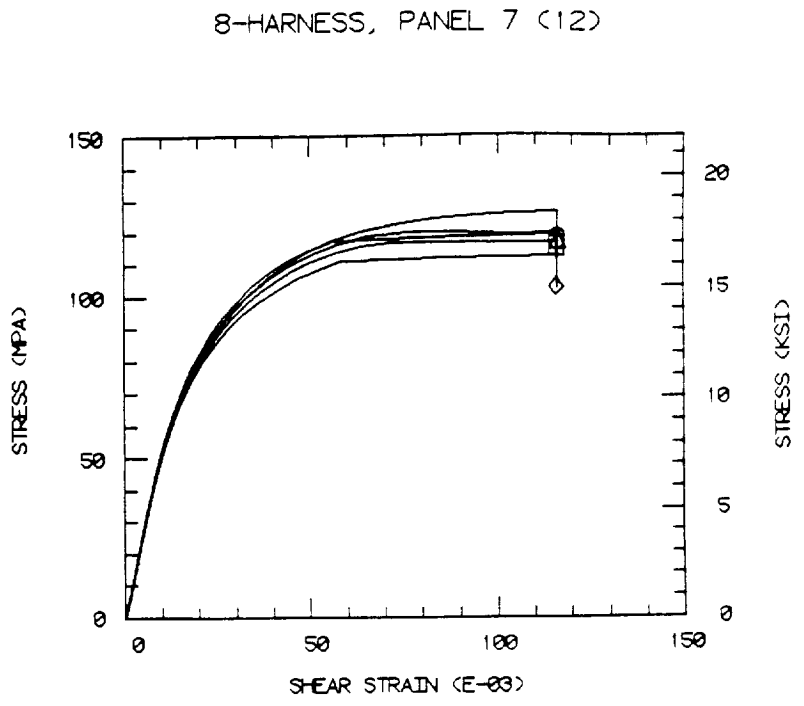

a. Stress-Strain Plot

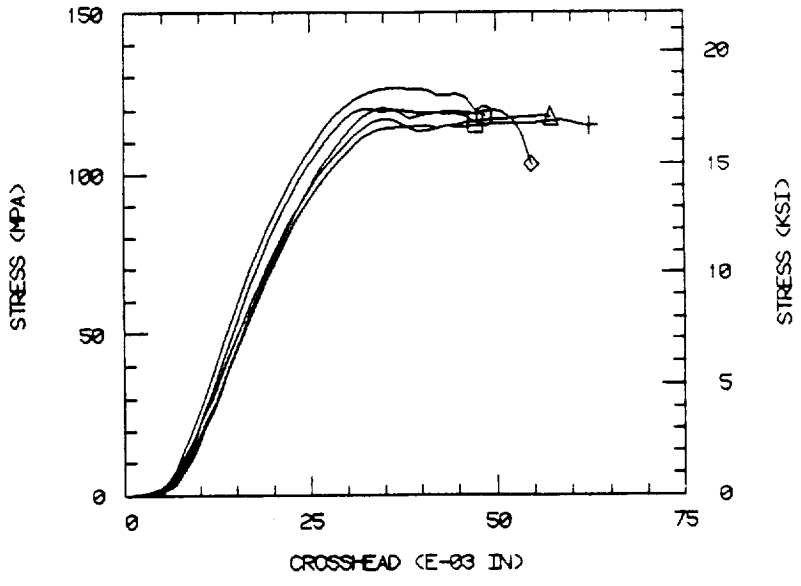

b. Stress-Displacement Plot

Figure B21. In-plane (12) Iosipescu Shear Stress-Strain and Stress-Displacement Plots for Orthogonal Layup 8-Harness Satin Weave T300/934 Graphite/Epoxy Composite, Panel No. 7.

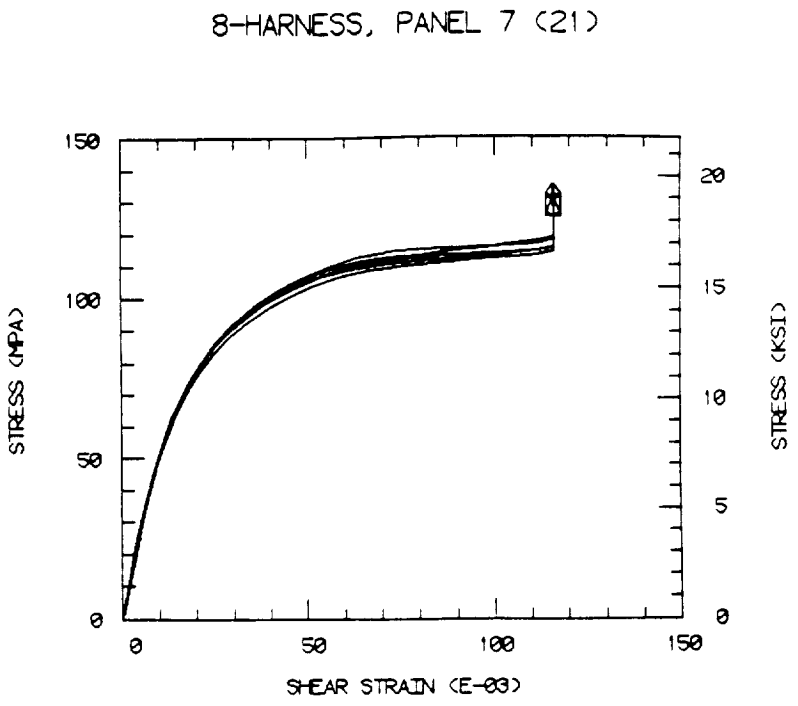

a. Stress-Strain Plot

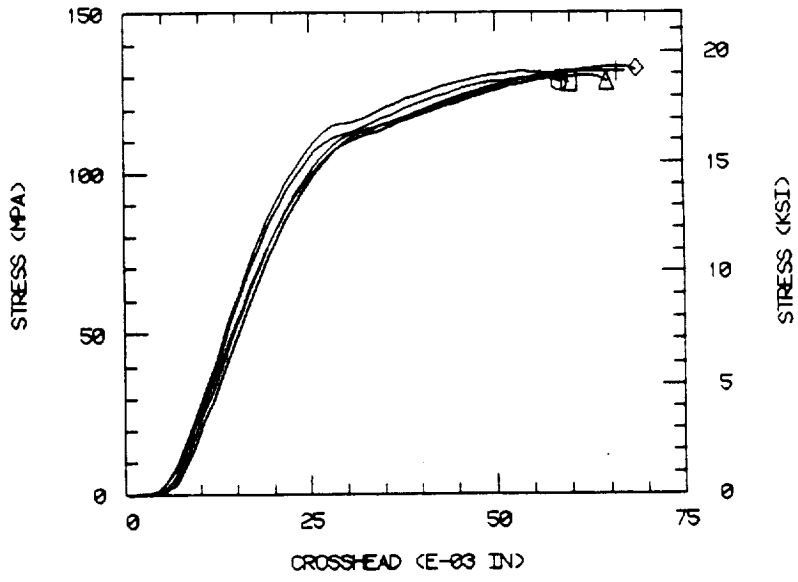

b. Stress-Displacement Plot

Figure B22. In-plane (21) Iosipescu Shear Stress-Strain and Stress-Displacement Plots for Orthogonal Layup 8-Harness Satin Weave T300/934 Graphite/Epoxy Composite, Panel No. 7.

TABLE B8

SHEAR STRENGTH AND SHEAR MODULUS OF ORTHOGONAL LAYUP 8-HARNESS SATIN WEAVE T300/934 GRAPHITE/EPOXY COMPOSITE, PANEL NO. 8

Test Orientation	Specimen No.	Strength (MPa)	Strength (ksi)	Modulus (GPa)	Modulus (Msi)
12	1	150	21.7	5.3	0.77
	2	143	20.7	4.8	0.69
	3	146	21.2	5.4	0.78
	Average	146	21.2	5.1	0.75
21	1	141	20.4	5.2	0.75
	2	123	17.9	5.2	0.76
	3	145	21.1	5.4	0.78
	Average	137	19.8	5.3	0.76
13	1	77	11.1	3.4	0.50
	4	72	10.4	3.2	0.47
	5	78	11.3	3.5	0.51
	6	78	11.3	3.4	0.49
	Average	76	11.0	3.4	0.49
	Std. Dev.	3	0.4	0.1	0.02
23	1	72	10.4	4.5	0.65
	2	70	10.2	3.7	0.54
	3	75	10.9	3.0	0.43
	4	52*	7.6*	3.2	0.46
	6	65	9.4	3.0	0.43
	Average	71	10.2	3.5	0.50
	Std. Dev.	4	0.6	0.6	0.1

*not included in average

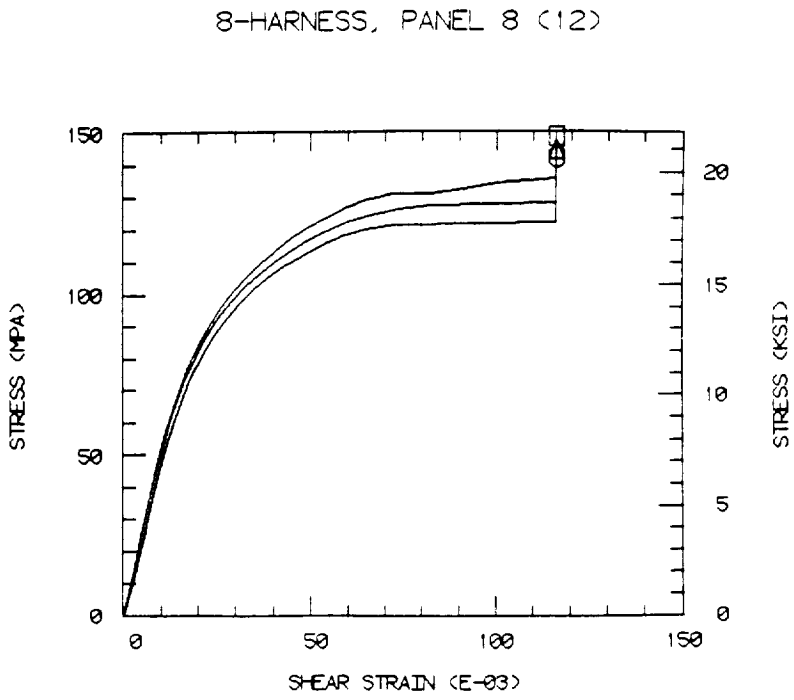

a. Stress-Strain Plot

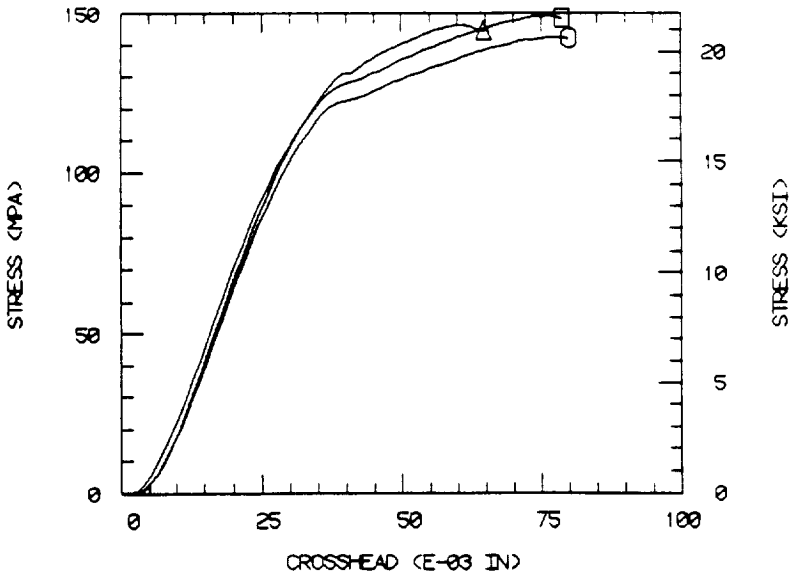

b. Stress-Displacement Plot

Figure B23. In-plane (12) Iosipescu Shear Stress-Strain and Stress-Displacement Plots for Orthogonal Layup 8-Harness Satin Weave T300/934 Graphite/Epoxy Composite, Panel No. 8.

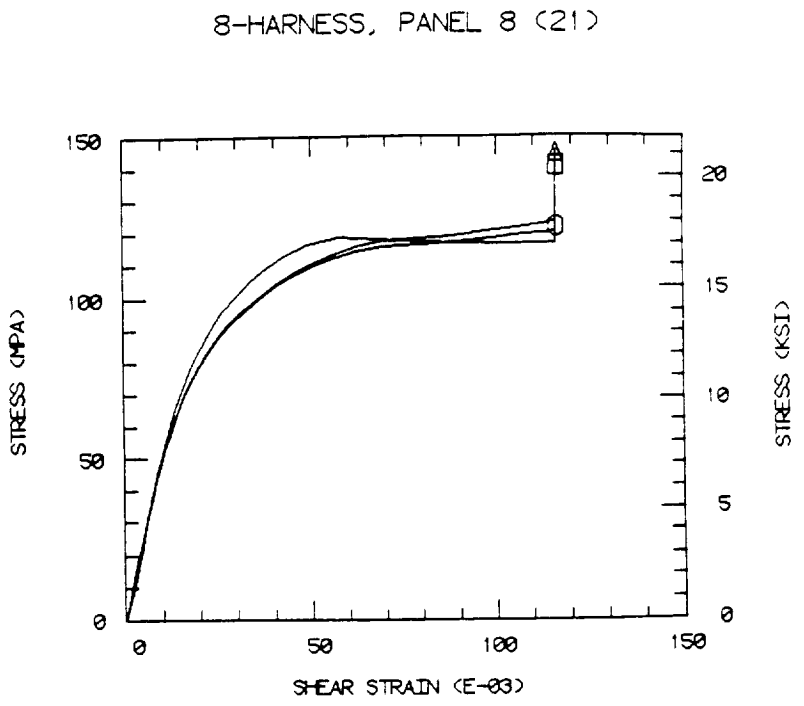

a. Stress-Strain Plot

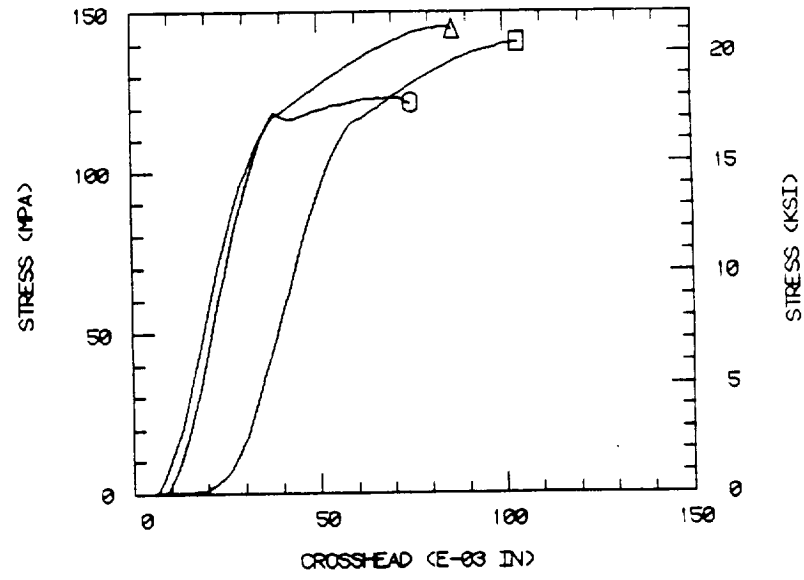

b. Stress-Displacement Plot

Figure B24. In-plane (21) Iosipescu Shear Stress-Strain and Stress-Displacement Plots for Orthogonal Layup 8-Harness Satin Weave T300/934 Graphite/Epoxy Composite, Panel No. 8.

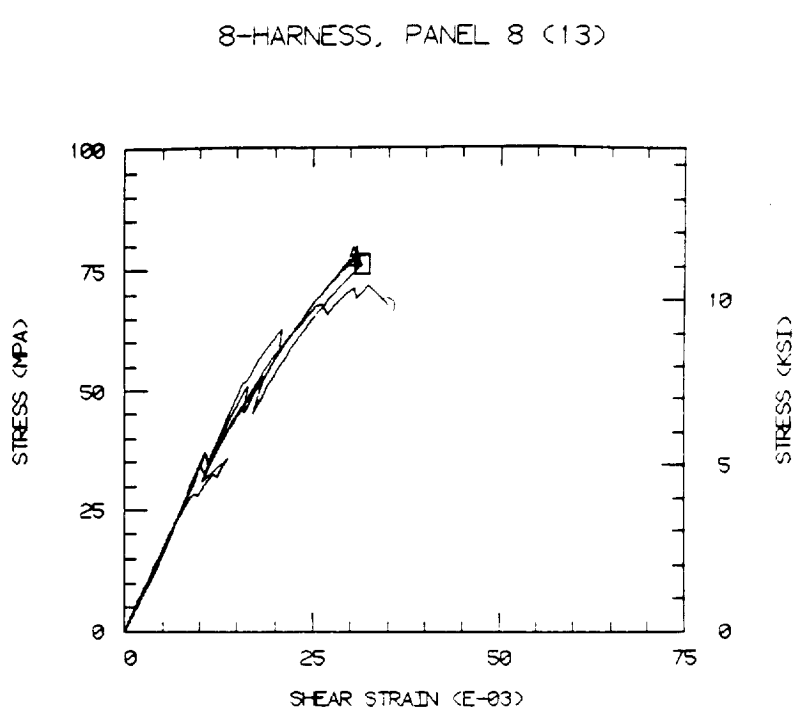

a. Stress-Strain Plot

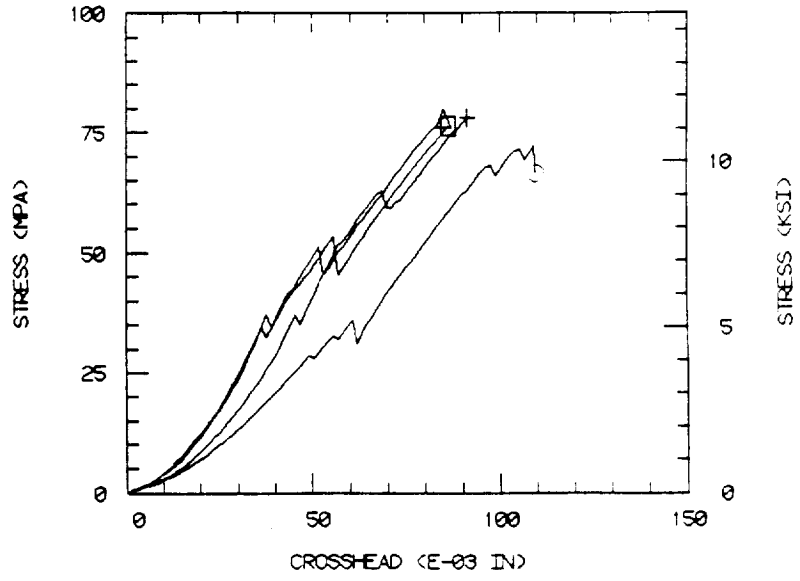

b. Stress-Displacement Plot

Figure B25. Interlaminar (13) Iosipescu Shear Stress-Strain and Stress-Displacement Plots for Orthogonal Layup 8-Harness Satin Weave T300/934 Graphite/Epoxy Composite, Panel No. 8.

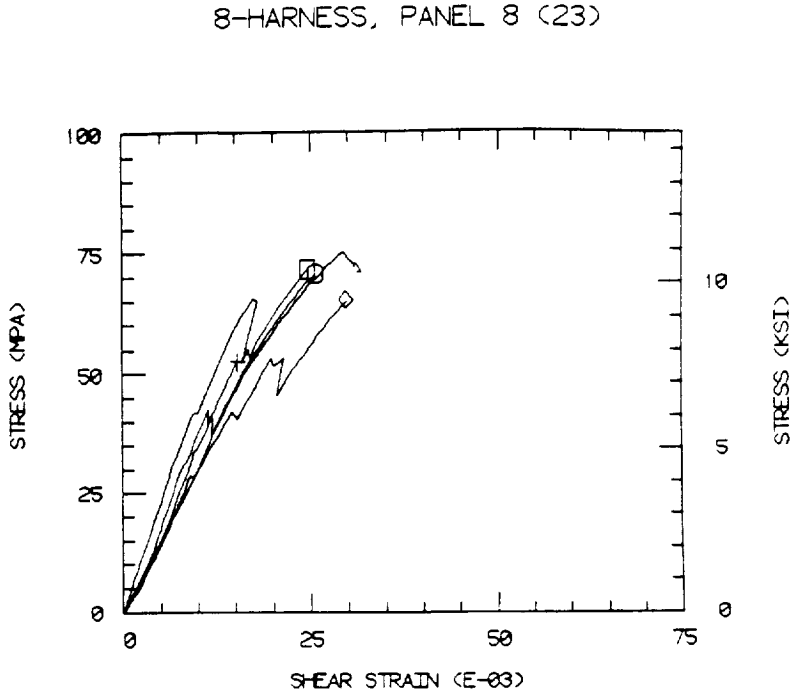

a. Stress-Strain Plot

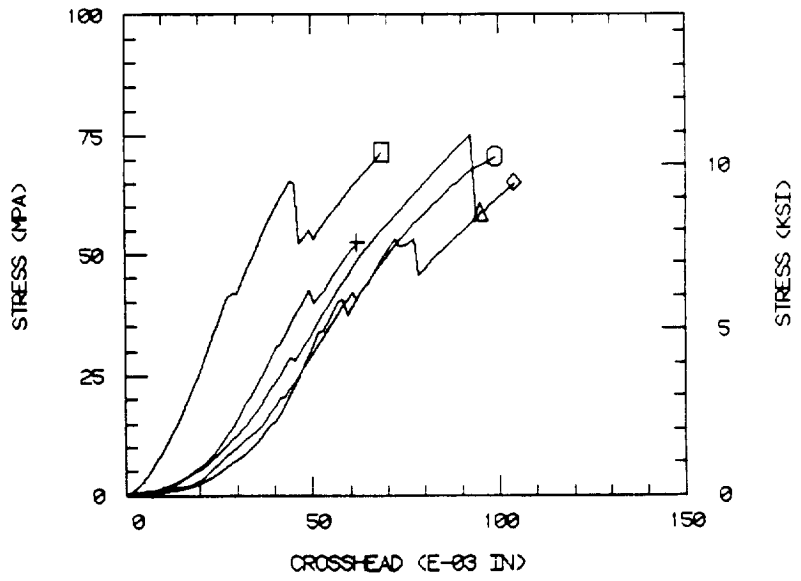

b. Stress-Displacement Plot

Figure B26. Interlaminar (23) Iosipescu Shear Stress-Strain and Stress-Displacement Plots for Orthogonal Layup 8-Harness Satin Weave T300/934 Graphite/Epoxy Composite, Panel No. 8.

TABLE B9

SHEAR STRENGTH AND SHEAR MODULUS OF QUASI-ISOTROPIC LAYUP 8-HARNESS SATIN WEAVE T300/934 GRAPHITE/EPOXY COMPOSITE, PANEL NO. 9

Test Orientation	Specimen No.	Strength (MPa)	Strength (ksi)	Modulus (GPa)	Modulus (Msi)
12	1	274	39.8	15.4	2.24
	2	276	40.0	15.2	2.20
	3	272	39.4	14.2	2.06
	4	270	39.2	14.1	2.04
	5	239	34.6	12.4*	1.80*
	Average	266	38.6	14.7	2.13
	Std. Dev.	16	2.3	0.7	0.10
21	2	250	36.2	15.6	2.26
	3	254	36.9	12.3	1.79
	4	261	37.9	16.3	2.36
	5	245	35.6	16.2	2.35
	Average	252	36.7	15.1	2.19
	Std. Dev.	7	1.0	1.9	0.27
13	1	56	8.1	3.5	0.51
	2	55	8.0	3.7	0.53
	3	67	9.7	4.3	0.62
	4	74	10.7	4.1	0.60
	Average	63	9.1	3.9	0.57
	Std. Dev.	9	1.3	0.4	0.05
23	1	48	7.0	3.7	0.53
	2	66	9.6	3.2	0.46
	3	52	7.6	4.1	0.59
	Average	56	8.1	3.7	0.53

*not included in average

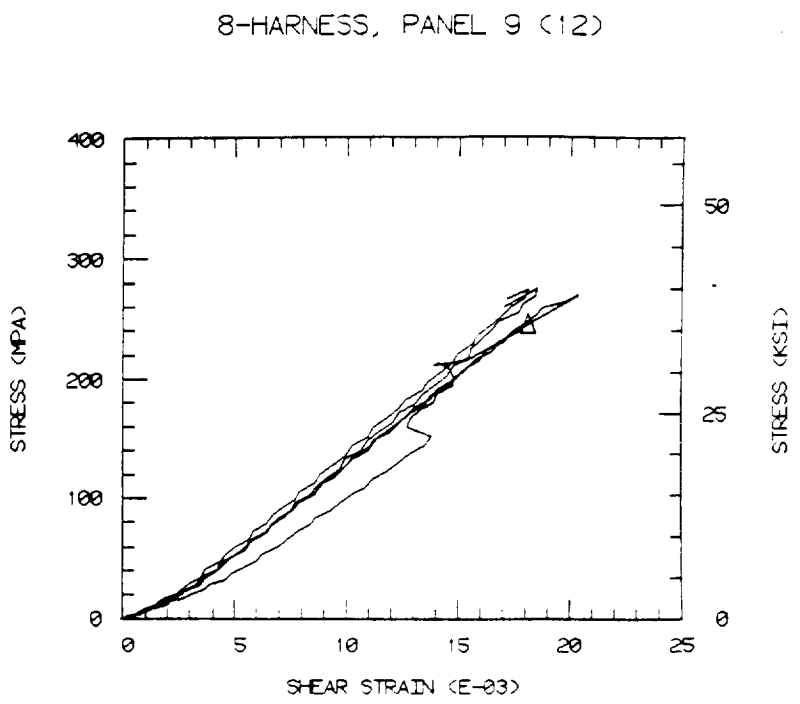

a. Stress-Strain Plot

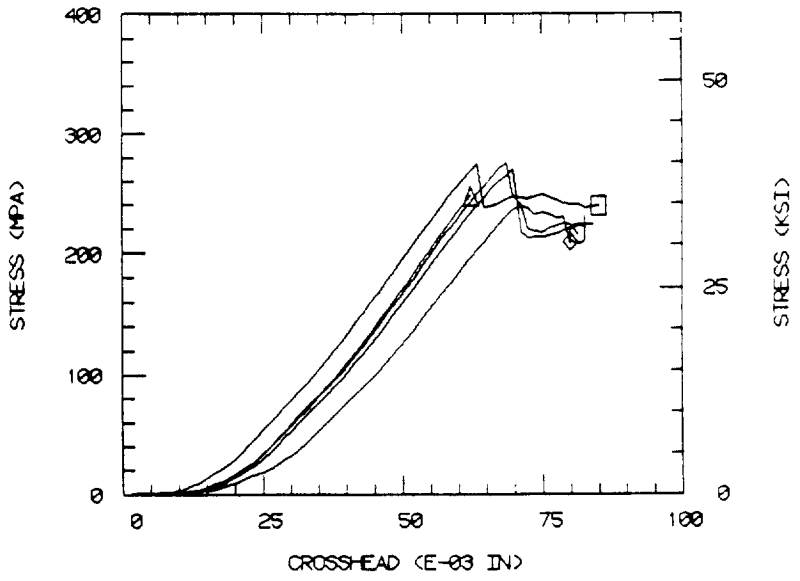

b. Stress-Displacement Plot

Figure B27. In-plane (12) Iosipescu Shear Stress-Strain and Stress-Displacement Plots for Quasi-Isotropic Layup 8-Harness Satin Weave T300/934 Graphite/Epoxy Composite, Panel No. 9.

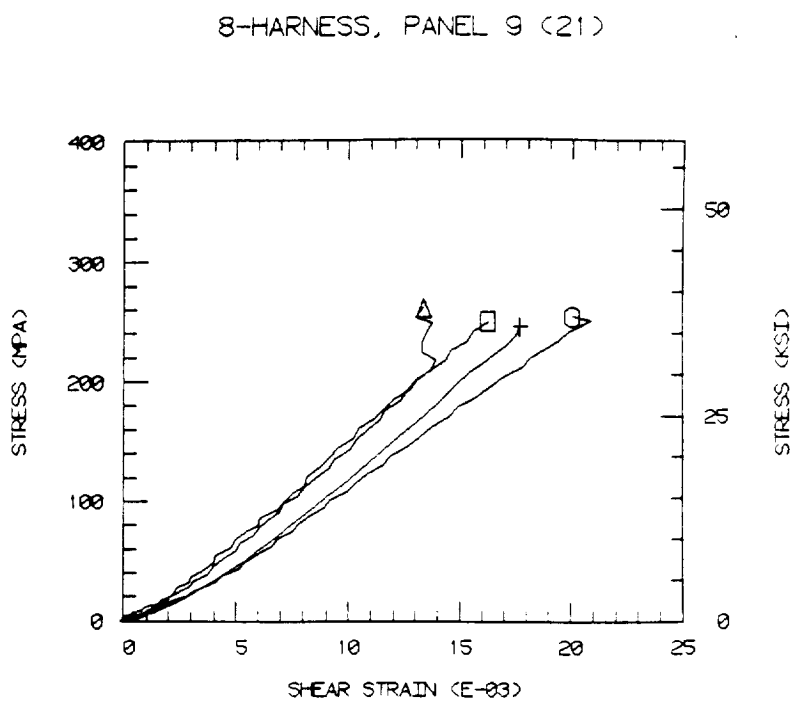

a. Stress-Strain Plot

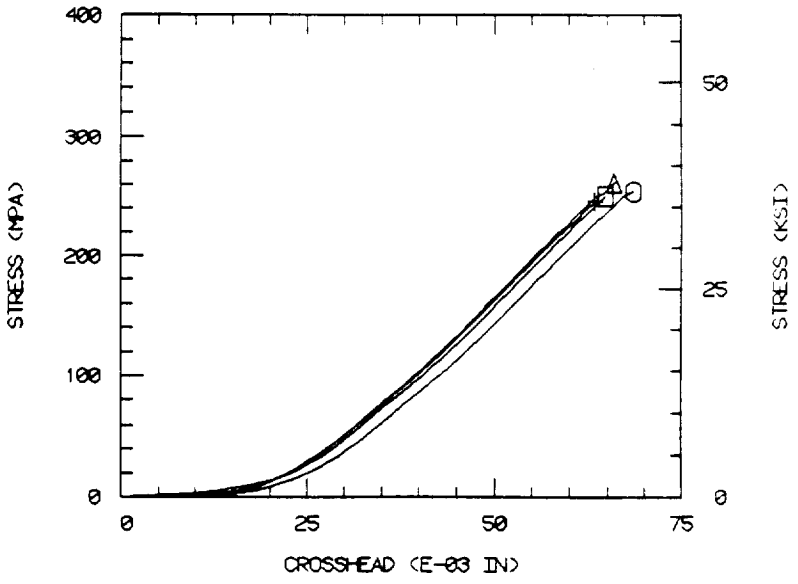

b. Stress-Displacement Plot

Figure B28. In-plane (21) Iosipescu Shear Stress-Strain and Stress-Displacement Plots for Quasi-Isotropic 8-Harness Satin Weave T300/934 Graphite/Epoxy Composite, Panel No. 9.

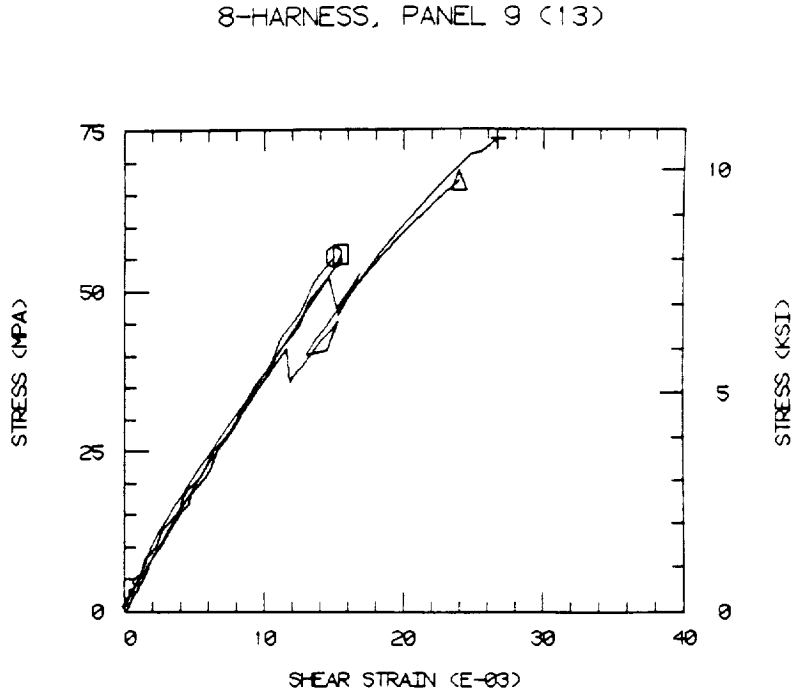

a. Stress-Strain Plot

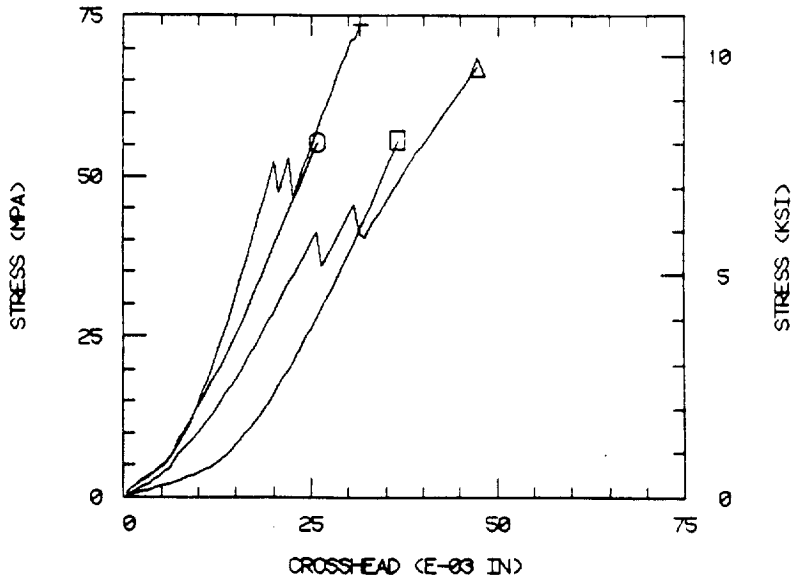

b. Stress-Displacement Plot

Figure B29. Interlaminar (13) Iosipescu Shear Stress-Strain and Stress-Displacement Plots for Quasi-Isotropic Layup 8-Harness Satin Weave T300/934 Graphite/Epoxy Composite, Panel No. 9.

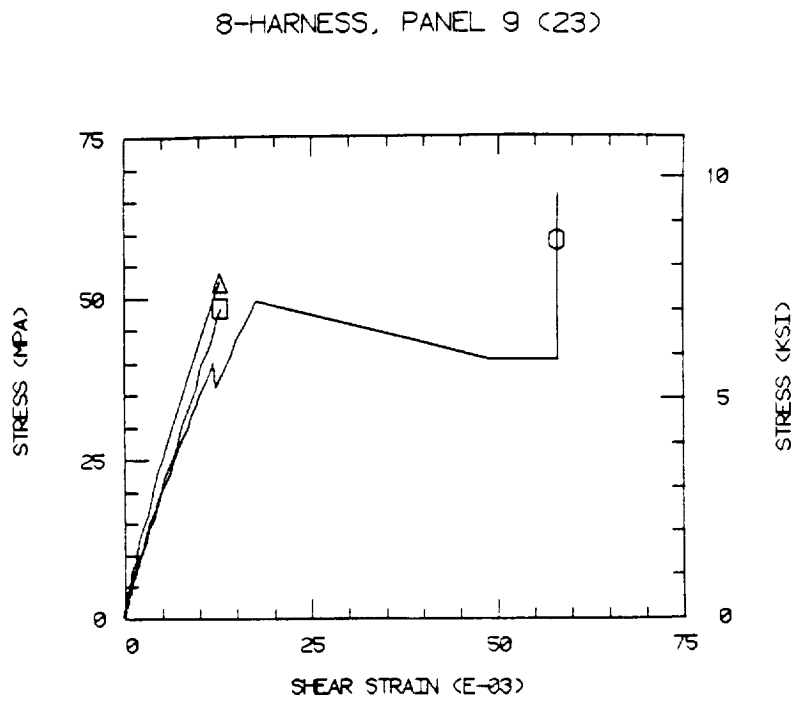

a. Stress-Strain Plot

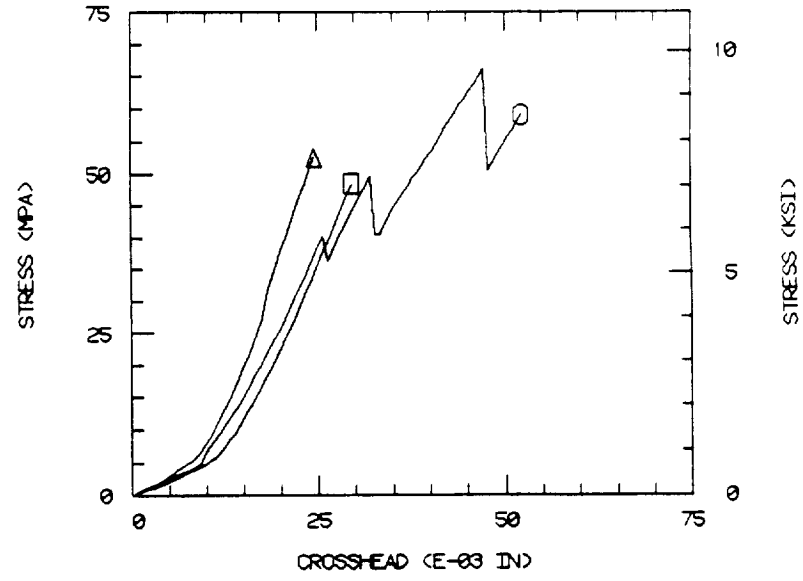

b. Stress-Displacement Plot

Figure B30. Interlaminar (23) Iosipescu Shear Stress-Strain and Stress-Displacement Plots for Quasi-Isotropic Layup 8-Harness Satin Weave T300/934 Graphite/Epoxy Composite, Panel No. 9.

TABLE B10

SHEAR STRENGTH AND SHEAR MODULUS OF ORTHOGONAL LAYUP PLAIN WEAVE AUXILIARY WARP T300/934 GRAPHITE/EPOXY COMPOSITE, PANEL NO. 18

Test Orientation	Specimen No.	Strength (MPa)	Strength (ksi)	Modulus (GPa)	Modulus (Msi)
12	1	121	17.6	3.7	0.54
	2	127	18.4	4.5	0.65
	3	121	17.5	3.4	0.50
	4	112	16.2	3.7	0.54
	5	103	14.9	3.9	0.57
	Average	117	16.9	3.9	0.56
	Std. Dev.	9	1.4	0.4	0.06
21	1	101	14.6	3.3	0.48
	2	100	14.5	3.7	0.53
	3	99	14.3	3.0	0.44
	4	108	15.6	3.7	0.54
	5	105	15.3	3.4	0.50
	Average	102	14.9	3.4	0.50
	Std. Dev.	4	0.6	0.3	0.04
13	1	57	8.3	4.3	0.63
	2	63	9.2	4.4	0.64
	3	67	9.7	4.5	0.65
	Average	63	9.1	4.4	0.64
23	1	41	5.9	2.9	0.43
	2	39	5.7	3.0	0.44
	3	34	4.9	3.3	0.48
	Average	38	5.5	3.1	0.45

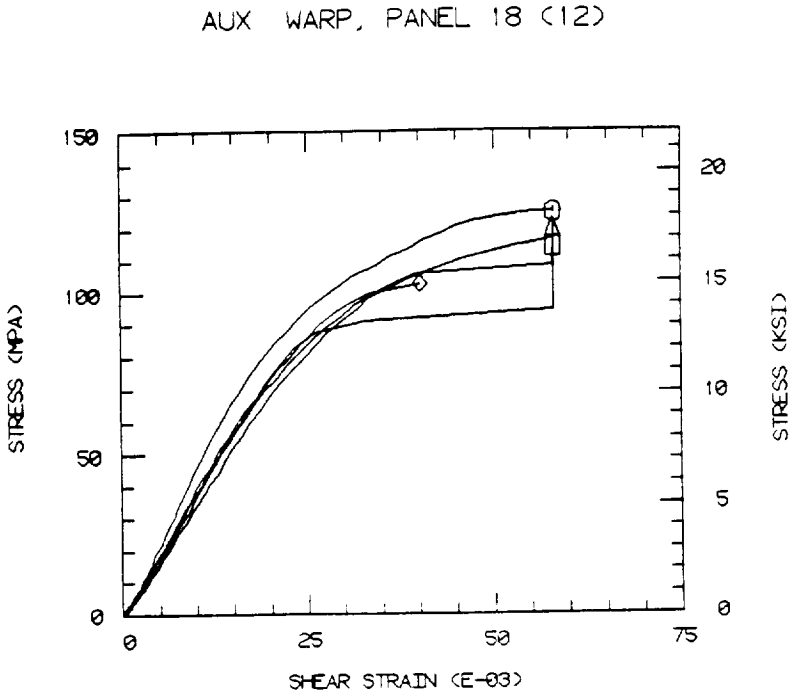

a. Stress-Strain Plot

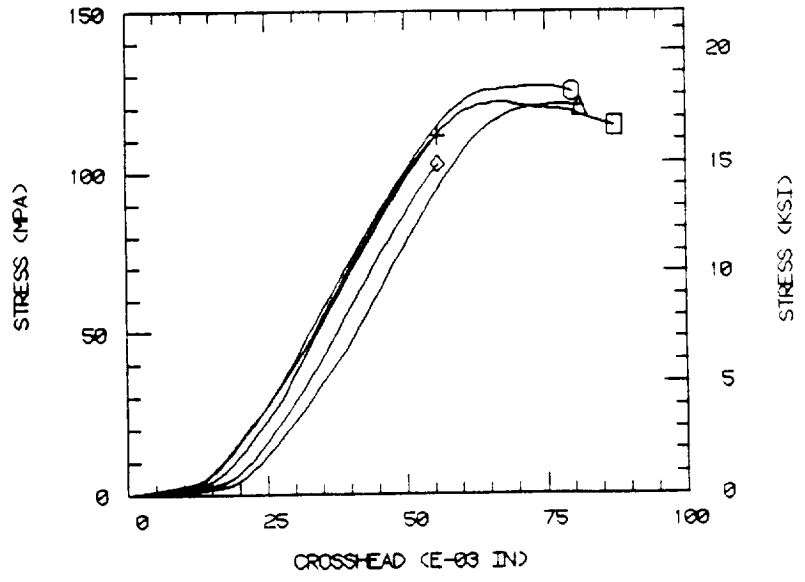

b. Stress-Displacement Plot

Figure B31. In-plane (12) Iosipescu Shear Stress-Strain and Stress-Displacement Plots for Orthogonal Layup Plain Weave, Auxiliary Warp T300/934 Graphite/Epoxy Composite, Panel No. 18.

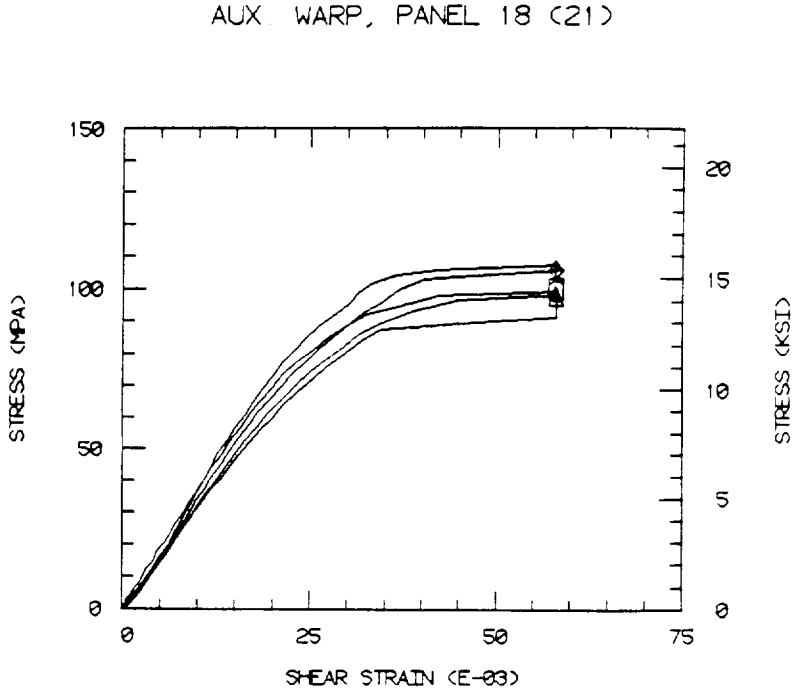

a. Stress-Strain Plot

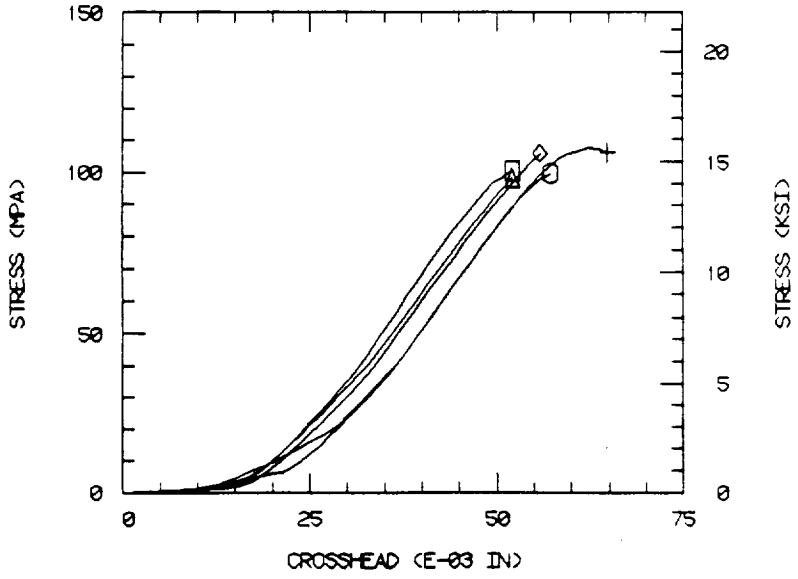

b. Stress-Displacement Plot

Figure B32. In-plane (21) Iosipescu Shear Stress-Strain and Stress-Displacement Plots for Orthogonal Layup Plain Weave, Auxiliary Warp T300/934 Graphite/Epoxy Composite, Panel No. 18.

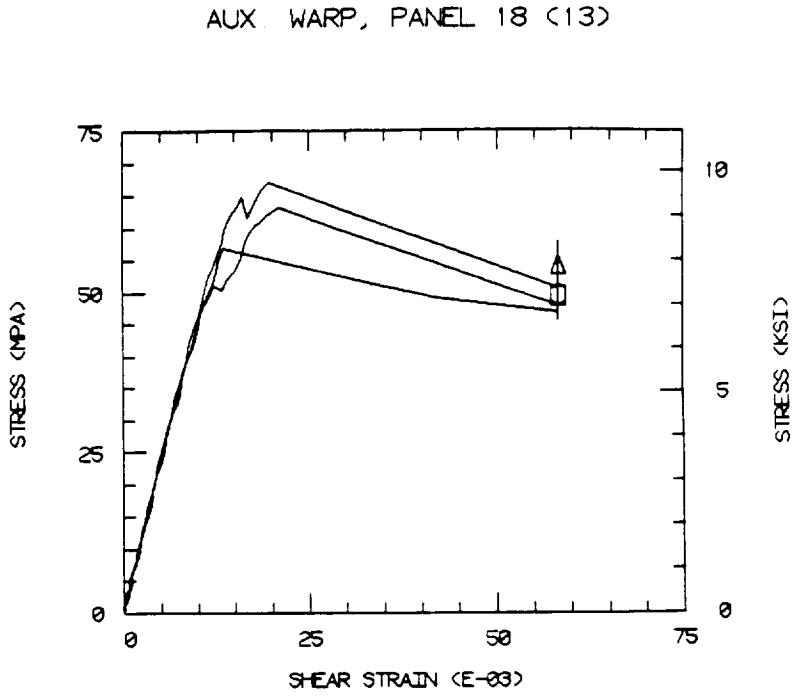

a. Stress-Strain Plot

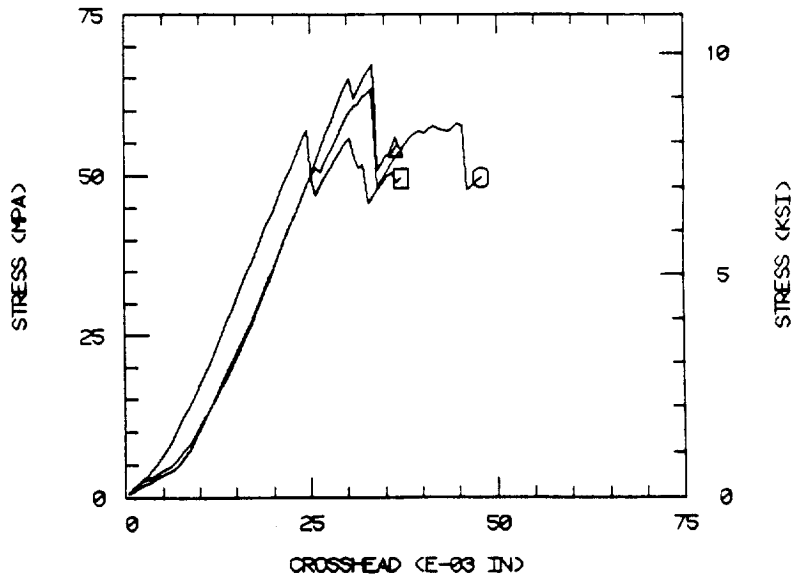

b. Stress-Displacement Plot

Figure B33. Interlaminar (13) Iosipescu Shear Stress-Strain and Stress-Displacement Plots for Orthogonally Layup Plain Weave, Auxiliary Warp T300/934 Graphite/Epoxy Composite, Panel No. 18.

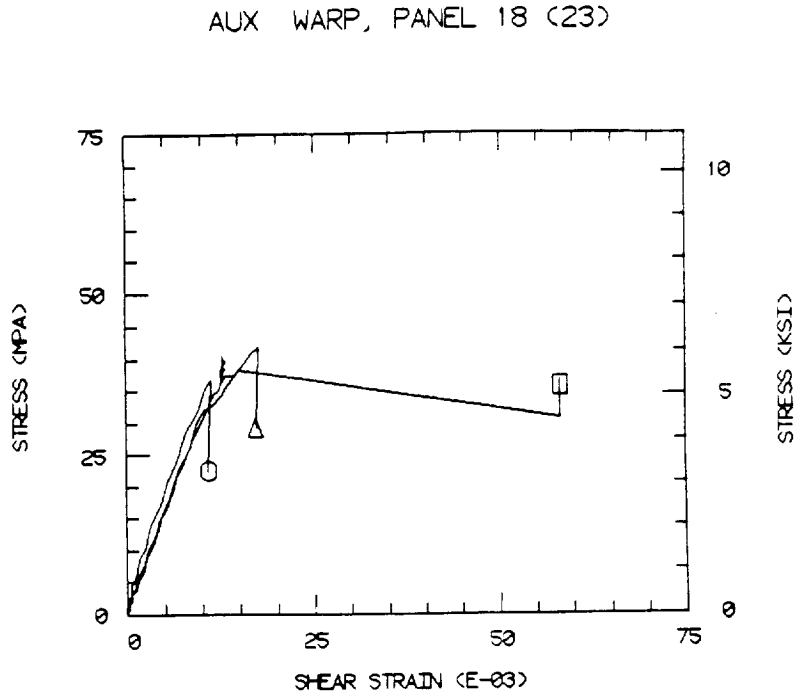

a. Stress-Strain Plot

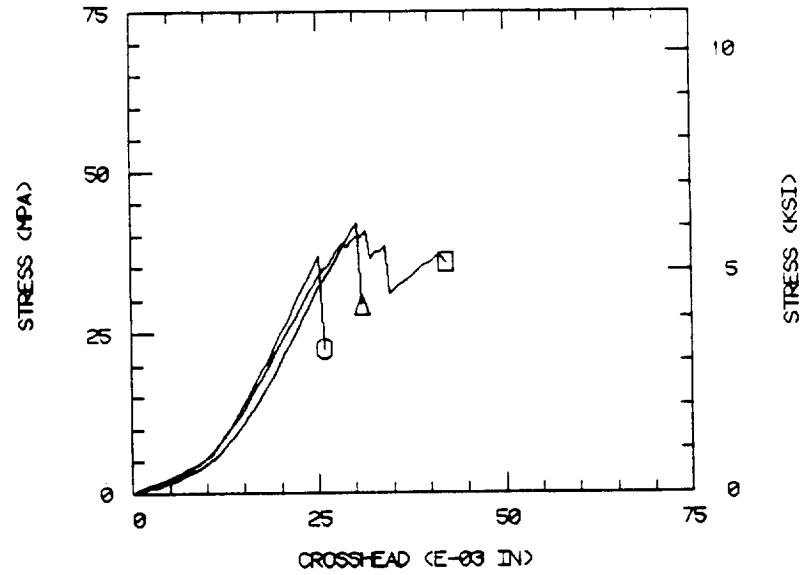

b. Stress-Displacement Plot

Figure B34. Interlaminar (23) Iosipescu Shear Stress-Strain and Stress-Displacement Plots for Orthogonal Layup Plain Weave, Auxiliary Warp T300/934 Graphite/Epoxy Composite, Panel No. 18.